THESIS

Comparative Analysis of Sodium Hydroxide, Silane and Acetylation Treated Luffa Cylindrica Enforced Polylactic Acid Bio-Composites

April/2021

MUHAMMAD JAHANZAIL KAMRAN
(102755302)
Swinburne University of Technology, Sarawak Campus
Faculty of Engineering, Computing and Science

ABSTRACT

Throughout the years, many researchers have been driven to concentrate on natural fibers and biodegradable polymer matrices made composite to fulfill the need of renewable, sustainable, and eco-friendly materials. In addition to that, these natural fibers are used due to their advantages, as they are inexpensive, require less production energy, consist of good mechanical properties, and most importantly, are biodegradable. In this thesis, analysis of the *Luffa Cylindrica* (LC) reinforced polylactic acid (PLA) bio-composites were discussed in detail. The LC surface was modified using three different chemical surface treatments, i.e., sodium hydroxide, silane, and acetylation, to enhance the compatibility of LC with PLA. Mechanical testing characterization was done on the chemically modified LC reinforced PLA bio-composites, i.e., tensile, flexural, hardness moreover, thermal, Fourier transform infrared spectroscopy, and morphological analysis were performed on each sample. Based on the experimental result, it showed that there was an increase in tensile and flexural strength of 7.1% and 6.9% for sodium hydroxide, 5.7% and 1.4% for silane, and 4.3% and 0.4% for acetylation chemical surface treatments respectively, especially to the surface treated samples at 15%wt fiber volume, and a decrease in water uptake (%). Furthermore, the FTIR analysis confirmed that the chemical surface treatments were successful, which provided an explanation of the results that were achieved. Thermal stability was enhanced due to improved interfacial bonding between LC and PLA due to the elimination of other constituents and impurities. Moreover, the morphological analysis (SEM) showed improved bonding compatibility between LC and PLA matrix.

ACKNOWLEDGEMENT

First and foremost, I would like to thank **God** because, with His will, I am able to finish this research and thesis. I would like to say that I sincerely appreciate the necessary facilities and equipment needed to conduct my research which was provided by **Swinburne University of Technology**, **Sarawak Campus**, and **University Malaysia Sarawak**. In addition, I would also wish to convey my appreciation towards the **Swinburne University of Technology, Sarawak Campus**, which provided the financial assistance for my conferences, for both local and international conferences.

Secondly, I would like to convey my genuine gratitude towards my supervisors, **Dr. Elammaran Jayamani**, **Dr. Soon Kok Heng**, and **Dr. Yat Choy Wong**, for their endless guidance and assistance in pursuing this research and for providing me with a broader perspective of the research. In addition, I am thankful for their insightful remarks, useful advice, technical guidance, and useful suggestions during the development of the research work.

Thirdly, I would like to say that I am thankful for the technical assistance provided by the lab technician from the **Swinburne University of Technology**, **Sarawak Campus**, **Mr. Fadillah Johari**, **Mr. Thomas Manggie**, and **other Staff Members**. Furthermore, I am thankful to the **lab technicians** from **University Malaysia Sarawak** for the supervision and guidance regarding the experimental facilities.

Finally, I would like to say thank you to **My Family** for their endless encouragement and support, be it emotionally, physically, or financially, throughout my research and thesis completion. I would also like to convey my gratitude to my friends and counterparts, **Mr. Hariprasanth P.V.S**, **Diana Jani Andrew**, and **Dr. Muhammad Khusairy bin Bakri** for their continual encouragement and support.

AUTHOR DECLARATION

I hereby announce that the thesis entitled "**Comparative Analysis of Sodium Hydroxide, Silane and Acetylation Treated Luffa Cylindrica Enforced Polylactic Acid Bio-Composite**" is the product of my own research work, except for quotes and citations which have been duly acknowledged and referenced. I further announce that it was not submitted to the Swinburne University of Technology, Sarawak Campus for any other master student before or simultaneously.

Name: Muhammad Jahanzail Kamran

Students ID: 102755302

Student Signature:

Date: 25th April 2021

Principal Coordinating Supervisor: Dr. Elammaran Jayamani

Co-Coordinating supervisor: Dr. Soon Kok Heng

Associate Supervisor: Yat Choy Wong

Principal Supervisor Signature:

Date: 25th April 2021

LIST OF JOURNAL PUBLICATIONS AND CONFERENCES

List of Journal Publications

2021	**Journal Title: Journal of Industrial Textiles (SAGE Journals)** **Paper Title:** A review: Surface Treatments, Production Techniques, Mechanical Properties and Characteristics of Luffa Cylindrica Bio-Composites. **Status:** Published, 5th January 2021 **DOI:** https://doi.org/10.1177/1528083720984094
2021	**Journal Title: Material Science Forum Vol. 1030** **Paper Title:** Comparison of Chemically Surface Treated Luffa Cylindrica Using Fourier Transform Infrared Spectroscopy (FTIR) and Thermal Analysis. **Status:** Published **DOI:** https://doi.org/10.4028/www.scientific.net/MSF.1030.53
2021	**Journal Title: Fibers and Polymers (Springer Journals)** **Paper Title:** Comparative and Characterization of Chemically Treated Luffa Cylindrica Reinforced Polylactic Acid Bio-Composites. **Status:** Under review, Awaiting Acceptance

List of Conference Publications

2020	**13th International UNIMAS Engineering Conference (ENCON 2020)** **Paper Title:** Comparison of Chemically Surface Treated Luffa Cylindrica Using Fourier Transform Infrared Spectroscopy (FTIR) and Thermal Analysis. **Status:** Accepted and Published
2021	**International Conference on Advances in Materials, Mechanics, Mechatronics & Manufacturing (IC4M 2021)** **Paper Title:** Optimization and Fabrication of Pure Polylactic Acid (PLA) Using Hot Press Compression Moulding. **Status:** Accepted and Published **DOI:** https://doi.org/10.1088/1757-899X/1136/1/012012
2021	**Symposium of Malaysian Chemical Engineers (SOMChE 2021)** **Paper Title:** Comparison of Chemically Surface Treated Luffa Cylindrica Using Scanning Electron Microscopy (SEM). **Status:** Accepted, Awaiting Publication

TABLE OF CONTENTS

LIST OF FIGURES

LIST OF TABLES

1 CHAPTER 1

1.1 INTRODUCTION

1.1.1 Natural Fibers

It is well known that the world is confronting a severe environmental pollution problem, which contributes to global warming. Researchers worldwide have been working on green materials to reduce specific areas of environmental pollution and, therefore, contribute to decreasing environmental pollution as a whole. This need has forced many researchers to focus on composites made from biodegradable materials. However, synthetic fibers such as glass fiber and carbon fiber have been utilized for several years in manufacturing composites. These synthetic fibres' enforced composites have been used significantly due to their remarkable mechanical properties. Synthetic fibers originate from petroleum; therefore, issues arise in recycling and biodegradability (Faris M. AL-Oqla 2013; Mohamad Alhijazi 2020). Synthetic fibers are not fully biodegradable; they are flammable and release huge smoke and toxic fumes. Therefore, to minimize environmental pollution, various researchers have started researching natural fibers because they are abundant, recyclable, and biodegradable (Debanth 2017; K. Majeed 2013). Natural fibers can be considered as multipurpose materials because they have decent mechanical properties, good soundproofing, and high impact resistance (C. Parida 2012; M.R. Sanjay 2018). The following Table 1 shows the advantages and disadvantages of natural fibers.

Table 1: Advantages and disadvantages of natural fibers (Ozbakkaloglu 2019).

Advantages	**Disadvantages**
Cheap	Moisture absorption is high.
Renewable source	Swelling (poor dimension stability)
Density is low	Poor resistance to microbes
High specific properties	Thermal resistance is lower.
High Young’s modulus	Fibers are not continuous.
Good tensile strength	Low transverse strength
It does not cause abrasion to tools and molds.	Low compressive strength
No skin irritation	Quality depends on the season.
Lesser consumption of energy	Demand and supply are inadequate.
CO_2 neutral	
No residues when destroyed	
Biodegradable	

Natural fibers have a higher content of fibers present; therefore, a small amount can provide equivalent performance, reducing the overall usage. Composites made using natural fibers are usually lightweight, and therefore, if utilized in the automotive industry, which improve automobiles' fuel efficiency. Ultimately leading to lesser environmental pollution (Ozbakkaloglu 2019).

Various types of natural fibers are available such as plant-based, animal-based, and mineral-based (asbestos) fibers (Campilho 2015). This research focuses on plant-based fibers, which are further divided into seed fiber, leaf fiber, bast fiber, fruit fiber, and stalk fiber, as shown in Figure 1. There are many different types of natural fibers and are categorized accordingly furthermore, the structure of plant fiber is shown in Figure 2. Discussion on the type of fiber used in this research is given in the upcoming section. Plant-based natural fibers consist of cellulose which is a crystalline region and usually consists of 80% crystalline region, hemicellulose, which is branched polysaccharides attached to cellulose, pectin, and lignin which is amorphous and also acts as a protective barrier (Breuer 2015; Omar Faruk 2012).

However, plant-based fibers are cellulosic fibers; therefore, they are hydrophilic in nature under normal conditions. Furthermore, due to being hydrophilic in nature, the fibber's moisture content can adversely affect the mechanical characteristics of the natural fiber-enforced composites or bio-composites (Ozbakkaloglu 2019).

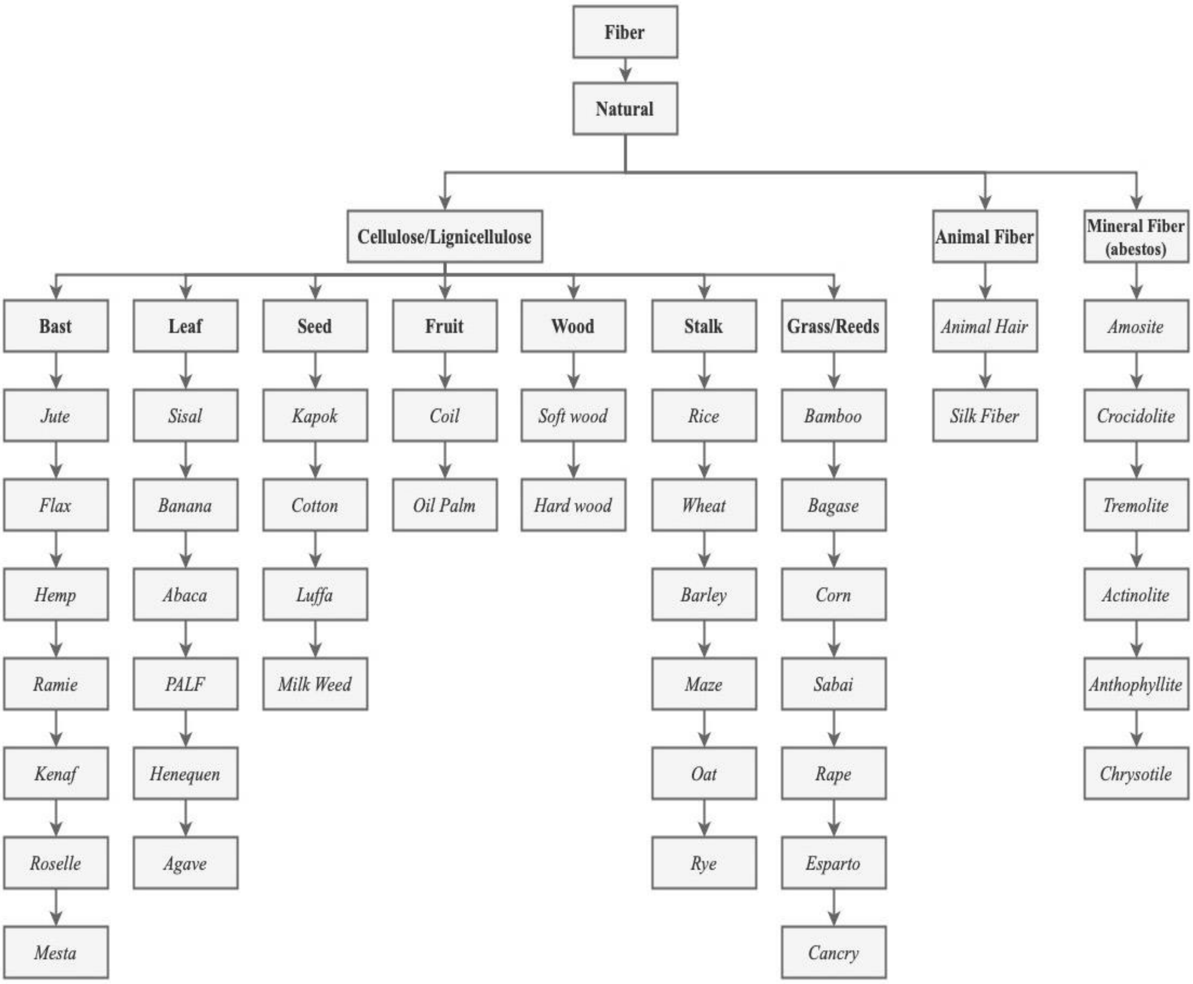

Figure 1: Classification of natural fibers (Ozbakkaloglu 2019).

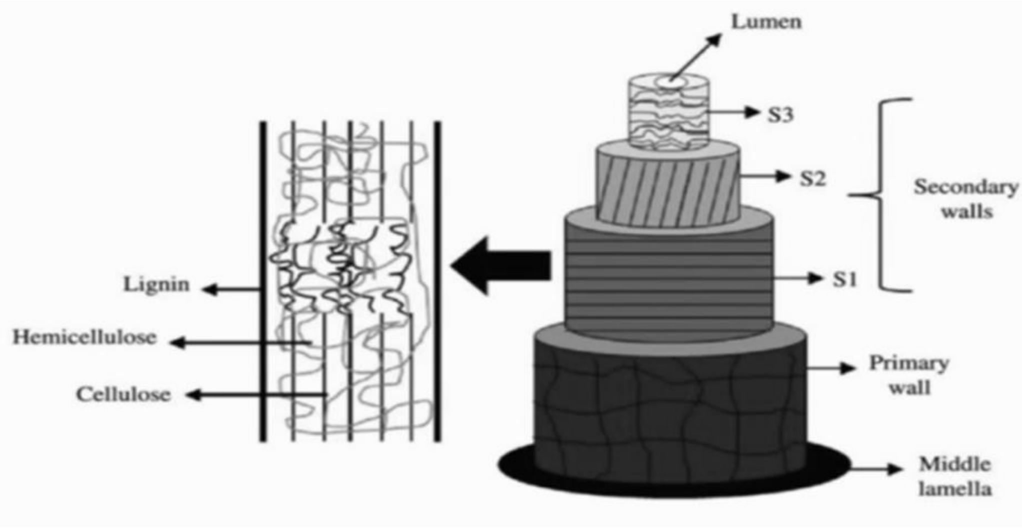

Figure 2: Structure of natural fiber (Debes Bhattacharyya 2015; Mukesh 2019).

The natural fibres' (plant-based) characteristics depend on various variables, such as size, orientation, crystallites, shape, and the thickness of the cell wall. Plant-based fibers are further characterized by low energy consumption, low cost, worldwide abundance, availability, low density, and non-abrasive nature (Anand R. Sanadi 1995; Campilho 2015). A comparison for various types of plant-based fibers can be seen in Table 2. These plant fibers are stiff/rigid; therefore, they are not damaged during various processing techniques like compression moulding, extrusion, or injection moulding. In contrast, synthetic fibers like glass fiber are brittle and get damaged during processing. These plant fibers are known for not having remarkable mechanical characteristics; however, some of the plant fibers have comparable strength and stiffness to glass fiber (Amar K. Mohanty 2005; Campilho 2015; Ozbakkaloglu 2019).

Better sound absorption is another advantage these plant fibers have on synthetic fibers. Therefore, in industries like automotive and construction, plant fibers can be utilized due to the mechanical characteristics and better sound absorption. Furthermore, this can mitigate the adverse impacts on the environment (Amar K. Mohanty 2005; Ozbakkaloglu 2019).

There are a different number of processing methods/techniques used to produce a natural fiber composite. Commonly used methods/techniques are injection moulding, compression moulding, roll milling, melt mixing, and solution mixing. Each of these techniques differs from the other by processing parameters and leads to different mechanical properties (Nhlapo 2010). Furthermore, the natural fibres' thermal stability, which eventually leads to thermal degradability, is at 200 °C and beyond. This has caused restrictions on many manufacturing techniques for mass production.

Table 2: Comparison for different types of plant-based natural fibers in terms of cellulose, hemicellulose, lignin, and waxes (average values) (Faris M. AL-Oqla 2014; Kuruvilla Joseph 1999; Ozbakkaloglu 2019).

Natural Fiber	**Cellulose (%wt)**	**Hemicellulose (%wt)**	**Lignin (%wt)**	**Waxes (%wt)**
Abaca fiber	60	23	8	3
Coir fiber	38	0.2	43	-
Cotton fiber	88	6	-	0.7-0.9
Flax fiber	71	19.6	2.4	1.8
Jute fiber	66	17	12.5	0.6
Kapok fiber	65	24	-	-
Kenaf fiber	71	20.6	9.3	-
Bamboo fiber	34.5	31	26	-
Hemp fiber	69	24	11	0.9
Pina fiber	82	-	12.9	-
Ramie fiber	72.4	14.5	0.8	0.4
Sisal fiber	66	13	10	2.3
Bagase fiber	55.4	16.9	25.2	-
Oil Palm fiber	66	-	27	-
Curaua fiber	73.8	12	7.9	-
Wheat Straw fiber	41.5	23	16	-
Rice Straw fiber	49	34	13.5	23
Rice Husk fiber	40	22	21	15.5
Luffa Cylindrica	62.5	15	16.5	-

1.1.2 Polymers

When it comes to composites polymer matrices and fibers are tied together with the help of interfacial adhesion. Tolerance to the atmosphere, surface aspect, and durability of the composite are the primary responsibilities of a polymer matrix (Campilho 2015). As the polymer matrix is stressed under the applied load, it evenly passes the external load on the fibers, which helps in preventing surface cracks and damage from spreading out entirely through the polymer matrix (Campilho 2015). Various researchers have been researching polymer matrices to substitute the petroleum-based polymer matrices due to the small supply of fossil fuels and to mitigate the effect on the environment caused due to the petroleum-based polymer matrices (Omar Faruk 2012; Ozbakkaloglu 2019). Natural fibers have been used on different occasions to produce composites that contain either a completely degradable, bio-based polymer matrices or partially degradable and petroleum-based polymer matrices to mitigate the effect on the environment. The Figure 3 shows various types of degradable and partially degradable polymer matrices.

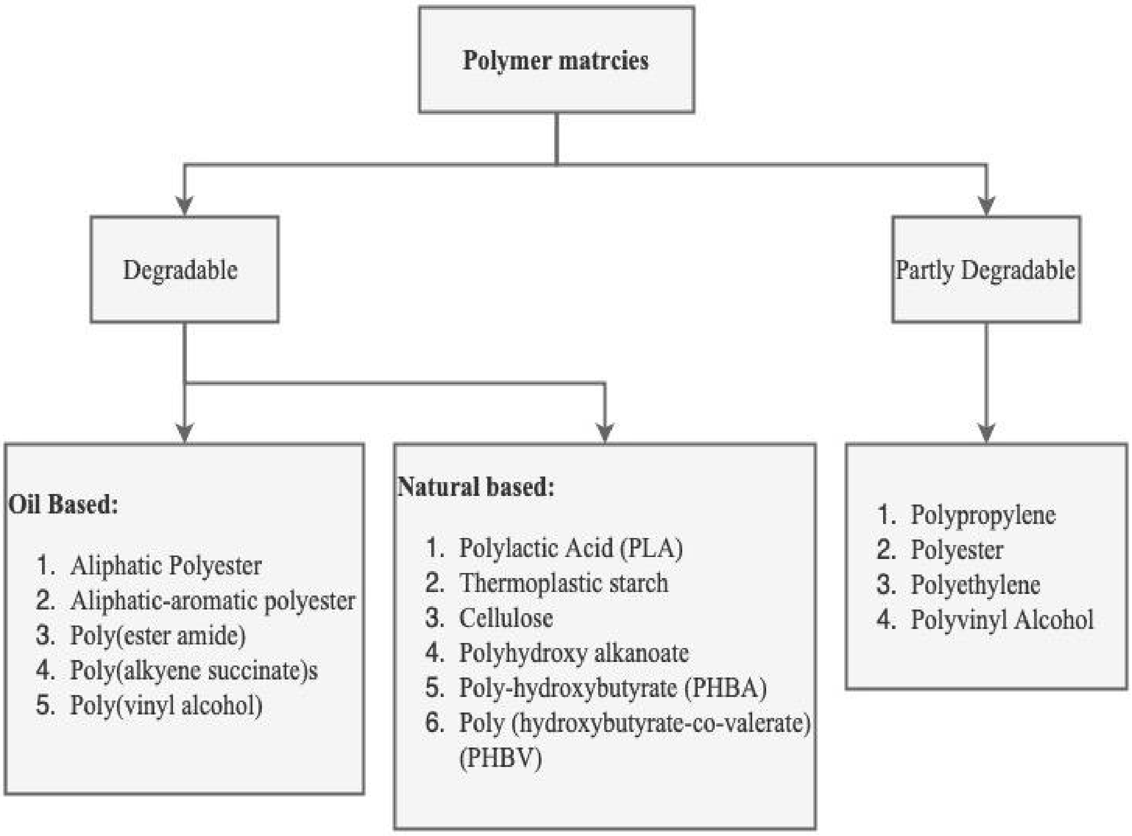

Figure 3: Various classifications of polymers (Ozbakkaloglu 2019).

1.1.2.1 Thermoplastics polymers

Thermoplastics are the type of polymer matrices that can be easily formed in different shapes just by heating and cooling cycles. The thermoplastic viscosity in the melted state is way greater than thermoset polymers (Campilho 2015; Omar Faruk 2012). Thermoplastics are in a solid-state at room temperature; therefore, with the help of various processing techniques such as compression moulding, extrusion, and injection moulding, they can be moulded into various types of shapes and sizes without any kind of chemical reactions or curing (Omar Faruk 2012). Furthermore, thermoplastics have high mechanical characteristics like tensile, flexural, and impact strength. However, the processing parameters like processing temperature and processing pressure are higher than thermosets and bio-based polymers (Ozbakkaloglu 2019). The Table 3 shows the most commonly used thermoplastic polymer resins, their advantages, and disadvantages.

Table 3: Advantage and disadvantages of various types of thermoplastic polymers (Lokensgard 2016; Ozbakkaloglu 2019).

Polymers	Advantages	Disadvantages
Polyethylene	High strength High impact strength Lightweight Low cost Less moisture absorption	Resistance to weather is low. Flammable High thermal expansion
Polypropylene	High resistance towards temperature High resistance towards dielectric Good chemical resistance High fatigue resistance	Processing is not easy. Expensive than some other types of thermoplastic polymers Availability is not easy.
Polystyrene	Good resistance for fatigue Good resistance from chemicals It does not crack easily under stress. Low moisture absorption	Flammable Low impact strength Brittle
Polyvinyl Chloride	Flame retardant Versatile Weather resistance Low cost Good dimensional stability	It does not have good resistance from UV Resistance is poor at low and high temperatures.

1.1.2.2 Thermoset Polymers

Thermoset polymer resins are different from thermoplastic resins because they are infusible materials. They are treated using a catalyst or heat (Sinha 2004). However, the main difference between thermosets and thermoplastic polymer resins is the thermoset polymer resins are not affected by heat; therefore, they cannot be melted and moulded into desired shapes and sizes (NAB 2007). Moreover, thermoset resins have high stability towards chemicals, heat, better water resistance, higher modulus, and crack resistance due to three-dimensional covalent bonds between the chains (Ozbakkaloglu 2019). However, at room temperature, thermosets are brittle and have a lower value of fractural toughness. The Table 4 shows commonly used thermoset polymer resins, their advantages, and disadvantages.

Table 4: Advantages and disadvantages of various types of thermoset polymers (Ozbakkaloglu 2019; Pritchard 2012; Takao Iijima 1991).

Polymers	Advantages	Disadvantages
Epoxy	High thermal and mechanical properties High moisture resistance It does not shrink when cured. Low cost	Expensive than some other types of thermoset polymers Hardener is corrosive Processing is not easy.
Polyester	Easier to handle than some other Low cost	Shrinkage, when cured, is high. Not easy to process or work on Mechanical properties are decent. Emissions are high
Vinyl ester	Resistance towards chemicals and the environment is very high. Better mechanical properties than some other resins	Shrinkage, when cured, is very high. Expensive than some other types of thermoset polymers It contains a high content of styrene. Curing is required post-processing.
Phenolic	Resistance from heat is very high.	Processing is not easy.

1.1.2.3 Biodegradable and bio-based resins

In the recent years, various researchers have started doing research on bio-based polymers because these polymers are derived as a whole or in parts from renewable sources. These bio-based polymers are either fully biodegradable or partly biodegradable. The most common types of bio-based polymers are polylactic acid (PLA), polyethylene terephthalate, and polypropylene (Campilho 2015). These polymer resins are made using cellulose and starch or through the polymerization of plants. Bio-based polymer resins are divided into three major categories: 1. partially bio-based and non-biodegradable, e.g., bio-polyethylene terephthalate, bio-polyethylene, and bio-polypropylene, 2. partially bio-based and fully biodegradable, e.g., polylactic acid (PLA) and 3. fully bio-based and biodegradable, e.g., polyhydroxyalkanoate (PHA) and starch (Campilho 2015; Omar Faruk 2012; Ozbakkaloglu 2019). The Table 5 shows commonly used bio-based polymer resins, their advantages, and disadvantages.

In the year of 2011, the production of bio-based polymers was recorded at around 3.5 million tons globally, while the production of petroleum-based polymers was around 235 million tons (Campilho 2015). In recent years, the rate of growth in the production of bio-based polymers was increased. Moreover, it was expected that by the end of 2020, the production of bio-based polymers would surpass 12 million tons annually (Campilho 2015). However, this volume of bio-based polymers is still much smaller than petroleum-based polymers. Therefore, in order to mitigate the adverse effects of petroleum-based polymers, the production of bio-based polymers should be increased dramatically (Ozbakkaloglu 2019).

Polylactic acid (PLA), which is a partially bio-based and fully biodegradable, is prepared using maize and starch, as mentioned earlier. In the past studies, it has been shown that the preparation of PLA utilizes 50% less oil and emits 60% lesser greenhouse gases in the air when degraded in comparison to petroleum-based polymers for similar applications (Campilho 2015; Ozbakkaloglu 2019).

Table 5: Advantages and disadvantages of various types of Bio-Based polymers (Kevin J. Edgar 2001; Mudhoo 2011; Ozbakkaloglu 2019; Volova 2004).

Polymers	Advantages	Disadvantages
Starch	Biodegradable Low cost	Brittle Processing is not easy. Water absorption is high.
Polylactic acid (PLA)	High modulus and high strength Fully biodegradable Nontoxic Low cost	Brittle Impact strength is low. Degrades at low temperature
Polyhydroxyalkanoate (PHA)	Molecular weight is high. Biodegradable	Low decomposition temperature Stability is low Brittle Deformability is low More expensive when compared to other types of biodegradable polymers
Cellulose	Plentiful Low cost Processing and modifications are easy. Not the best impact strength but better than some other biodegradable polymers Not the best heat resistance but better than some other biodegradable polymers	Moisture absorbance is high. Low decomposition temperature

Polylactic acid (PLA), which is also known as polylactide is produced using micro-organism activity. It is a polyester that can be biodegraded and comes under the category of aliphatic (Tueen 2019). In recent years, PLA has been increasingly used in the production of environmentally friendly composites. The mechanical properties of PLA typically differ between soft and high strength materials therefore, properties are typically in accordance with the result. The properties are uniquely influenced by various parameters, such as crystallinity, materials composition mixing, molecular weight, and orientation. With the help of the research in the past on PLA, it was evident that PLA previously had been used to make composites with several natural fibers, i.e. flax, pulp, hemp, and kenaf (Jae-Kyoo Lim 2007; K. Oksman 2003b; Panayiotis Georgiopoulos 2018b; Yicheng Du 2014b). Going through various researchers' work, processing temperature value may vary from one processing technique to another. In addition, the processing temperature for injection molding machines varies in the range of 170-180 °C (Jae-Kyoo Lim 2007). Furthermore, in another research, it was seen that an extrusion machine was utilized, and the processing temperature value was between 180-190 °C (Shin Serizawa 2005b). In addition, a temperature range of 150-170 °C had been widely used to produce PLA composites using compression molding. It was also observed that pure PLA samples or its composites are widely produced using injection molding, compression molding, and extrusion. Furthermore, different processing methods eventually lead up to different properties.

There are numerous types of natural fibers, but throughout this research, *Luffa cylindrica* (LC) was the focus. LC, which refers to as loofa or sponge gourd, is part of a vegetable sponges' family and the plant is richly accessible in nations such as China, India, and Japan. LC is graded as a cellulose/lignocellulose natural fiber (Valcineide O.A. Tanobe 2005). Furthermore, the cellulose content is (55-70 %), hemicellulose content is (8-22 %) and lignin content is (10-23 %) (N. Karthi 2020; Saw 2017). Fibrous LC mat has high mechanical properties, including high strength, stiffness, and energy absorption. Taking LC's mechanical properties into account, several researchers had made LC composites with various types of polymers like polypropylene, polyester, thermoplastic starch, and epoxy in recent years (Saw 2017; Sha Yin 2019). Commonly used processing techniques to prepare LC composites were hand lay-up, compression molding, extrusion (twin/single screw), and injection molding (Kaewta Kaewtatip 2012; M. Sakthivel 2014; Sun-Mou Lai 2016; Vinay Kumar Patel 2016). Furthermore, the highest tensile strength it could achieved was 192.70 MPa, which was recorded for LC-epoxy composite (D.Mohana krishnudu 2018). Whereas, the lowest tensile strength of 1.24 MPa was recorded for LC-thermoplastic starch composites (Kaewta Kaewtatip 2012). In addition, LC is also widely used to prepare packing mediums, mats, soundproofing, and remove heavy metals from wastewater (Al-Snafi 2019). Moreover, some of the LC composites were created for the removal of metal ions.

Fiber surface treatment is essential for the development of bio-composites using natural fiber. These surface treatments are obligatory to enhance the adhesion between LC and any polymer. Surface treatments contributed to removing hydroxyl groups and waxy impurities that add inadequate adherence between the fiber and the polymer. Furthermore, various researchers have extensively used sodium hydroxide chemical surface treatment to modify the surface of LC to enhance the interfacial adhesion between LC and polymer due to the ease of availability and usage (Chhatrapati Parida 2015a; Saw 2017). Moreover, it aids in eliminating the waxy impurities from the surface of LC, while LC's mercerization enhances the interlocking between LC, whereas its improved improving the interfacial adhesion of the polymer (Hossein Ebrahimnezhad-Khaljiri 2020; Kaewta Kaewtatip 2012; R.Panneerdhass 2014).

1.1.3 Research Gap

With the assistance of past studies on LC, it was evident that LC-PLA bio-composites were scarcely studied. Compared to other forms of chemical surface treatments, most of the past studies mainly focused on sodium hydroxide chemical surface treatment. Thereby, this research provides a thorough analysis of LC-PLA bio-composites by understanding the significance of the subject. The thesis compares the effects of sodium hydroxide, silane, and acetylation chemical surface treatments. These chemical surface treatments were performed to enhance the interfacial compatibility of LC with PLA by modifying the surface of LC. Moreover, the untreated and chemically surface treated LC-PLA bio-composites were evaluated in terms of mechanical characteristics, water uptake (%), thermal properties, FTIR, and morphological properties.

1.1.4 Research Scope

The scope of this research was to identify and analyse the effects on cellulose, hemicellulose, and lignin present in the microstructure of *Luffa Cylindrica* (LC) due to sodium hydroxide, silane, and acetylation chemical surface treatments. The changes in the microstructure of LC due to sodium hydroxide, silanol, and acetyl functional groups were analysed using Fourier Transform Infrared Spectroscopy (FTIR). In addition, Scanning Electron Microscopy (SEM) was utilized to analyse the improvements in interfacial adhesion between LC and Polylactic

Acid (PLA). Moreover, analyse the improvements on the mechanical characteristics and water uptake (%) of LC-PLA bio-composites due to sodium hydroxide, silane, and acetylation chemical surface treatments. Last but not least, analyse the thermal behaviour of LC, PLA, and LC-PLA bio-composite with the aid of thermogravimetry analysis (TGA), Derivative thermogravimetry (DTG), and Differential Scanning Calorimetry (DSC).

1.1.5 Objectives

- To optimize compression moulding processing parameters for pure PLA samples.
- To fabricate LC-PLA bio-composite samples using hot press compression moulding.
- To analyse the effects on hemicellulose, cellulose, and lignin due to sodium hydroxide, silanol, and acetyl functional groups chemical surface treatments using FTIR.
- To analyse the adhesion between LC and PLA due to sodium hydroxide, silane, and acetylation chemical surface treatments using SEM.
- To analyse the mechanical characteristics (tensile, flexural, and hardness), water absorption (uptake %), and thermal stability using TGA, DTG, and DSC for LC-PLA bio-composite due to sodium hydroxide, silane, and acetylation chemical surface treatments.

1.1.6 Flowchart

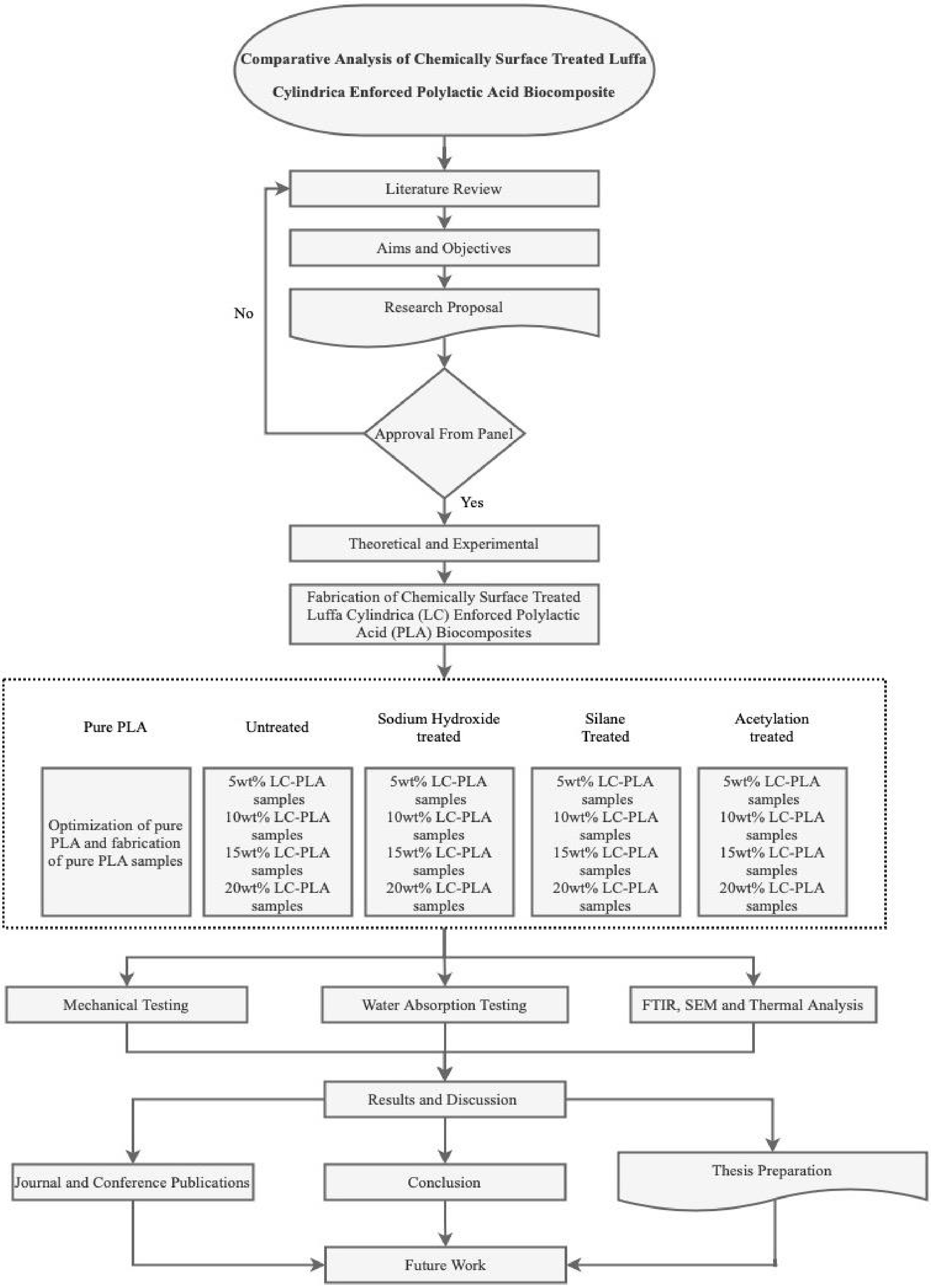

Figure 4: Research project flowchart

1.2 SUMMARY

Different natural fibers and polymers were addressed in this chapter. Various natural fibers such as lignocellulose/cellulose, animal, and mineral fibers (asbestos) are accessible. Lignocellulose/cellulose natural fibers became the focus of this research because LC falls under the category of lignocellulose/cellulose natural fibers. Therefore, a comparison of the chemical composition was given for different types of lignocellulose and cellulose natural fibers. Furthermore, the structure of natural fiber was also discussed. Several processing techniques were used for the preparation of natural fiber composites, for example, injection moulding, extrusion, and compression moulding. Thermoplastic resins, thermoset resins, bio-based resins, and partly bio-based resins were also explained in this chapter. Advantages and disadvantages were also discussed in detail for each type of polymer resin. Last but not least, the chapter also discussed the scope, objectives, and research gap for this research.

The literature review of LC and polylactic acid (PLA), physical characteristics, chemical surface treatments and techniques, processing parameters and techniques, applications, and discussion on various LC and PLA composites are discussed in the upcoming Chapter (Chapter 2).

2 CHAPTER 2

2.1 LITERATURE REVIEW

2.1.1 Luffa Cylindrica (LC)

LC is commonly known as loofa or sponge gourd and belongs to a vegetable sponges family (D. Kocak 2015). The plant is available abundantly in countries like China, India, and Japan. Young luffa plants can be consumed as a vegetable and for medical purposes (Valcineide O.A. Tanobe 2005). LC comes under the category of cellulose/lignocellulose natural fibers. During the growth of the LC plant, cells elongate and form a fibrous structure. This fibrous structure consists of cellulose, hemicellulose, and lignin (Sha Yin 2019). LC fibrous mat shown in Figure 5 possesses great mechanical properties such as high strength, stiffness, and energy absorption (Deepak Pathania 2017; Niharika Mohanta 2015; Saw 2017). Considering LC's mechanical properties, several researchers have used LC to make composites, whereas other researchers are motivated to make composites for metal-ion removal (Shouzheng Su 2018). Moreover, LC's other commonly used applications are packing mediums, mats, soundproof linings, and removal of heavy metals from wastewater. In addition to that, treatment for asthma, sinus, chronic bronchitis, inflammation, and jaundice are some of LC's medicinal uses (Al-Snafi 2019; Musibau Adewuyi Azeez 2013).

Figure 5: Luffa fiber (Sudhir Kumar Saw 2013).

As reported by various other researchers, LC contains high content of cellulose 55-70%, hemicellulose 8-22%, lignin 10-23%, extractives 3.2% and ash 0.4% (C. Parida 2012; Debes Bhattacharyya 2015; Hasan Koruk 2019; Mukesh 2019; Saw 2017). and the molecular structure of cellulose, hemicellulose, and lignin can be seen in Figure 6. In addition to that, the density of LC lies between 0.82-0.92 g cm$^{-3,}$ which is not that high compared to other commonly used natural fibers like sisal or hemp (Gilberto Siqueira 2013; K. Anbukarasi 2015; Kuruvilla Joseph 1999). Other than that, LC and other commonly used natural fibres' mechanical properties can be seen in Table 6.Another advantage is that natural fibers such as LC have a higher fiber content than synthetic fibers; therefore, a small amount of natural fiber can provide equivalent performance, thus reducing the fibber's overall usage (H. Demir 2006).

Table 6: Comparison of luffa fiber mechanical properties with other commonly used natural fiber (A. Stamboulisa 2001; Govind Pathak 2018; Harpreet Singh 2018; Jianhu Shen 2012; N. Karthi 2020; S.Salit 2017; Saw 2017).

Mechanical Properties	**Luffa Fiber**	**Hemp Fiber**	**Sisal Fiber**	**Kenaf Fiber**	**Flax Fiber**	**Jute Fiber**
Tensile strength (MPa)	202.3	550	600	930	1.339	860
Young's modulus (GPa)	4.5	70	38	53	58	60
Elongation at break (%)	2.5	1.6	2	1.6	3.2	2
Density (g/cm^3)	1.2	1.5	1.3	1.1	1.5	1.5

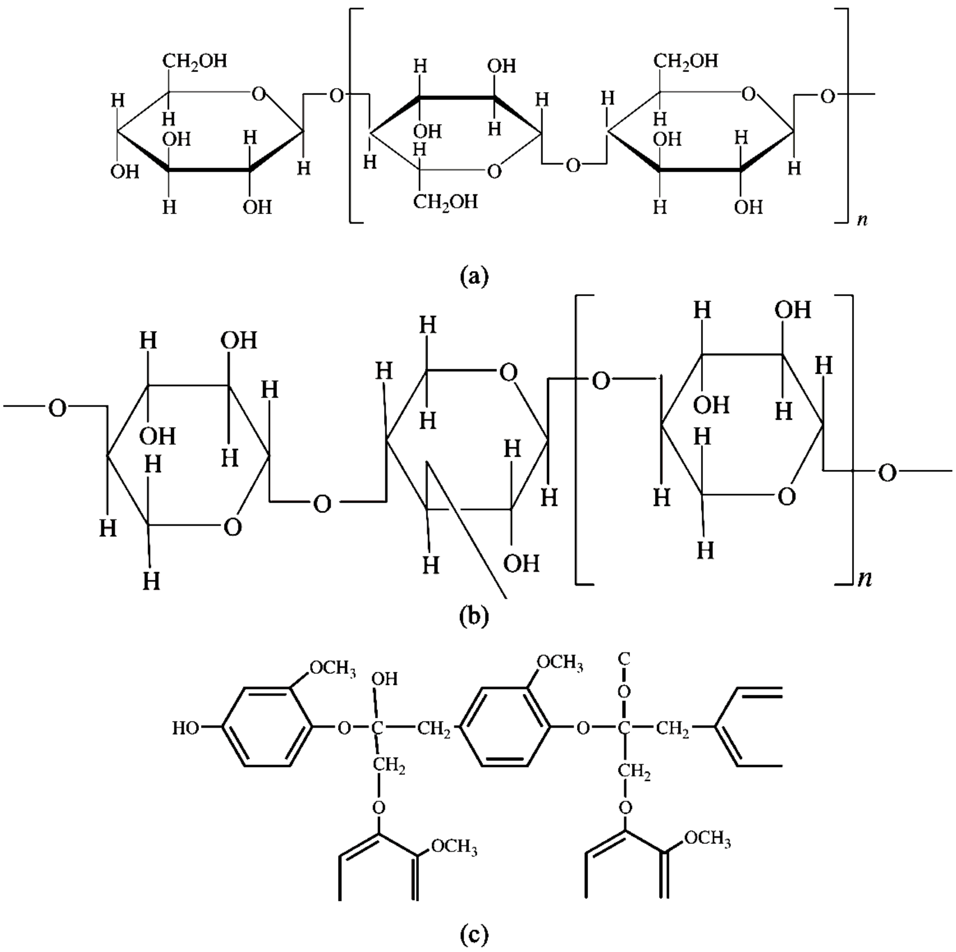

Figure 6: Molecular structure of (a) cellulose, (b) hemicellulose and (c) lignin (MM Alam 2014; Mukesh 2019).

2.1.2 Chemical Surface Treatments and Techniques

In order to enhance the mechanical characteristics of a composite, it is important to improve the adhesion between the fiber and the polymer matrix using chemical fiber surface treatments. Natural fibers generally consist of a waxy surface and hydroxyl groups responsible for poor adhesion between the fiber and the polymer matrix. Therefore, it is important to thoroughly study various chemical fiber surface treatments because each of the surface treatments has its own benefits (A. Arbelaiz 2005; Éder J. Siqueira 2013). Moreover, some of the most commonly used chemical fiber surface treatments for LC are sodium hydroxide, silane, and acetylation surface treatments (Adewale Adewuyi 2017; Jerico Biagiotti 2004; Xue Li 2007)

2.1.2.1 Sodium Hydroxide Surface Treatment

One of the most commonly utilized fiber surface treatments is sodium hydroxide surface treatment. With the help of sodium hydroxide treatment, there is a disruption of hydrogen bonding, improving the surface roughness. Moreover, sodium hydroxide surface treatment causes depolymerization of cellulose, which then exposes short length crystallites (Xue Li 2007). There are many different ways through which this treatment can be performed to improve the adhesion (L. Ghali 2009). Various researchers have shown various techniques to improve the adhesion using sodium hydroxide surface treatment in the past. Different values of concentrations, immersion times, immersion temperatures, and catalysts or coupling agents have been adapted by researchers (Shu Hong 2020). The most used techniques can be found in Table 7. Furthermore, the equation shown underneath explains the chemical reaction between the fiber and sodium hydroxide (Arun Kumar Gupta 2012; Mukesh 2019):

$$\mathrm{Fiber-OH+NaOH\ \rightarrow Fiber-O-Na+H_2O} \tag{1}$$

Table 7: Various methods of using sodium hydroxide surface treatment.

Solution	**Immersion time**	**Immersion temperature**	**Coupling agent/Catalyst**	**Natural fiber**	**Reference**
1 N of NaOH solution in distilled water	1 hour	Room temperature	-	Sisal fiber	(Arun Kumar Gupta 2012)
6% of NaOH solution in distilled water	48 and 144 hours	Room temperature	-	Kenaf fiber	(V. Fiore 2015)
`5%, 10% and 15% NaOH solutions in distilled water and 2.5% HCL	30 minutes	Room temperature	-	Borassus fiber	(L. Boopathi 2012)

2% NaOH solution in distilled water	30 minutes	Room temperature	-	-	(M.A. Norul Izani 2013)
NaOH solution in distilled water	30 minutes	Room temperature	-	Banana fiber	(N. Venkateshwaran 2013)
2 and 10% NaOH solution in distilled water	1 hour	Room temperature	-	Banana fiber	(Sherely Annie Paul 2008)
1% NaOH solution in distilled water	3 hours	Room temperature	-	Bagasse fiber	(V. Vilay 2008)
3%,6%, and 9% NaOH solution in distilled water	3 hours	Room temperature and 95 °C	-	Kenaf fibers	(A.M. Mohd Edeerozey 2007)
3% NaOH solution in distilled water	1 hour	Room temperature	-	Sisal fiber	(Siddesh Naik V 2017)
20%wt aqueous NaOH solution in distilled water with few drops of acetic acid	1 hour	Room temperature	-	Sisal fiber	(zquez 2003)
4% NaOH solution in distilled water	2 hours	100 °C	Hydrogen Peroxide 10%	Luffa fiber	(Lassaad Ghali & Sakli 2011)

5% NaOH solution in distilled water	1 hour	80 °C	-	Luffa fiber	(Chhatrapati Parida 2015a)
2%wt NaOH solution in distilled water	5 hours	80 °C	-	Luffa fiber	(Adewale Adewuyi 2017)
5% NaOH solution with 5% hydrogen peroxide in distilled water	1 hour	85 °C			
10% NaOH and 20% acetic acid solution in distilled water	1 hour	40 °C	-	Luffa fiber	(Yuxia Chen 2018)
18% NaOH solution with 1.6% urea in distilled water	30 minutes	80 °C			
5% NaOH solution in distilled water	30 minutes	Room temperature	-	Luffa fiber	(Vinod Kumar Guptaa 2014)
10% NaOH solution in distilled water	1 hour	30 °C	-	Raffia palm fiber	(Anike David Chukwudi 2015)

Studies regarding different concentrations, immersion times, and immersion temperatures have been made by various researchers, which leads to the existence of various techniques to perform sodium hydroxide surface treatment. All of the magnitudes mentioned above can influence the mechanical properties of a composite in a slightly different way. Moreover, sodium hydroxide surface-treated fiber composites have always shown superior mechanical properties compared to untreated fiber composites. This insinuates that surface treatment using sodium hydroxide enhances the adhesion between a fiber and a polymer. In some studies where numerous concentrations of sodium hydroxide solutions were compared, the results had shown a decrease in composite strength when the concentration was increased. This result can be expected due to the concentration being high enough to destroy the fiber surface leading to poor adhesion. In addition to that, the increase in immersion time, such as 144 hours, also leads to the destruction of the fiber surface. Furthermore, various studies showed fiber immersion at elevated temperature because better cleaning of fiber surface can be expected at elevated temperature compared to room temperature.

2.1.2.2 Silane Surface Treatment

Silane is a powerful coupling agent used to adhere to glass fiber with a polymer matrix. To show a reduction in cellulose hydroxyl groups in the fiber matrix, silane has been used to surface treat the natural fibers (Xue Li 2007). Silanol forms in the presence of moisture and, therefore, reacts with the hydroxyl groups, resulting in the formation of covalent bonds on the surface of the fiber (Arun Kumar Gupta 2012; M.S. Huda 2007; Xue Li 2007).

Several types of silane coupling agents are available for silane surface treatment. However, the most commonly used silane coupling agents are aminopropyltriethoxy silane, vinyltris (2-methoxyethoxy) silane, 3-aminopropyltrimethoxy silane, n-octyltrimethoxy silane, bis [3-(triethoxysilyl) propyl] tetrasulfide, and 3-trimethoxysilyl propyl mathacrylate (Kumar 2010). Various researchers adapted different approaches to perform silane surface treatment (Mukesh 2019). These techniques were adapted to varying concentrations, coupling agents, immersion time, and immersion temperature. The most commonly used techniques to perform silane surface treatments are mentioned in Table 8.

$$\mathrm{CH_2CHSi(OC_2H_5)_3} \rightarrow \mathrm{CH_2CHSi(OH)_3 + 3C_2H_5OH} \tag{2}$$

$$\mathrm{CH_2CHSi(OC_2H_5)_3 + Fiber - OH} \rightarrow \mathrm{CH_2CHSi(OH)_2O - Fiber + H_2O} \tag{3}$$

Table 8: Various methods of using silane surface treatment.

Solution	Immersion time	Immersion temperature	Coupling agent/Catalyst	Natural fiber	Reference
5%wt silane solution in an alcohol-water mixture (60:40) and acetic acid	1 hour	Room temperature	Bis-(3-triethoxysilylpropyl) and 3-amino propyl-triethoxysilane	Sisal fiber	(Arun Kumar Gupta 2012)
0.003L chemical diluted in 0.997L distilled water with acetic acid	15 minutes	Room temperature	Vinyltrimethoxy silane 98% concentration	-	(W. Z. W. Zahari 2015)
Silane aqueous solution 2% volume ratio with acetic acid	3 hours	Room temperature	-	Ijuk fiber	(A. Orue 2016)
1% silane and 0.5% dicumyl peroxide weight percentage in respect to fiber and acetic acid in methanol mixture with water	1 hour	Room temperature	-	Sisal fiber	(P.J. Herrera-Franco 2005)
0.2 mol/L concentration of silane in ethanol and water mixture with acetic acid	72 hours	Room temperature	3-amino-propyl-triethoxysilane and 3-amino-propyl-trimethoxysilane with a ratio of (80:20)	Henequen fiber	(Feng Zhou 2014)

0.5%wt silane in distilled water containing acetic acid	24 hours		γ-amino-propyl-triethoxy silane		
0.033%wt aqueous solution with 0.5%wt dicumyl peroxide as a catalyst and acetic acid	1 hour		Vinyltris (2-methoxyethoxy) silane		
1% silane solution in acetone solution with acetic acid	2 hours		3-amino-propyl-trimethoxy silane	Bamboo fiber	
1%wt silane with respect to fiber mat solution in ethanol	1 hour	Room temperature	N-octyl-trimethoxy silane and Bis [3-(triethoxysilyl) propyl] tetrasulfide		(Kumar 2010)
0.5%wt silane with respect to fiber mat in de-ionized water	2 hours		3-trimethoxy-silyl propyl methacrylate		
1, 5, 9, and 13 %wt silane solution in absolute ethyl	1 hour	Room temperature	-	Sisal fiber	(Yucheng Liu 2019)

alcohol-water					
6wt % GX 560 silane solution in ethanol	5 hours	Room temperature	-	Cornstalk fiber	(Hamid Abdelhafid Ghouti 2019)

As mentioned earlier, several types of silane coupling agents are available; therefore, they affect the fiber differently, leading to slightly different mechanical properties. One of the most frequently used silanes coupling agents is 3-aminopropyltrimethoxy silane because it is easily and widely available. In addition to that, silane surface-treated fiber composites showed better mechanical properties than untreated fiber composites. It can be concluded that silane surface treatment improves the adhesion between the fiber and the polymer. From various techniques, as mentioned above, longer immersion times are adapted by various researchers. It is important to have a longer immersion time to ensure silane can diffuse properly with the fibre's cell walls. However, a higher immersion temperature value will eventually speed up the process of diffusion between silane and fiber cell walls.

2.1.2.3 Acetylation Surface Treatment

The whole purpose of acetylation surface treatment is to introduce acetyl functional groups. Acetylation surface treatment can be referred to as esterification of the cellulosic fiber as this surface treatment introduces acetyl functional groups in the microstructure of the fiber; therefore, making the fiber more hydrophobic (Xue Li 2007). The chemical reaction that takes place can be seen in the equation (Arun Kumar Gupta 2012; Mukesh 2019; Xue Li 2007).

$$\mathrm{Fiber} - \mathrm{OH} + \mathrm{CH_3} - \mathrm{C(=O)} - \mathrm{O} - \mathrm{C(=O)} - \mathrm{CH_3} \rightarrow \mathrm{Fiber} - \mathrm{OCOCH_3} + \mathrm{CH_3COOH} \qquad (4)$$

Acetylation surface treatment of natural fiber can be attained in several ways. Different values of concentration, temperature, immersion time, and catalyst can be used. No matter what the technique is, the end purpose is to make the fiber more hydrophobic. Commonly used techniques by various researchers can be seen in Table 9.

Table 9: Various methods of using acetylation surface treatment.

Solution	**Immersion time**	**Immersion temperature**	**Coupling agent/Catalyst**	**Natural fiber**	**Reference**
Acetic acid and 50 ml of acetic anhydride	1 hour in acetic acid and 5 minutes in acetic anhydride	Room temperature	2 drops of concentrated sulphuric acid	Basalt fiber	(M. A. Martins 2003)
10 ml of acetic anhydride	-	30 °C	0.1 and 0.4 volume % of concentrated sulphuric acid	Sisal fiber	(Giovanna Frisoni 2001)
The ratio of 1:1.5 of acetic anhydride to acetic acid	2 hours	90 °C	Few drops of concentrated sulphuric acid	Flax fiber	(Hamideh Hajiha 2014)
Acetic acid and 6mL of acetic anhydride	1 hour in acetic acid and 5 minutes in acetic anhydride	Room temperature	10-20 µL of concentrated sulphuric acid	Hemp and Sisal fiber	(Seung Goo Lee 2003)
The mixture of pyridine and acetic anhydride at a volume ratio of 0.6	1 hour	Slowly heated to 110 °C	-	Flax fiber	(Jintao Wang 2013)
606g of glacial acetic acid and 264g of acetic anhydride	1 hour and 45 minutes immersion with acetic acid, then 3 hours more in the mixture of glacial acetic acid and acetic anhydride.	35 °C, cooled down to 18 °C, then slowly increased to 50-55 °C	0.6 mL of concentrated sulphuric acid with glacial acetic acid, then 3.6 mL was added again with the addition of acetic anhydride	Kapok fiber	(S.M. Luz 2008)

1:1 of acetic acid and acetic anhydride	-	Room temperature	1 mL of concentrated sulphuric acid	Sisal fiber	(Arun Kumar Gupta 2012)
Glacial acetic acid solution followed by acetic anhydride solution in distilled water	30 minutes in glacial acetic acid solution	30 °C	Few drops of concentrated sulphuric acid	Raffia palm fiber	(Anike David Chukwudi 2015)

Various techniques adapted by researchers have shown different immersion times, immersion temperatures, and concentration values. Acetylation surface-treated fiber composites show better mechanical properties when compared to untreated fiber composites. This can be due to better adhesion between the polymer and the fiber. This is because the acetylation surface treatment replaces hydroxyl functional groups with acetyl functional groups. Higher concentration values lead to poor mechanical properties because the fiber surface gets damaged. Furthermore, high immersion time leads to better bending strength but the deflection of the composite decreases.

2.1.3 Luffa Fiber composites and Processing Techniques

Various researchers have adopted numerous techniques in the past to produce LC composites. In some cases, several processing techniques were utilized to manufacture LC composites. Only a few techniques are used to produce LC composites with various types of polymer matrices. LC composites and their processing techniques with processing magnitudes are shown in Table 10.

Table 10: Various processing techniques used by researchers to manufacture luffa fiber composites.

Composite	**Processing technique**	**Parameters**	**Reference**
Luffa fiber reinforced epoxy composite	Hand lay-up and compression moulding	*Hand lay-up:* The pressure of 5 MPa at room temperature and was left for 24 hours. *Compression moulding:* Fiber and the epoxy were compressed for a few minutes before adding another layer of epoxy. The second layer of epoxy and fiber was compressed again and curing time for 24 hours.	(R.Panneerdhass 2014), (K. Anbukarasi 2015), (Saw 2017), (D.Mohana krishnudu 2018), (Sudhir Kumar Saw 2013) and (Niharika Mohanta 2015)
Thermoplastic starch/Luffa fiber composite	Compression moulding	Temperature value of 150 °C, time 10 minutes, and pressure of 200 kg/cm^2.	(D. Kocak 2015) and (Kaewta Kaewtatip 2012)
Luffa/Polyester composite	Hand lay-up, cold pressing, and compression moulding	*Hand lay-up:* A load of 25kg was applied, and the mould was left at room temperature for 24 hours. *Cold pressing:* - *Compression moulding:*	(Vinay Kumar Patel 2016), (Anil Dhanola 2018), (Yuxia Chen 2020), (C. A. Boynard 2003), (Lassaad Ghali 2011), (Lassaad Ghali & Sakli 2011) (Valcineide O.A. Tanobe 2014) and (Yuxia Chen 2020)

		The pressure of 13 MPa. The pressure of 3.6 MPa, time 2 hours, and temperature 70 °C.	
Poly(butylene succinate-co-lactate)/starch blend/Luffa-based composites	Twin-screw extrusion	Twin-screw extruder with L/D of 40 in co-rotating mode, screw speed at 360rpm and temperature range of 90-120 °C	(Sun-Mou Lai 2016)
Luffa/Polyester resin/Epoxy composite	Hand lay-up	-	(C. Sivakandhan 2018)
Luffa/Polypropylene composite	Torque rheometer (Thermo Haake Rheomix), compression moulding, and injection moulding	*Torque rheometer:* Mixing temperature 190 °C, rotor speed 60rpm, and mixing time 10 minutes. *Compression moulding:* Temperature value of 190 °C, the pressure of 10 bar, and time 10 minutes. *Injection moulding:* -	(H. Demir 2006), (M. Sakthivel 2014) and (A. K. Mohanty 2002)
Luffa/Groundnut/Epoxy composite	Hand lay-up	-	(R.Panneerdhass 2014)
Luffa/Coir/Polypropylene composites	Injection moulding	-	(M. Sakthivel 2014)
Poly(lactic) Acid/Luffa composites	Single screw extrusion	Rotation speed of 100rpm, the temperature of 170 °C mixing time 10 minutes	(Chhatrapati Parida 2015a)

Luffa/coir fiber reinforced epoxy composites	Hand lay-up	Components were mixed, and pressure of 600 kg cm-2 for 12 hours. Curing was performed for 12 hours in sealed conditions. Post curing was performed at 80 °C for 5 hours	(Saw 2017)

2.1.4 Mechanical Properties of Luffa fiber Composites

Processing techniques and fiber surface modification techniques discussed earlier have different effects on mechanical properties. These effects are discussed in the following sections. Furthermore, Table 11 shows flexural strength, tensile strength, and hardness for all the mentioned LC composites and the type of fiber surface treatment utilized.

2.1.4.1 Tensile Properties

In a study regarding LC enforced epoxy composites, the comparison was shown between treated and untreated LC with varying %wt. The results revealed that treated LC composites had higher tensile strength relative to untreated LC composites. Furthermore, 40% of fiber volume composites showed the highest tensile strength compared to 30% and 50% fiber volume composites (D.Mohana krishnudu 2018; K. Anbukarasi 2015). In another study, LC filled poly (butylene succinate-co-lactate)/ starch blend composites were compared with kenaf fiber-filled poly (butylene succinate-co-lactate)/ starch blend composites. Both the fibers were surface treated using the same concentration of sodium hydroxide. Furthermore, the mixing ratio was unchanged, as well. The result showed that the tensile strength of kenaf fiber enforced composite was higher than LC enforced composite. Moreover, the difference between the tensile strength was less than 4 MPa (Sun-Mou Lai 2016; Weifeng Cao 2018). In another study, LC polyester composites were tested before and after adding calcium carbonate, aluminium oxide, and titanium dioxide as micro fillers. Fiber volume of 5%wt and 10%wt were used in this study, and the micro fillers were used at 5%wt. The result showed that there was a significant increase in tensile strength. However, calcium carbonate fillers and 5%wt fiber showed the overall highest tensile strength (Vinay Kumar Patel 2016). In a different study, natural fillers such as rice husk, groundnut, and wood powder were used to increase the tensile strength of luffa fiber enforced polyester composites. Additionally, 30%wt of LC was used throughout all the samples, whereas %wt of 3, 7, and 11 were used for fillers. The results showed a decrease in tensile strength in the case of rice husk and wood fiber as the %wt went from 3 to 11. However, there was an increase in tensile strength when groundnut %wt went from 3 to 11. It was concluded that this was due to the difference in the fillers' size (Anil Dhanola 2018). The effects of stacking patterns were tested in another study. LC and coir fiber were used to make epoxy enforced composites. Both of the fibers were surface treated using the same concentration of sodium hydroxide. Tri-stacking (Luffa/Coir/Luffa), tri-stacking (Coir/Luffa/Coir), and bi-stacking (Luffa/Coir) were tested in this study. The results showed the highest tensile strength for the tri-stacking (Luffa/Coir/Luffa) method. However, tri-stacking (Coir/Luffa/Coir) showed the lowest tensile strength (Saw 2017).

As shown in the studies performed by various researchers, more than one factor can affect the tensile strength. Different concentrations of chemicals and the volume of the fiber are two main factors affecting the tensile strength. Furthermore, different methods of stacking can affect tensile strength as well. Another approach adopted by researchers of adding nanofillers can also affect the tensile strength. However, when adding fillers, it is recommended to change the %wt of nanofillers in the composite to study the effects on tensile strength thoroughly.

2.1.4.2 Flexural Properties

In order to make sure that a natural fiber polymer composite is suitable for desired applications, it is important to determine flexural modulus, flexural strength, flexural load, and deflection at break (Jianhu Shen 2013; M.R. Sanjay 2018). There have been various studies on flexural strength, focusing on fiber volume, fiber length, and fiber surface treatment.

A study related to LC polyester composite showed a comparison between acetylation, combined process, and cyanoethylating treated and untreated LC polyester composites. The study results showed that the acetylated treated fiber recorded the highest amount of flexural strength, modulus, and elongation at break (Lassaad Ghali & Sakli 2011; Lassaad Ghali 2011; Valcineide O.A. Tanobe 2014). In a different study, LC and groundnut enforced epoxy composites were tested for flexural strength. This study focused on fiber volume in the composites. Different fiber volumes ranging from 10 to 50% were utilized to produce composites. The study showed a gradual increase in the strength as the fiber volume increased from 10 to 40%. However, an unexpected drop in flexural strength was observed when the fiber volume reached 50% (Niharika Mohanta 2015; R.Panneerdhass 2014; Sudhir Kumar Saw 2013). In a study regarding LC/polypropylene composites, the composites were tested for flexural rigidity. LC was treated using sodium hydroxide surface treatment. Results from this research showed that with the addition of 20% LC in the composite, the flexural rigidity of the composite was almost doubled when compared to 100% polypropylene samples (Gonzalo Martínez-Barrera 2013; M. Sakthivel 2014). In another study, LC and polylactic acid (PLA) composites were tested for flexural strength. LC in this research was treated using sodium hydroxide surface treatment. A fiber volume of 2%, 5%, and 10% was used to produce composites with PLA. It was concluded in the research that the composite with 2% LC showed the highest value of flexural stress and flexural strain. However, composites prepared using 5% LC indicated the highest flexural modulus value (Chhatrapati Parida 2015b).

A different approach of the study was conducted regarding bio nanocomposites of LC. Two samples were prepared in which the fiber was modified using calcium carbonate and resin with a weight proportion of 1:1 and 2:1, respectively. It was observed that the sample with 1:1 mixing had better flexural properties in comparison to 2:1 mixing composites (C. Parida 2012).

As can be seen in the studies performed by various researchers, more than one factor can affect the flexural strength of the composite; it is possible to conclude that fiber surface treatment and a certain amount of fiber volume % in the composite lead to better flexural properties. However, different concentrations of chemicals in fiber surface treatments and different fiber % in the composites can lead to a different outcome. Therefore, it is recommended to analyse the composites and conditions thoroughly.

2.1.4.3 Hardness Properties

A study showed a comparison between glass fiber epoxy composite, glass fiber/LC epoxy hybrid composite, ceramic epoxy composite, and ceramic/LC hybrid epoxy composite. The research concluded that the ceramic/LC epoxy hybrid composite showed the greatest value for hardness (C. Sivakandhan 2018). In a different study, micro fillers like calcium carbonate, aluminium oxide, and titanium dioxide were added to create LC polyester composites. Similar %wt of fillers were used; however, fiber %wt changed from 5%wt to 10%wt. The study concluded that polyester with 10%wt LC and 5 %wt aluminium oxide showed the highest value of hardness, 12.9 Hv (Vinay Kumar Patel 2016). In another study regarding fillers, natural fillers like rice husk, wood powder, and groundnut were used. LC %wt of 30 was kept constants for all the samples; however, the %wt of 3%, 7%, and 11% was utilized for fillers. It was concluded in the study that as the %wt of rice husk and wood powder fillers increased, there was a decrease in hardness value. However, in the case of groundnut, the hardness value increased as the %wt of filler increased. The highest value of hardness, 13.3 Hv, was recorded when 11% of the groundnut was used (Anil Dhanola 2018). In other research, the effects of fiber surface treatment were reviewed. LC was surface treated using sodium hydroxide concentration of 10%. The treated and untreated LC polypropylene composite samples were tested for the Rockwell hardness number. The result concluded that treated LC polypropylene composites have better Rockwell hardness numbers than untreated LC polypropylene composites (M. Sakthivel 2014).

As shown in the studies performed by various researchers, more than one factor can affect the hardness value. Two main factors affecting the hardness value are different concentrations of the chemical and volume of the fiber. Micro fillers such as calcium carbonate, aluminium oxide, and titanium dioxide were added, and all of them showed better hardness value. However, when adding micro fillers, it is recommended to change the percentage of the fillers in the composite to study the effects that the fillers have on the hardness.

Table 11: Fiber treatment and the mechanical properties of various LC composites.

Composite	Fiber Treatment	Tensile strength (MPa)	Flexural strength (MPa)	Hardness	Reference
Luffa fiber reinforced epoxy composite	Sodium hydroxide	192.70, 17.63, 23 and 17.97	-, 39.1, 110 and 106.67	-, 50Hv	(R.Panneerdhass 2014), (K. Anbukarasi 2015), (Saw 2017), (D.Mohana krishnudu 2018), (Sudhir Kumar Saw 2013) and (Niharika Mohanta 2015)
Thermoplastic starch/Luffa fiber composite	-	1.24	-	-	(D. Kocak 2015) and (Kaewta Kaewtatip 2012)
Luffa/Polyester composite	Acetylation	-	52.3 and 41.96	-	(Vinay Kumar Patel 2016), (Anil Dhanola 2018), (Yuxia Chen 2020), (C. A. Boynard
	Sodium hydroxide	16-19	46.4and 40.25	-	

	-	19	-	4.4Hv	2003), (Lassaad Ghali 2011), (Lassaad Ghali & Sakli 2011) (Valcineide O.A. Tanobe 2014) and (Yuxia Chen 2020)
Poly(butylene succinate-co-lactate)/starch blend/Luffa-based composites	Sodium hydroxide	16	35	-	(Sun-Mou Lai 2016)
Luffa/Polyester resin/Epoxy composite	-	64.15	-	20.3Hv	(C. Sivakandhan 2018)
Luffa/Polypropylene composite	Silane	33-35	-	-	(H. Demir 2006), (M. Sakthivel 2014) and (A. K. Mohanty 2002)
Luffa/Groundnut/Epoxy composite	Sodium Hydroxide	20	65	-	(R.Panneerdhass 2014)
Luffa/Coir/Polypropylene composites	Sodium hydroxide	24	10	50 HRA	(M. Sakthivel 2014)
Poly(lactic) Acid/Luffa composites	Sodium hydroxide	36.45	48.64	-	(Chhatrapati Parida 2015a)
Luffa/coir fiber reinforced epoxy composites	Sodium hydroxide	27	72	-	(Saw 2017)

2.1.5

2.1.6 Characteristics of Luffa Fiber composites

2.1.6.1 Scanning Electron Microscopy (SEM)

SEM analysis for sodium hydroxide surface treated samples, as shown in Table 7, concluded that the untreated fiber samples consist of impurities, as shown in Figure 7-(a). These impurities will lead to poor fiber and polymer adhesion. In addition to that, a smooth surface was seen due to the presence of waxy impurities on the surface. Samples with an immersion time of 48 hours shown in Figure 7-(b) showed no sign of impurities, eventually leading to better adhesion between the fiber and the polymer. In addition to that, a rough surface was seen, confirming the removal of waxy impurities. However, samples immersed for 144 hours indicated in Figure 7-(c) showed complete annihilation of the fiber surface, and cracks were seen throughout the fibber's surface (V. Fiore 2015).

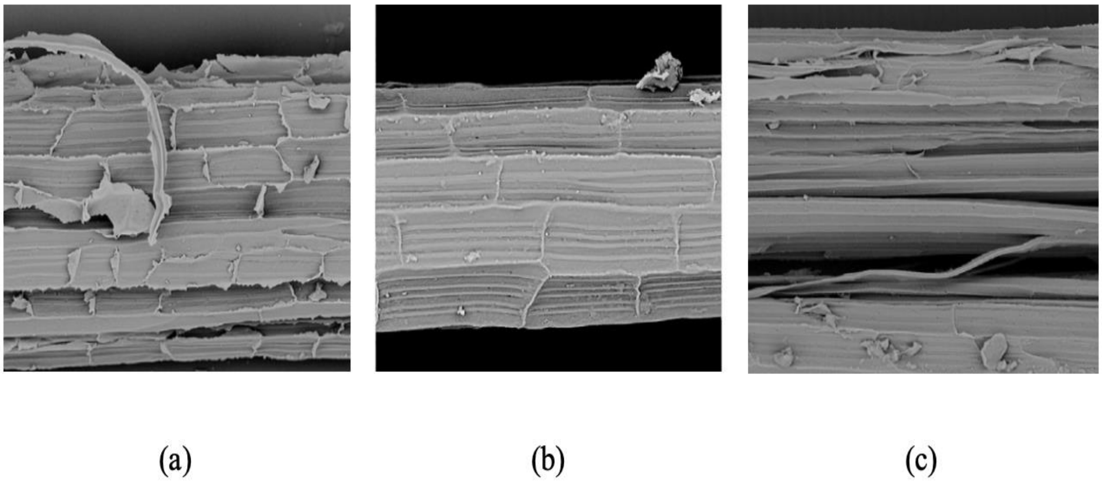

Figure 7: SEM samples, (a) untreated, (b) sodium hydroxide treated 48 h, and (c) sodium hydroxide treated 144 h (V. Fiore 2015).

Sodium hydroxide and silane surface-treated fiber samples were compared using SEM analysis. Surface treatment was performed using the techniques mentioned in Table 7 and Table 8. With the help of Figure 8-(a), it was evident that the surface of the fiber was smooth due to the presence of waxy impurities. In addition to that, linkages were present on the surface due to the fiber being rich in lignin. As shown in Figure 8-(b), the fiber surface after the sodium hydroxide surface treatment Figure 8 was much rougher due to waxy impurities' removal. Another noticeable difference was the removal of linkages from the surface due to the removal of lignin. However, the silane surface-treated sample indicated in Figure 8-(c) showed a smooth surface. This is due to silane sticking on the surface of the fiber (Feng Zhou 2014).

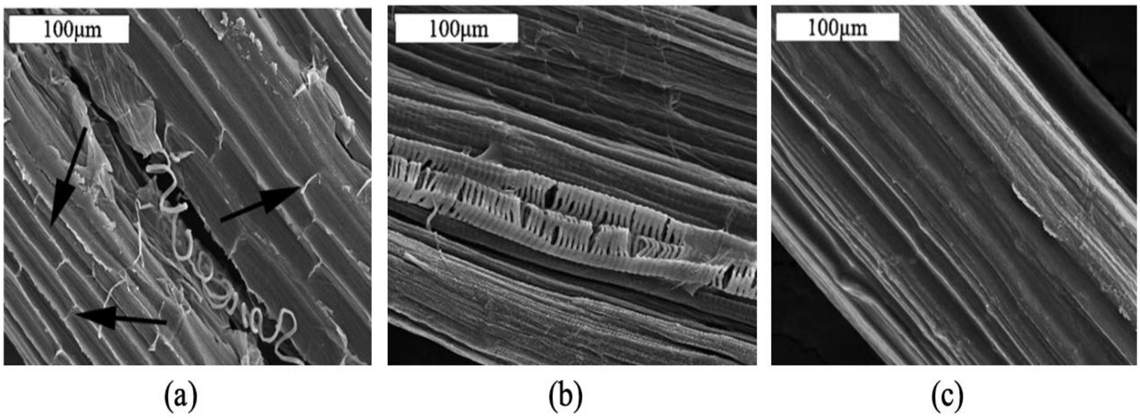

Figure 8: SEM samples, (a) untreated, (b) sodium hydroxide treated samples, and (c) silane treated samples (Feng Zhou 2014).

Another study regarding SEM analysis for untreated, sodium hydroxide, silane, and acetylated surface-treated fiber samples was conducted. As shown in Figure 9-(a), untreated fiber samples showed impurities on the surface. These impurities were seen in the form of wax and lignin. Sodium hydroxide surface-treated samples indicated in Figure 9-(b) showed a rough surface due to the removal of waxy impurities. This observation confirms that sodium hydroxide surface treatment was successful. Furthermore, the adhesion between the fiber and the polymer was improved due to the surface being rough. The silane surface-treated sample shown in Figure 9-(c) did not show any specific changes because the fibber's surface was still smooth. This was due to the silane particles sticking on the surface of the fiber. However, the acetylated surface treated sample indicated in Figure 9-(d) showed complete removal of impurities. In addition to that, the surface of the fiber was still smooth due to the replacement of hydroxyl groups with acetyl groups (Hamideh Hajiha 2014).

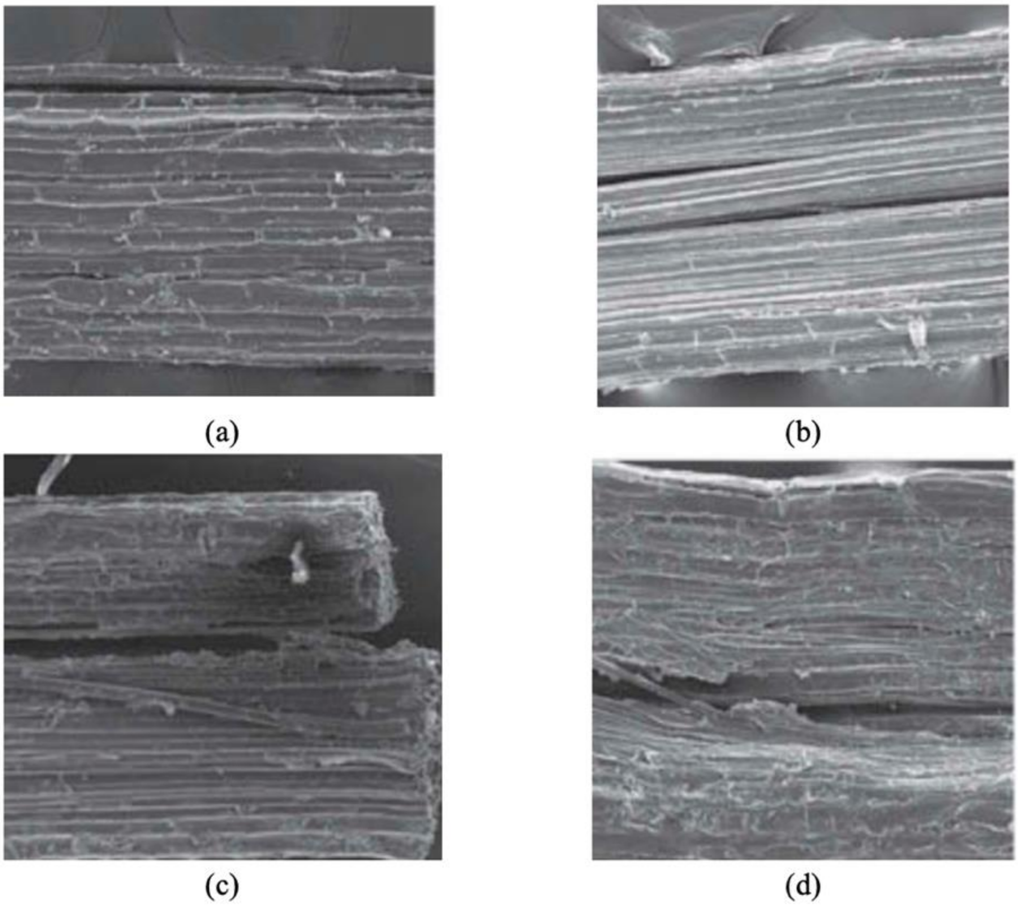

(a) (b) (c) (d)

Figure 9: SEM samples, (a) untreated, (b) sodium hydroxide treated samples, (c) silane treated samples, and (d) acetylated treated samples (Hamideh Hajiha 2014).

2.1.6.2 Fourier Transform Infrared Spectroscopy (FTIR)

FTIR is an analytical technique that is based on an interferometer. Spectrum bands for the IR usually range from 4000-400 cm^{-1} (Dutta 2017; Nicole M. Stark 2004). Various researchers follow the standards provided by the American Society for Testing and Materials (ASTM). In order to perform FTIR, researchers usually utilize ASTM E168-16 and ASTM E1252-98 standards to conduct qualitative and quantitative analysis. Furthermore, FTIR helps in understanding the functional groups which are present in the fiber. A comparison between the peaks of untreated, sodium hydroxide, silane treated, and acetylated LC can be seen in Figure 10.

FTIR results for silane treated LC samples, as shown in Table 8, indicate asymmetric stretching between Si-O-Si linkage and Si-O-cellulose bonds. This stretching is visible in the range of 950 and 1150 cm^{-1}. Bands ranging from 936 and 1366 cm^{-1} confirm the bonding between silane and cellulose. In addition to that, Si-O-cellulose's bond is also confirmed with the stretching of the bands. Bands ranging from 1200 and 1366 cm^{-1} also confirm the presence of Si-O-Si and Si-O-cellulose bonds (H. Demir 2006).

Sodium hydroxide treated LC samples indicated in Table 7 have shown peaks in the range of 1500 and 1000 cm^{-1}. This concluded the bending of CH_2, O-H, and stretching of C-OR. Furthermore, the untreated LC sample showed a vibration of C=O at the range of 1735 cm^{-1}. This can be due to the presence of carbonyl and acetyl groups in hemicellulose and lignin. However, sodium hydroxide treated LC samples showed no peak at 1735 cm^{-1}. Therefore, successful removal of hemicellulose and lignin can be concluded (Sun-Mou Lai 2016).

Acetylated LC samples shown in Table 9 showed peaks in the range of 1735 and 1737 cm^{-1}, which confirms the absorbance. Furthermore, the C-H bond present in lignin showed bending at the peak value of 1500 cm^{-1}. Stretching and vibration of the carbonyl group C=O are caused due to the process known as esterification of hydroxyl groups; therefore, the stretching can be seen in the range of 1735 and 1737 cm^{-1}. Furthermore, ester linkages between acetyl and hydroxyl groups are confirmed with the peak shown at 2372 cm^{-1} (Arun Kumar Gupta 2012).

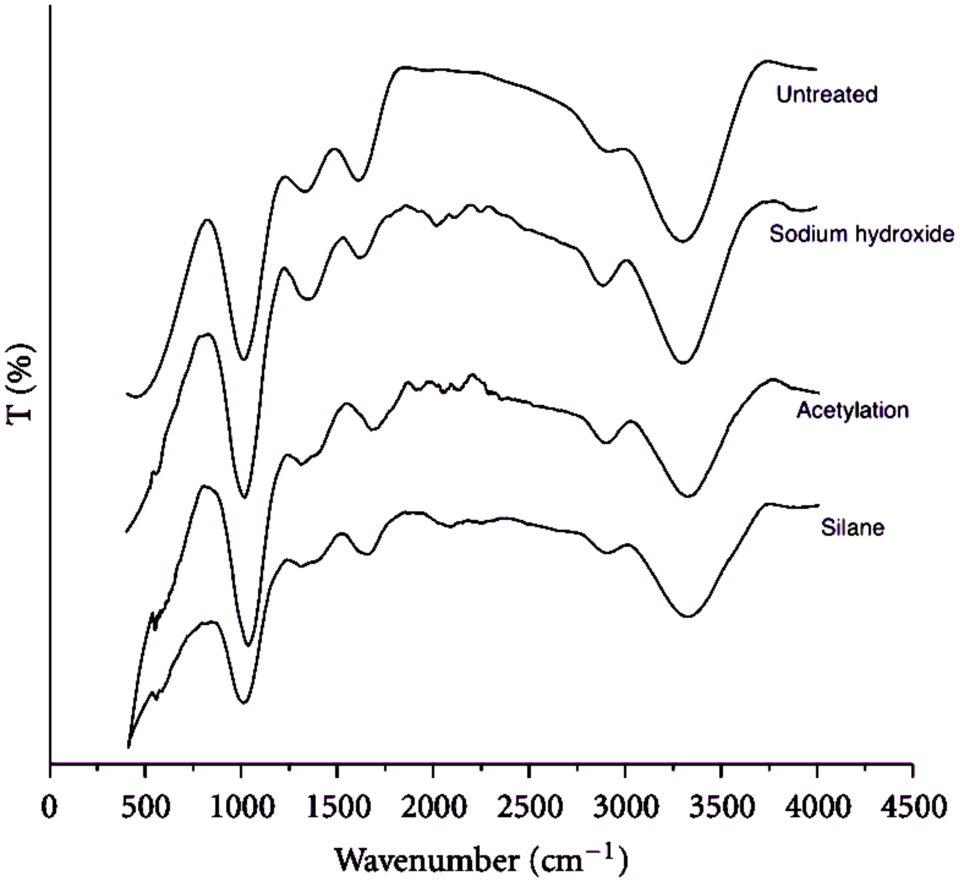

Figure 10: Comparison between FTIR peaks using different chemical surface treatments (Arun Kumar Gupta 2012).

2.1.6.3 Thermal Analysis

TGA is a method adapted by various researchers to study composites' decomposition and thermal stability (Kaewta Kaewtatip 2012; S. N. Pandey 1993). This method can be used to compare the composites' thermal decomposition with varying concentrations of chemicals used for chemical surface treatments, varying fiber volumes, and the addition of fillers or nanocomposites.

Thermal analysis was performed on thermoplastic starch/LC composites with varying fiber %wt. The processing technique can be seen in Table 10. The study concludes that the weight loss of 5%wt LC composite started at 100-200 °C, which could be attributed to the presence of moisture in the composite. Furthermore, the maximum amount of weight loss occurred at 333 °C due to thermoplastic starch degradation. However, at the temperature value of 389 °C, maximum weight loss occurred due to the cellulose and hemicellulose's thermal decomposition present in LC. In the case of 10%wt LC composite, the initial weight loss was at a similar temperature of 100-200 °C however, maximum weight loss occurred at 336 °C. In addition to that, composite with 20%wt LC showed similar weight loss initially at 100-200 °C; however, maximum weight loss occurred at 343 °C (Kaewta Kaewtatip 2012).

In another study regarding TGA, untreated and surface-treated LC composites were compared. Sodium hydroxide surface treatment was utilized in this research, as shown in Table 7. Another surface treatment, known as FA-grafted composites, was utilized as well. The results can be seen in Figure 11. The study concluded that the FA-grafted composites showed maximum temperature value for the maximum rate of mass loss followed by sodium hydroxide treated composites and then by untreated composites (Sudhir Kumar Saw 2013).

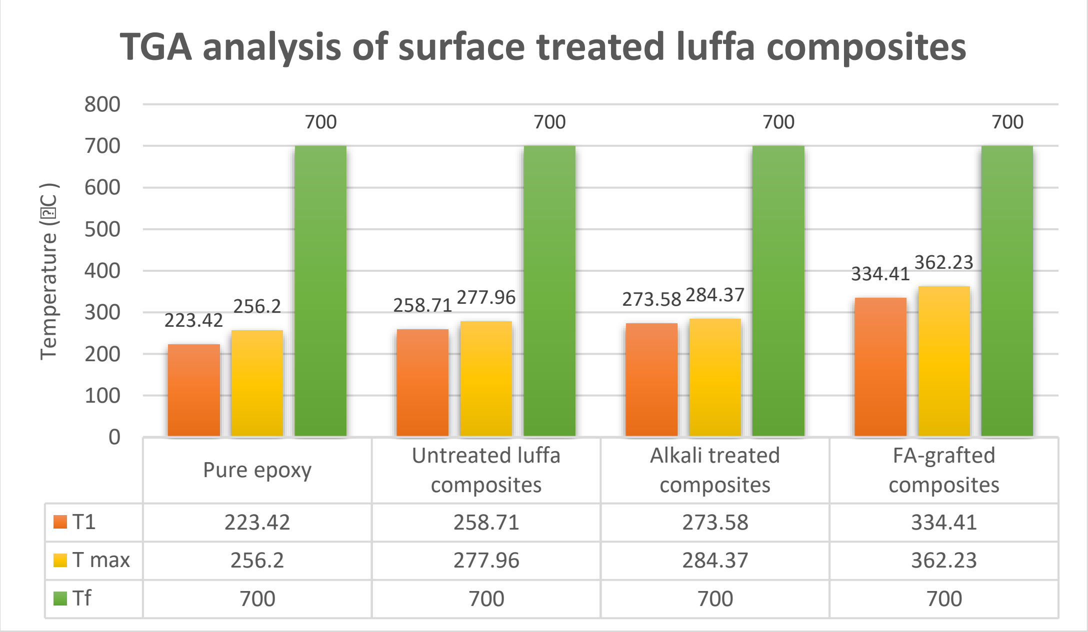

	Pure epoxy	Untreated luffa composites	Alkali treated composites	FA-grafted composites
🟧 T1	223.42	258.71	273.58	334.41
🟨 T max	256.2	277.96	284.37	362.23
🟩 Tf	700	700	700	700

Figure 11: TGA analysis of surface-treated luffa fiber epoxy composites.

Where T_1, onset degradation temperature, T_{max}, the temperature of the maximum rate of weight loss, T_f, final degradation temperature.

Another study regarding TGA compared LC nanocomposites modified calcium carbonate and calcium phosphate. The result can be seen in Figure 12. Four samples were tested; B1 [calcium carbonate modified LC – resorcinol nanocomposites (1:1)], B2 [calcium carbonate modified LC – resorcinol nanocomposites (2:1)], B3 [calcium phosphate modified LC – resorcinol nanocomposites (1:1)] and B4 [calcium phosphate modified LC – resorcinol nanocomposites (2:1)] (C. Parida 2012).

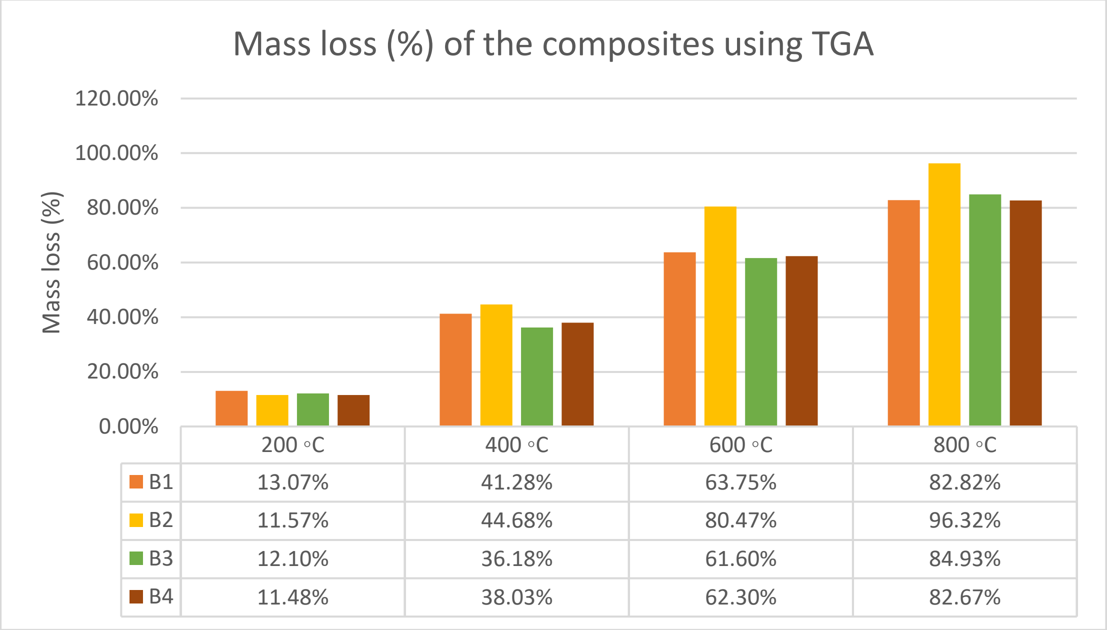

	200 ◦C	400 ◦C	600 ◦C	800 ◦C
B1	13.07%	41.28%	63.75%	82.82%
B2	11.57%	44.68%	80.47%	96.32%
B3	12.10%	36.18%	61.60%	84.93%
B4	11.48%	38.03%	62.30%	82.67%

Figure 12: Mass loss (%) using TGA.

2.1.7 Luffa fiber Composites and Water Absorption

It is important to have a study related to water absorption because these studies help researchers to discover the impacts due to the moisture on natural fiber composites. Moisture leads to debonding between the fiber and the polymer matrix, deforms the composite's shape, and eventually leads to poor mechanical strength (M.R. Sanjay 2018; Shun Li 2019). In addition to that, natural fibers like LC and cotton fiber have poor hydrophobicity (Chaohong Dong 2019; Lu 2020). Therefore, it is important to make sure that natural fibers and their composites have good water repellence.

LC composites had been tested for water absorption on various occasions. In a study, sodium hydroxide treated, and untreated LC enforced epoxy composites were tested according to the American Society for Testing and Materials (ASTM) D570 standard. Specimens were initially oven-dried to obliterate the moisture. This assessment procedure took 48 days, during which the weight and the dimensions of the immersed specimens were recorded every 24 hours. The results showed that the treated composites absorbed 13.8% less water than the untreated composites (K. Anbukarasi 2015). In another study, fiber bundles of LC were tested. These samples were surface treated using a varying percentage of sodium hydroxide. According to the American Society for Testing and Materials (ASTM) D 2654-89a standard, the samples were tested. Thirty samples of each type of treatment were placed in an oven for 4 hours at 105 °C to completely eliminate the moisture. The samples were weighed and measured before being placed in the humidity chamber at 65% relative humidity at 24 °C for 24 hours. The results concluded that the untreated fiber absorbed the highest amount of moisture; however, sodium hydroxide treated fiber showed a decrease of 29%. Furthermore, as the percentage of sodium hydroxide increased in the solution, a higher amount of moisture absorption was recorded (Yadong Wu 2018; Yuxia Chen 2018). Another study was conducted on polypropylene/LC composites were tested before and after silane and MAPP surface treatment for water absorption. The samples were immersed in distilled water at room temperature, where the measurements and differences in weight were recorded frequently. The untreated fiber samples showed a 2.8%wt increase; however, a decrease of 39 and 28.4% was seen for silane and MAPP treated fiber samples, respectively (H. Demir 2006; Hasan Koruk 2019). LC in another research was tested for water absorption after sodium hydroxide, grafted, and hydrolysed surface treatments. The samples were immersed in 500 ml of de-ionized water, which was heated from 10 °C to 60 °C. The researchers were monitoring all kinds of changes in the samples' weight after a certain amount of time. The result indicated that for sodium hydroxide and hydrolysed treated samples, water absorption increased as the temperature increased. However, grafted samples indicated that water absorption decreased as the temperature increased (Qiuping Yang 2018; Zhi Liu 2016).

According to other researchers' findings, there are numerous ways to assess water absorption in the sample. One of the approaches is to utilize moisture regain %, and the other is to find uptake % (H. Demir 2006; Yuxia Chen 2018).

$$\%\ \mathrm{Uptake} = \frac{\mathrm{M_t} - \mathrm{M_0}}{\mathrm{M_0}} \times 100 \tag{5}$$

Where; $M_t$is the mass of the sample at a certain time whereas, M_0 is at t = 0

$$\mathrm{MR} = \frac{\mathrm{M_h} - \mathrm{M_d}}{\mathrm{M_d}} \times 100 \tag{6}$$

Where; M_h is the mass of the sample after being exposed to humidity whereas, M_d is the mass of the dried sample.

$$\text{Water absorption (\%)} = \frac{\mathrm{W_F} - \mathrm{W_I}}{\mathrm{W_I}} \times 100\% \tag{7}$$

Where; W_I is the weight of fiber before immersion whereas, W_F is the weight of fiber after immersion.

On multiple occasions, bio-nano composites reinforced with LC were tested for water absorption as well (Gilberto Siqueira 2013). The experiment was implemented at 25 °C using a temperature-controlled incubator. Water activity was set in the range of 0 to 0.95. Samples weighing approximately 20 mg were exposed to nitrogen flux inside the chamber. The readings were taken until there were no further changes (Nadège Follaina 2013). In another research, an LC sponge was used to test the absorption of oil. The fiber was surface treated using 2%wt aminopropylisobutyl POSS with hexane as a solvent and 2%wt trisilanophenyl POSS with ethanol as a solvent. These samples were immersed in motor oil, pump oil, olive oil, vegetable oil, and diesel oil. The result showed that 2%wt aminopropylisobutyl POSS with hexane as a solvent treated LC sponge had better absorption capacity (mL/g) when compared to 2%wt trisilanophenyl POSS with ethanol as a solvent treated LC sponge (Zhe Wang 2017). Absorption capacity was calculated using the formula below:

$$\text{Absorption capacity} = \frac{(\mathrm{W2} - \mathrm{W1})}{\rho \mathrm{W1}} \tag{8}$$

Where, W1 and W2 represent the fibber's weight before and after the absorption of oil, and ρ shows the oil's density.

2.1.8 Polylactic Acid (PLA)

Polylactic acid, which is also known as polylactide (PLA), is produced using the help of micro-organisms activity. It is a biodegradable polyester and comes under the category of aliphatics. PLA has gained researchers' interest in the past several years because the focus is on developing environmentally friendly composites. Molecular structure for PLA can be seen in Figure 13. These polymers degrade naturally; therefore, once they are disposed pollution rate is lowered compared to non-biodegradable polymers. Polymers like polyethylene, polyvinyl chloride, polypropylene, and polystyrene can be produced cheaply, leading to exploitation in disposable packaging manufacturing. These polymers do not degrade; thus, polymer pollution has become a huge concern (Marius Murariu 2016; Tueen 2019).

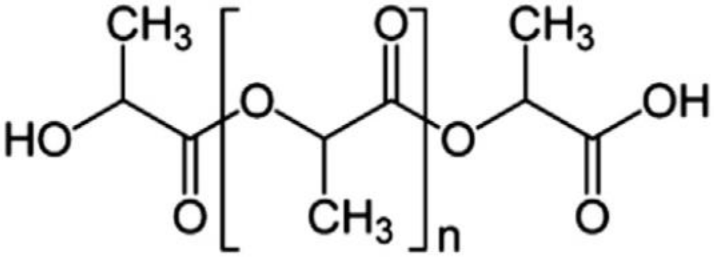

Figure 13: Molecular structure of PLA.

Mechanical properties of PLA usually vary around from soft elastic materials to high strength materials. Properties are usually manipulated depending on the kind of outcome that is expected. Different parameters such as crystallinity, a material formulation that includes composites, blends, molecular weight, and orientation, affect the properties differently. Even though the properties can be manipulated, PLA is a brittle material with low impact strength and elongation at break. However, other mechanical properties like tensile strength and modulus are comparable with polyethylene terephthalate (PET) (Tueen 2019).

Mechanical properties of PLA can be seen in Table 12 underneath. However, with the improvement of the processing using ring-opening polymerization, the properties of PLA are therefore substantially improved. The path requires an intermediate substance known as lactide. It can be in the form of L-lactide, Meso-lactide, and D-lactide in the shape of the cyclic dimer of lactic acid. Molecular structure for various types of lactide groups can be seen in Figure 14. The lactic acid used in this procedure can be produced using the fermentation of carbohydrates such as starch and cellulose. Primary sources of these carbohydrates are corn and cassava (Lee Tin Sin 2019). Furthermore, various types of domestic, engineering and biomedical applications of PLA can be seen in Table 13, (Lee Tin Sin 2019).

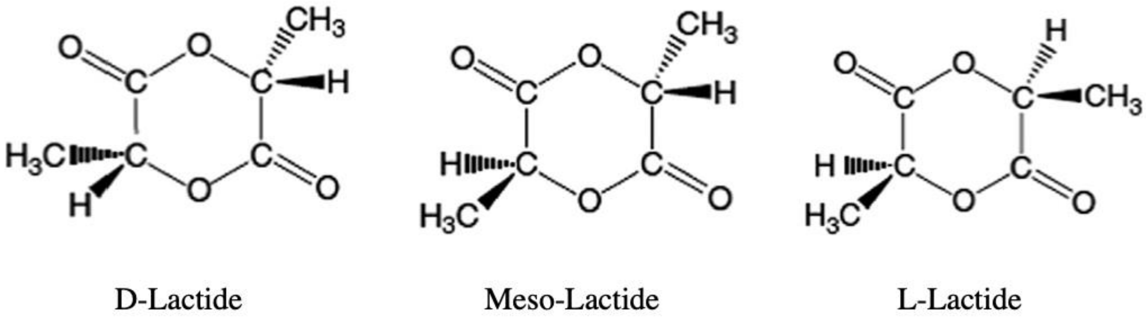

Figure 14: Molecular structure of different types of lactides.

Table 12: Mechanical properties of PLA.

Mechanical properties	**Polylactic Acid (PLA)**
Tensile strength (MPa)	53
Yield Strength (MPa)	60
Young's modulus (GPa)	3.5
Elongation at break (%)	6.0
Notched Izod impact (J/m)	12.81
Flexural strength (MPa)	83
Flexural modulus (GPa)	3.8

Table 13: Shows various types of domestic, engineering, and biomedical applications of PLA.

Type of applications	**Applications**	**Reference**
Domestic applications currently being used	Apparel and household (jackets and hats) Bottles (shampoo bottles) Cups and food service ware Food Packaging (containers) Films Business cards Rigid consumer goods (phones and tablets) Home textiles (cushions) Nonwoven products (packaging) Foam trays (meat packaging) Expanded foams Children toys Fashion products (bike helmets and shoes)	(Lee Tin Sin 2019)
Engineering applications currently being used	Engineering materials (drainage pipes) Automotive industry (foot mats and panels) Building materials (flooring) 3D printing Electrical and electronics (cable coating) Agricultural (clips and water hoses) Hygiene (napkins and nursing)	
Biomedical applications currently being used	Surgical implants (anchors and bone plugs) Drug carriers	

2.1.8.1 Polylactic acid (PLA) and Natural Fiber Composites

PLA composites had been produced with a variety of natural fibers such as flax, pulp, hemp, and kenaf (Jae-Kyoo Lim 2007; K. Oksman 2003b; Panayiotis Georgiopoulos 2018b; Yicheng Du 2014b). Going through various researchers' work, it can be seen that processing temperature value varies around. Various types of PLA and natural fiber composites, processing techniques and processing parameters can be seen in the Table 14. In addition, the processing temperature for injection moulding machine varies around in the range of 170-180 °C (Jae-Kyoo Lim 2007). Furthermore, in another research, it was seen that an extrusion machine was utilized, and the processing temperature value was between 180-190 °C (Shin Serizawa 2005b). In addition, a temperature range of 150-170 °C had been widely used to produce PLA composites using compression moulding. By going through different researchers' work, it was observed that pure PLA samples or PLA composites are widely produced using injection moulding, compression moulding, and extrusion. Furthermore, different processing methods eventually lead up to different properties.

Table 14: PLA and natural fiber composites, processing techniques and mechanical properties.

Composite	**Processing Technique/s**	**Tensile strength (MPa)**	**Flexural strength (MPa)**	**Reference**
Poly(lactic) Acid + Jute Fiber composite	Extrusion, Hot press compression moulding and 3-D printing	81.9, 150-200, 75, 40.8 and 17.8-22.1	175-225, 64.6 and 18-38.0	(A.K. Bledzki 2010), (Bhanu K. Goriparthi 2012), (Sean A. Hinchcliffe 2016) and (S. Ravi Theja Reddy 2020)
Poly(lactic) Acid + Abaca Fiber composite	Extrusion	74.0	-	(A.K. Bledzki 2010)
Poly(lactic) Acid + Hemp Fiber composite	Hot press compression moulding, 3-D printing, and Twin-screw extrusion	85.7 and 87.3	87.2	(M.S. Islam 2010), (M.G. Aruan Efendy 2016), (Sean A. Hinchcliffe 2016), (V. Mazzanti 2019) and (K.L. Pickering 2016)
Poly(lactic) Acid + Kenaf Fiber composite	Hot press compression moulding, Extrusion and Twin-screw extrusion	82.0, 58-62 and 46.8-91.5	93-132	(Nina Graupner 2011), (Intan S.M.A. Tawakkal 2014), (Po-Yuan Chen 2017), (Shin Serizawa 2005a) and (Panayiotis Georgiopoulos 2018a)
Poly(lactic) Acid + Rice Fiber composite	Injection moulding	53.4-63.1		(Yang Zhao 2011) and (Longxiang Zhu 2019)
Poly(lactic) Acid + Coconut Fiber composite	Hot press compression moulding	72.6 and 30-50	-	(Jun Young Jang 2012)

Poly(lactic) Acid + Sisal Fiber composite	Hot press compression moulding, 3-D printing, and Hand layup	36.0 and 52.5-59.3	125.0	(Pramendra KumarBajpai 2013), (Sean A. Hinchcliffe 2016), (Parul Sahu 2018) and (M. K. Gupta 2018)
Poly(lactic) Acid + Bamboo Fiber composite	Twin screw extruder	30-52	-	(Wassamon Sujaritjun & Hamada 2013)
Poly(lactic) Acid + Flax Fiber composite	Extrusion, 3-D printing, and Hot press compression moulding	49.7, 8.27-30.58 and 44-52	70.5	(Thomas Bayerl 2014), (Sean A. Hinchcliffe 2016), (Suneel Motru 2020) and (K. Oksman 2003a)
Poly(lactic) Acid + Harakeke Fiber composite	Hot press compression moulding	101.6		(M.G. Aruan Efendy 2016) and (K.L. Pickering 2016)
Poly(lactic) Acid + Luffa Fiber composite	Extrusion	36.45	48.64	(Chhatrapati Parida 2015a)
Poly(lactic) Acid + Pulp Fiber composite	Hot press compression moulding	88-122	-	(Yicheng Du 2014a)

2.2 SUMMARY

This chapter explained the research on LC and PLA done by various researchers in the past. The chapter begins with an overview of LC and then explores the chemical surface treatments and methods that different researchers have utilized in the past. In addition, different polymers and manufacturing methods were shown. Effects of chemical surface treatment were shown for mechanical characteristics (i.e., tensile, flexural, and hardness), morphological analysis (i.e., scanning electron microscopy), infrared spectroscopy (i.e., Fourier transform infrared spectroscopy), water absorption (water uptake %), and thermal analysis (i.e., thermogravimetry analysis). Comparison between different types of LC composites was made with mechanical characteristics to the extent that chemical surface treatments and manufacturing techniques may influence mechanical characteristics. In the second section of this chapter addressed the research done on PLA in the past. Also explained were mechanical properties and lactide groups. The different application was explained (i.e., residential, medical, and engineering). Last but not least, the chapter analysed and compared different types of PLA and natural fiber composites based on mechanical characteristics. Sodium hydroxide was used as the most frequent method of chemical surface treatment using the literature. Moreover, compression moulding has also been observed to produce the most mechanically efficient composites overall.

Optimization for pure PLA, untreated LC-PLA bio-composite, and chemically surface treated LC-PLA bio-composite is shown in the upcoming chapter. Furthermore, adapted methodologies for chemical surface treatments and physical characteristics are explained in the upcoming chapter (Chapter 3).

3 CHAPTER 3

3.1 METHODOLOGY

3.1.1 Materials

In this research, the white solid powdered PLA form was used. The PLA's density was 1.24 g/cc, and the grade was AI - 1001 which was purchased from the SHENZEN ESUN Industrial Co., Ltd. The LC sponge was acquired from a local supplier to be used in this research. Sodium hydroxide and acetic anhydride were purchased from Thermo Fisher Scientific, acetic acid and sulphuric acid were purchased from LabChem Inc., silane and 3-amino propyltriethoxysilane (APS) were purchased from Merck (Malaysia) Sdn. Bhd. and Bis-(3-triethoxysilypropyl) was purchased from GELEST Inc.

3.1.2 Optimization of Pure PLA

A limited amount of research was available regarding the production of pure PLA samples or composites using hot press compression moulding; therefore, this research aimed to optimize PLA using a hot press compression moulding machine. American Society for Testing and Materials (ASTM) (D790-17, D2240-15e1, D638-14, and D570-98(2018)) specimens were moulded for flexural, flexural, hardness, tensile, and water uptake (%) tests (ASTM 2010, 2014a, 2015, 2017). Various combinations and techniques were utilized to attain optimized specimens (*Polymer Blends Handbook* 2014). Different magnitudes of processing temperature, processing pressure, compression time, and cooling time were analysed. Since the hot press compression moulding was not a widely used technique to prepare samples for PLA; therefore, optimization was an essential step. Furthermore, in another research, it was stated that the hot press compression moulding process produces samples with far better mechanical characteristics when compared with samples made using injection moulding or extrusion (Garkhail 1999). In this research, the white solid powdered PLA form was used. The PLA's density was 1.24 g/cc, which was purchased from the SHENZEN ESUN Industrial Co., Ltd.

3.1.2.1 Mould Preparation

In order to fabricate the samples, ASTM D790-17, D2240-15e1, D638-14, and D570-98(2018) were utilized (ASTM 2010, 2014a, 2015, 2017; B V Lingesh 2014; Suhara Panthapulakkal 2006). The following Figure 15 and Figure 16 show the molds that were utilized and their dimensions, respectively. A releasing agent was applied to the molds to prevent the sticking of samples to the molds and ease specimens' removal. GOTECH hot press compression moulding machine was utilized for optimization and can be seen in Figure 17.

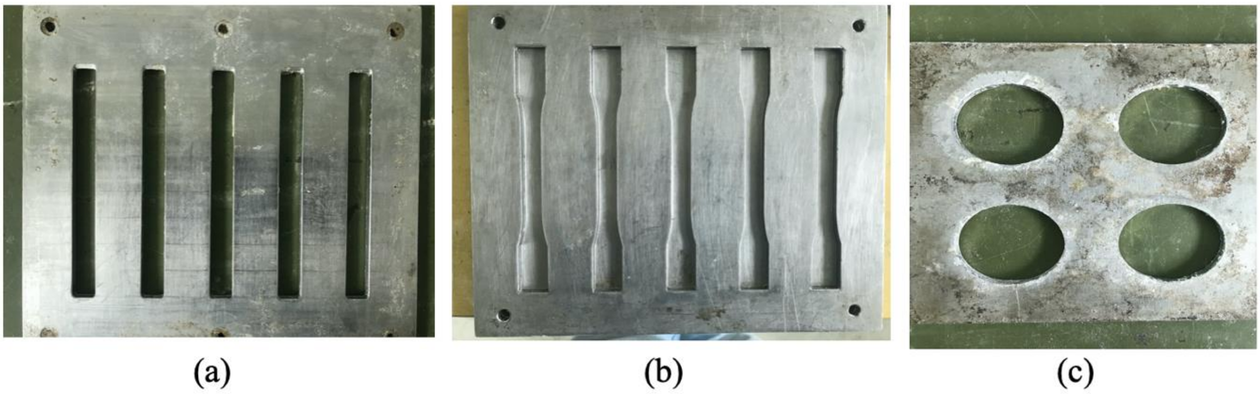
(a) (b) (c)

Figure 15: Molds used to fabricate (a) flexural, (b) tensile and (c) water uptake (%) samples.

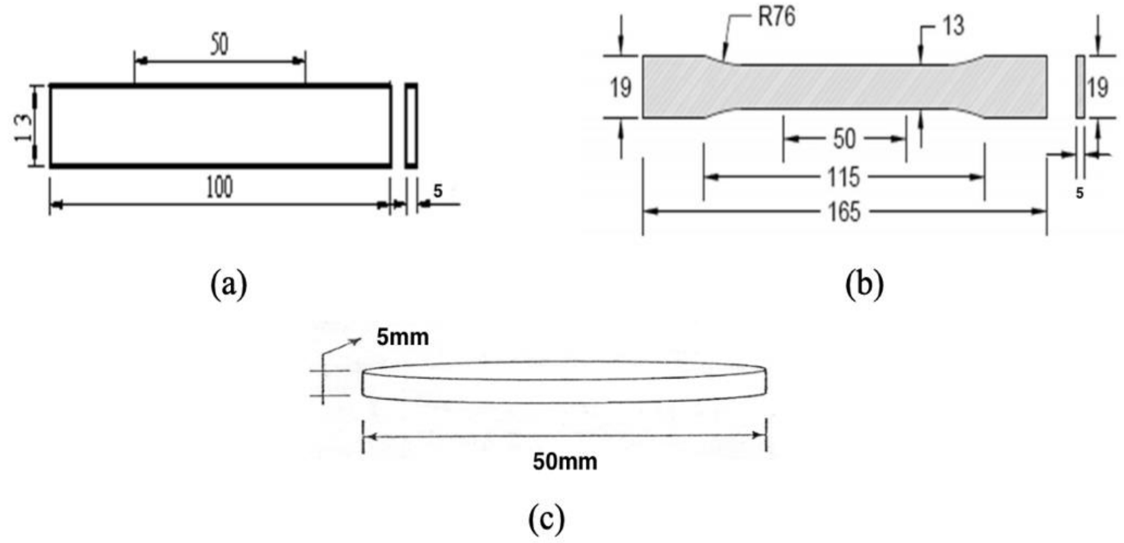

Figure 16: Dimensions for (a) flexural, (b) tensile and (c) water uptake (%) samples in mm.

Figure 17: GOTECH hot press compression moulding machine.

3.1.2.2 Flexural Samples

PLA is a brittle material in nature with low percentage elongation; therefore, optimization was a critical step to achieve good mechanical properties. Furthermore, optimization was also required for hot press compression moulding. Different processing variables such as temperature, pressure, time, cooling time, and even the mould's condition played considerable roles in optimizing the samples. Slight variations in any of these magnitudes can affect the resultant mechanical properties.

With the help of TGA analysis, it was noticed that the melting temperature of this specific PLA used in this research was in the range of 150-155 °C. Therefore, the first batch of samples was kept at 155 °C, with the pressure of 140 MPa, compression time was set at 25 minutes, and cooling time was set at 3 hours. Once the mould was removed from the machine, it was clearly visible that the samples were wrecked. This was due to the pressure value of 140 MPa being too high. Furthermore, a temperature value of 155 °C was not enough to melt the samples entirely and evenly, as seen in Figure 18. By referring to previous researchers' work, it seemed optimum that a longer cooling time ensures that the samples would settle perfectly in the mould (Heather Simmons 2019; Pumchusak 2014).

Figure 18: Uneven melting of PLA at 155 °C.

The second batch of the samples was placed with a processing temperature of 175 °C; however, the pressure was significantly reduced to 60 MPa, whereas compression time and cooling time were not changed. When the mould was opened, the same overflow issue was present; however, the samples were evenly melted throughout, and bubbles were present on the surface. The overflow of the sample can be seen in Figure 19. High processing temperature was utilized in this batch because higher temperature values were used during extrusion and injection moulding of PLA (A. Rubio-López 2015; C. Parida 2012; Justine Muller 2017).

Figure 19: Massive amount of overflow due to high pressure.

In the third batch of samples, the mould was replaced from a male-female setup seen in Figure 20-(a) to flat plates, which were used on top and bottom, whereas the mould was in the middle, which can be seen in Figure 20-(b), underneath. Similar conditions for processing temperature, processing pressure, compression time, and cooling time were applied. With flat plates on top and bottom, overflow was reduced; however, it was not eliminated.

Figure 20: (a) male-female mould used in the first runs and (b) flat plates used afterward.

In the fourth batch of samples, all the conditions were kept the same; however, the pressure was reduced further down to 30 MPa. Nevertheless, when the mould was opened to remove the samples, overflow was reduced significantly whereas, cracks were present on the sample's surface. Due to these cracks, all the samples broke during the removal from the mould.

In the fifth batch of samples, further changes were made. Processing temperature was reduced to 160 °C, processing pressure was maintained at 30 MPa, compression time was increased to 30 minutes, and mould was pre-heated to 160 °C, and the cooling time was still at 3 hours. With the help of these changes, even melting throughout the sample was witnessed; overflow was still present; however, cracks were removed, but bubbles and voids were present on the samples, as seen in Figure 21.

Figure 21: Voids caused due to the overflow of the polymer from the mould.

In the sixth batch of samples, all the conditions were kept the same; however, the processing pressure was reduced significantly to 6 MPa. Reducing the pressure to 6 MPa helped in reducing the overflow even more. However, the bubbles were still not removed.

In the seventh batch of samples, the baking paper was utilized between the mould and plates. Utilizing baking paper, making sure that samples were not sticking with the plates. Furthermore, the baking paper helped to cool samples evenly. With the help of previous runs, all the magnitudes were finalized. The processing temperature value was set at 160 °C, processing pressure was set to 6 MPa, compression time was set to 30 minutes, mould was pre-heated to 160 °C, and cooling time was 3 hours. When the mould was removed and opened, it was evident that all five samples were perfect, and can be seen in Figure 23. To be certain, another batch of samples was placed in a hot press compression moulding machine with the same conditions, and the second run was also successful. Step by step procedure to prepare the mould with baking paper can be seen in Figure 22. Therefore, optimization of flexural samples was completed. The samples were removed from the mould carefully and were placed in an airtight container for two weeks before testing (Lee Tin Sin 2019). These samples were then tested using GOTECH universal testing machine using ASTM D790-17, and the average value was recorded (A. Rubio-López 2015). Moreover, the flexural strength was calculated using the equation shown:

$$\sigma = \frac{3FL}{2wd^2} \tag{9}$$

$\sigma = Flexural\ strength$

$F = Force$

$A = Surface\ area$

$L = Length\ of\ the\ sample$

$w = width\ of\ the\ sample$

$d = depth\ of\ the\ sample$

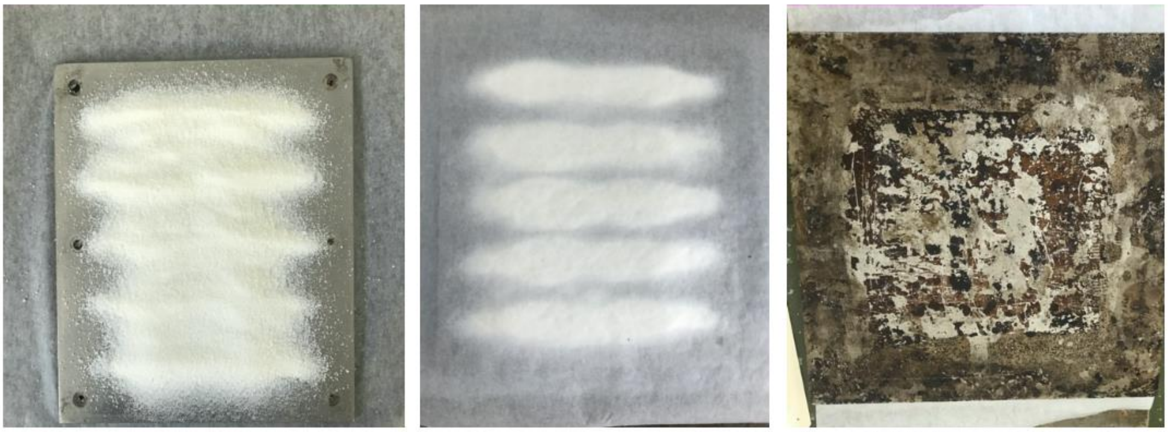

Step 1: Flat plate was placed with baking sheet on top of it. Then the **Mold** was placed with PLA powder.

Step 2: Another baking sheet was placed on top of the PLA powder.

Step 3: Flat metal plate was placed on top of the baking sheet and the sample was placed inside the hot press compression moulding machine.

Figure 22: Step-by-step guide to achieving optimized samples using baking paper.

Figure 23: Optimized flexural sample achieved using optimization.

3.1.3 Tensile Samples

Optimization of flexural samples made things much more straightforward. It was noticed that the processing temperature range for even melting throughout the sample was achieved in the range of 160-170 °C while maintaining the processing pressure around 6 MPa. It was noticed that compression time could be adjusted between 20-30 minutes, and cooling time can range from 2 hours to 24 hours. Furthermore, with baking paper, bubbles were removed, and the overflow was controlled significantly.

With this knowledge, the first batch of tensile samples was placed inside the hot press compression moulding machine. Processing temperature was set at 160 °C, processing pressure was at 6 MPa, hot press machine was pre-heated to 160 °C, compression time was 30 minutes, cooling time was 3 hours, and just like flexural samples, the baking paper was utilized. It turned out that the samples were not melted evenly, which led to the cracking of samples, as seen in Figure 24-(a). Uneven melting occurred due to the higher amount of PLA volume present in the tensile mould than flexural mould.

With the second batch, all of the conditions were kept the same; however, compression time was increased from 30 minutes to 40 minutes. This change was considered in order to improve the melting of PLA and remove the cracks. By increasing the compression time, cracks were removed; however, samples were still not appropriately melted; therefore, they broke while being removed from the mould, as seen in Figure 24-(b). Furthermore, voids were present on the surface of the samples as well.

The third batch of samples was placed, and two changes were made. Processing temperature was increased from 160 to 170 °C, and compression time was reduced back to 30 minutes. Samples in the mould showed even melting; however, bubbles were present, as seen in Figure 24-(c). Moreover, the samples cracked, and some broke as soon as pressure was removed. This showed that a temperature of 170 °C makes the samples more brittle.

The fourth batch of samples was placed, and the processing temperature was reduced to 165 °C. Even melting was witnessed, and there were no cracks. However, again when pressure was removed, samples cracked, as seen in Figure 24-(d).

Constant cracking and breaking of samples led to the inspection of mould. With the help of inspection, it was concluded that the mould was slightly bent; therefore, when pressure was removed, the samples would crack or break. The mould was replaced, and the fifth batch of samples was placed. Processing temperature was set at 165 °C, and mould was pre-heated to 165 °C, processing pressure of 6 MPa was applied, compression time was 30 minutes, and cooling was done for 3 hours at room temperature. When the mould was removed, it was evident that all five samples were optimized. The optimized tensile sample can be seen in Figure 25. Samples were removed carefully and placed in an airtight container for two weeks before testing (Lee Tin Sin 2019). Mechanical testing was carried out using GOTECH universal testing machine, and hardness was found using the SHORE hardness meter. Hardness values were then converted to the Rockwell hardness C scale. All five samples were tested for tensile strength (ASTM D638-14) and hardness (ASTM D2240-15e1), and the average value was recorded (A. Rubio-López 2015). Moreover, the tensile strength was calculated using the equation shown:

$$\sigma_{tensile} = \frac{F}{A} \tag{10}$$

$\sigma_{tensile} = Tensile\ strength$

$F = Force$

$A = Surface\ area$

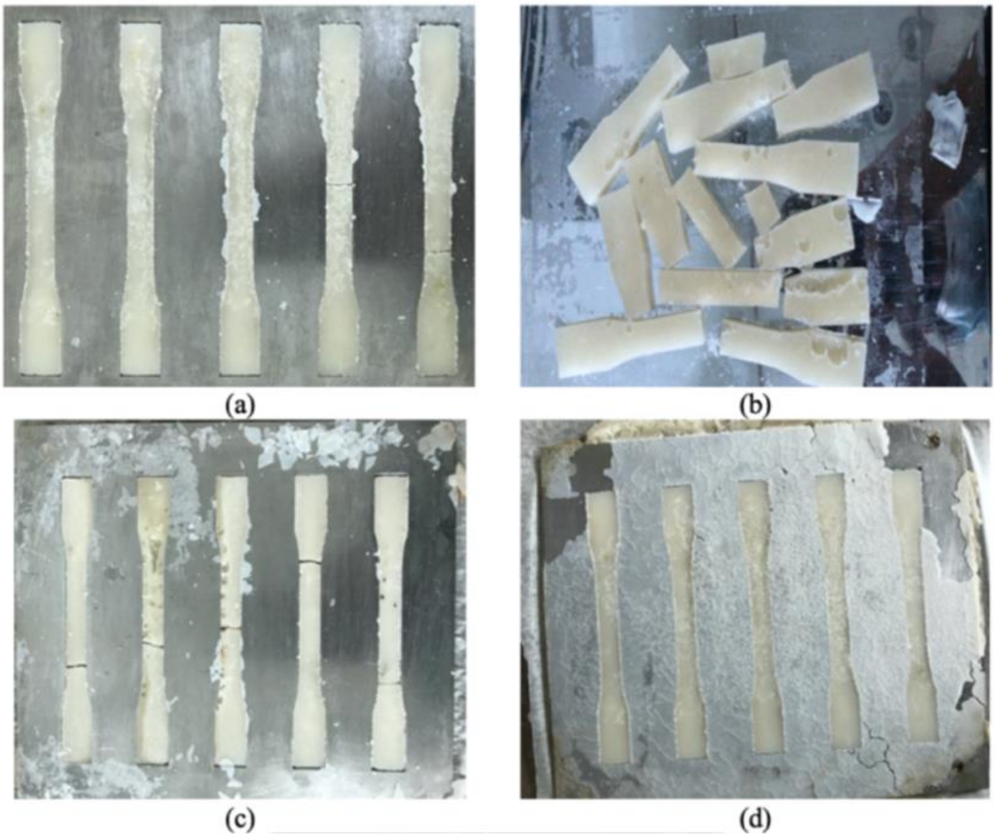

Figure 24: Optimization process of tensile samples, (a) uneven melting and cracks, (b) cracks and voids, (c) cracks and voids, and (d) minor cracks and bubbles.

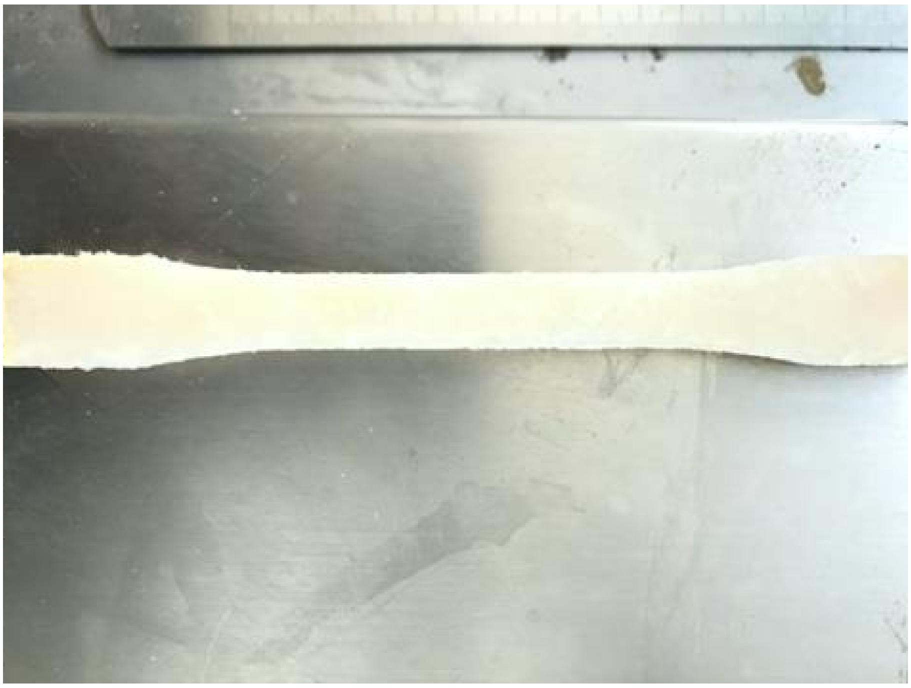

Figure 25: Optimized tensile sample achieved using optimization.

3.1.3.1 Water Uptake (%) Samples

Fabrication of flexural and tensile samples provided a clear idea regarding the magnitudes. Optimization of water uptake (%) samples was the easiest among all the optimizations. The processing temperature was set at 165 °C, and the hot press compression machine was pre-heated to 165 °C. Processing pressure was set at 6 MPa, compression time was 30 minutes, and the cooling time was approximately 3 hours. Moreover, cooling was done at room temperature. The baking paper was utilized the same way it was utilized for tensile and flexural samples. When the mould was opened, it was evident that all the samples were perfect. There were no cracks, bubbles, or uneven melting of the samples. A perfect optimized sample seen in Figure 26. Samples were placed in an airtight container for two weeks before they were tested ted (Lee Tin Sin 2019)

Figure 26: Optimized water uptake (%) sample achieved using optimization.

3.1.4 Preparation of Luffa Fiber

3.1.4.1 Luffa Fiber Surface Modification

The LC was acquired from a local supplier to be used in this research. Fiber surface treatment was essential for the development of bio-composites using natural fiber. These surface treatments were obligatory to enhance the adhesion between LC and any polymer. Surface treatments would also contribute to removing hydroxyl groups and waxy impurities that add inadequate adherence between the fiber and the polymer. Prior to performing any surface treatment, LC was chopped with a chopper. Five mm chopped pieces of fiber were removed from the batch with the aid of a sieve.

A necessary step before undergoing any type of chemical surface treatment is fiber surface modification. LC samples were submerged in a mild detergent solution at 60 °C for 2 hours. This step leads to the removal, for example, of any kind of surface impurities like dust and seeds. LC samples were removed from the solution and washed with distilled water till the detergent was removed entirely from the surface and the LC samples were no longer slippery. In addition, LC samples were dried for three days at room temperature. In their past work, multiple researchers had standardized this approach (Arun Kumar Gupta 2012).

3.1.4.2 Luffa Fiber Chemical Surface Treatments

3.1.4.2.1 Sodium Hydroxide Surface Treatment

Dry five mm LC samples were submerged into a 1N sodium hydroxide and distilled water solution for one hour at room temperature. The samples of LC were then washed with distilled water, containing few drops of acetic acid, which helped neutralize the samples. Furthermore, samples of LC were washed using a continuous flow of distilled water to ensure that sodium hydroxide was completely eliminated and that the fiber samples did not had any soapy like feeling on the surface. Sodium hydroxide surface-treated LC samples were then left for drying for 24 hours at room temperature and then in the oven for 12 hours, at 80 °C (Arun Kumar Gupta 2012; V. Vilay 2008). Submergence of LC seen in Figure 27.

3.1.4.2.2 Silane Surface Treatment

Dried five mm samples of LC were submerged into ethanol-water (60:40) solution containing 5%wt silane for 1 hour at room temperature. Bis-(3-triethoxysilypropyl) and 3-amino propyltriethoxysilane (APS) coupling agents were used as well. In addition, a few drops of acetic acid were added in order to maintain the pH value of the solution at 4. Following an hour of submergence time, LC samples were removed from the solution. In order to altogether remove all the traces of the solution from the surface, LC samples were washed thoroughly using distilled water. Silane surface-treated LC samples were dried at room temperature for 24 hours. Moreover, the samples were dried in an oven at 80 °C for 12 hours (Arun Kumar Gupta 2012; Kumar 2010). Submergence of LC seen in Figure 27.

3.1.4.2.3 Acetylation Surface Treatment

LC five mm dried samples were submerged in a solution containing 1:1 acetic acid and acetic anhydride. In addition to that, concentrated sulphuric acid (1ml) was added as a catalyst. LC samples were submerged in the solution for one hour at room temperature. After an hour of submergence, fiber samples were vigorously washed with distilled water in order to remove the chemical solution entirely from the fibber's surface. Cleaned samples of LC were kept for drying at room temperature for 24 hours and then in the oven at 80 °C for 12 hours (Arun Kumar Gupta 2012; Hamideh Hajiha 2014). Submergence of LC seen in Figure 27.

Figure 27: Submergence of LC in chemical solution for chemical surface treatment.

3.1.5 Characteristics of Luffa Fiber Samples

3.1.5.1 Scanning Electron Microscopy (SEM)

The Scanning Electron Microscopy (SEM) study is one of the most commonly used electron microscopies to conduct a morphological analysis on the bio-composites. Hitachi Analytical table (Tabletop Microscope-3030) equipment was utilized to perform SEM analysis. Moreover, ASTM E2015-04 was utilized (ASTM 2014b). Initially, the specimens were cut and placed on metal plugs. In addition, the samples were partially coated with gold film for 60 seconds. Thickness was found out to be at 10 nm with 0.1 Torr and 18 mA. The accelerating voltage was set to 20KV with a working distance of 20 mm. The magnifications of 100x, 500x, and 800x were utilized for a detailed study on the surface of the bio-composite. Different researchers in the past with different parameters had employed a similar standard approach to perform SEM analysis (A. Oushabi 2017; Saw 2017).

3.1.5.2 Thermal Analysis

Thermal analysis (thermogravimetry analysis) was performed utilizing Perkin Elmer, simultaneous thermal analyzer, model: STA8000. Samples weighing 4.5mg were utilized in this analysis. Purified nitrogen gas was utilized to ensure test samples only react to temperature during this degradation. A temperature increment of 20 °C/min was utilized. The test was repeated twice for every untreated, sodium hydroxide treated, silane treated, and acetylated LC samples. The temperature value toward the beginning of the test was set at 50 °C, and the final temperature was 900 °C for complete degradation of LC. Thermal analysis was performed according to ASTM E1641-18 (ASTM 2018). This way to perform TGA has been institutionalized by different researchers in their work (Kaewta Kaewtatip 2012; Sudhir Kumar Saw 2013).

3.1.5.3 Fourier Transform Infrared Spectroscopy (FTIR)

The Fourier Transform Infrared Spectroscopy (FTIR) analysis for sodium hydroxide, silane, and acetylated chemical surface treated and untreated LC samples were performed. The scans were recorded using the SHIMADZU IRAffinity-1S model. It was made sure scans were taken consecutively in the range of 500-4000 cm^{-1}. Furthermore, all the scans were recorded at a resolution of 4 cm^{-1}. The IR spectrum information from the investigation was used to plot the FTIR plots under the compliance of ASTM E168-16 and ASTM E1252-98e1 standards (ASTM 2013, 2016). This approach to performing FTIR analysis has been standardized by various other researchers (Arun Kumar Gupta 2012; Mizi Fan 2012).

3.1.6 Preparation of Luffa Fiber/PLA Bio-Composites

Utilizing the GOTECH hot press compression moulding machine, the samples were prepared. LC with 5 %wt, 10 %wt, 15 %wt, and 20 %wt volume was utilized to manufacture bio-composites with PLA to forecast the bio-composites overall mechanical characteristics. Dimensions for the samples were shown in Figure 16. All of the samples were prepared using the parameters shown in Table 15. American Society of Testing and Materials (ASTM) standards had been used (B V Lingesh 2014). For the preparation of flexural, hardness, tensile, and water absorption samples, respectively, the standards ASTM D790-17, D2240-15e1, D638-14, and D570-98(2018) were used (ASTM 2010, 2014a, 2015, 2017; Suhara Panthapulakkal 2006). The preparation procedure seen in Figure 28. However, untreated, and chemically surface treated LC-PLA composites seen in Figure 29 and Figure 30, respectively.

Table 15: Processing parameters used to prepare samples for flexural, tensile and water uptake (%).

Magnitudes	**Flexural**	**Tensile**	**Water uptake (%)**
Processing temperature (°C)	160	165	165
Processing pressure (MPa)	6	6	6
Compression time (min)	30	30	30
Cooling time (h)	3	3	3
Pre heat	Yes	Yes	Yes

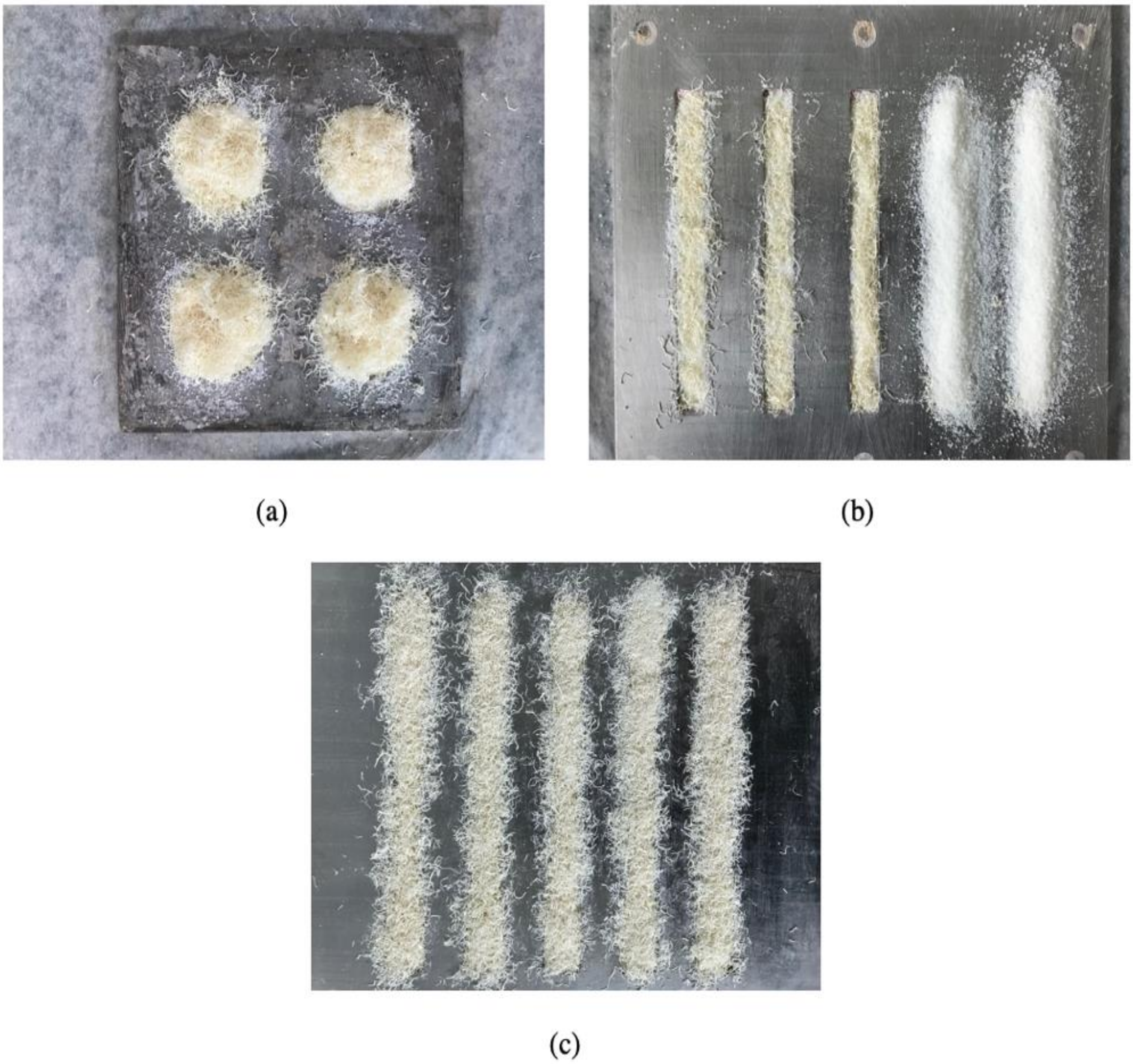

Figure 28: Preparation procedure for (a) water uptake (%) samples, (b) flexural samples and (c) tensile samples.

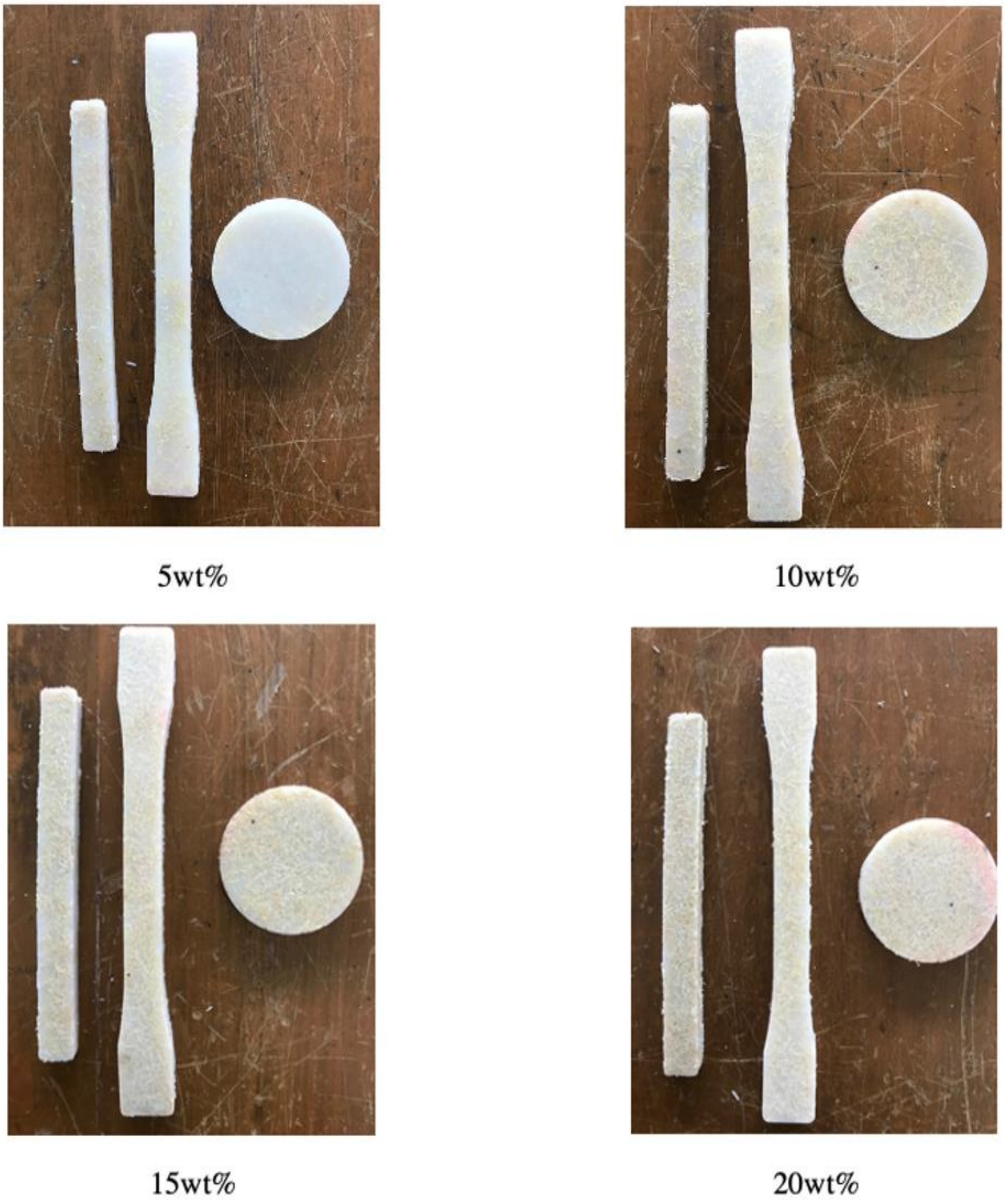

5wt%

10wt%

15wt%

20wt%

Figure 29: Untreated LC-PLA composites with varying fiber volumes (5-20 %wt).

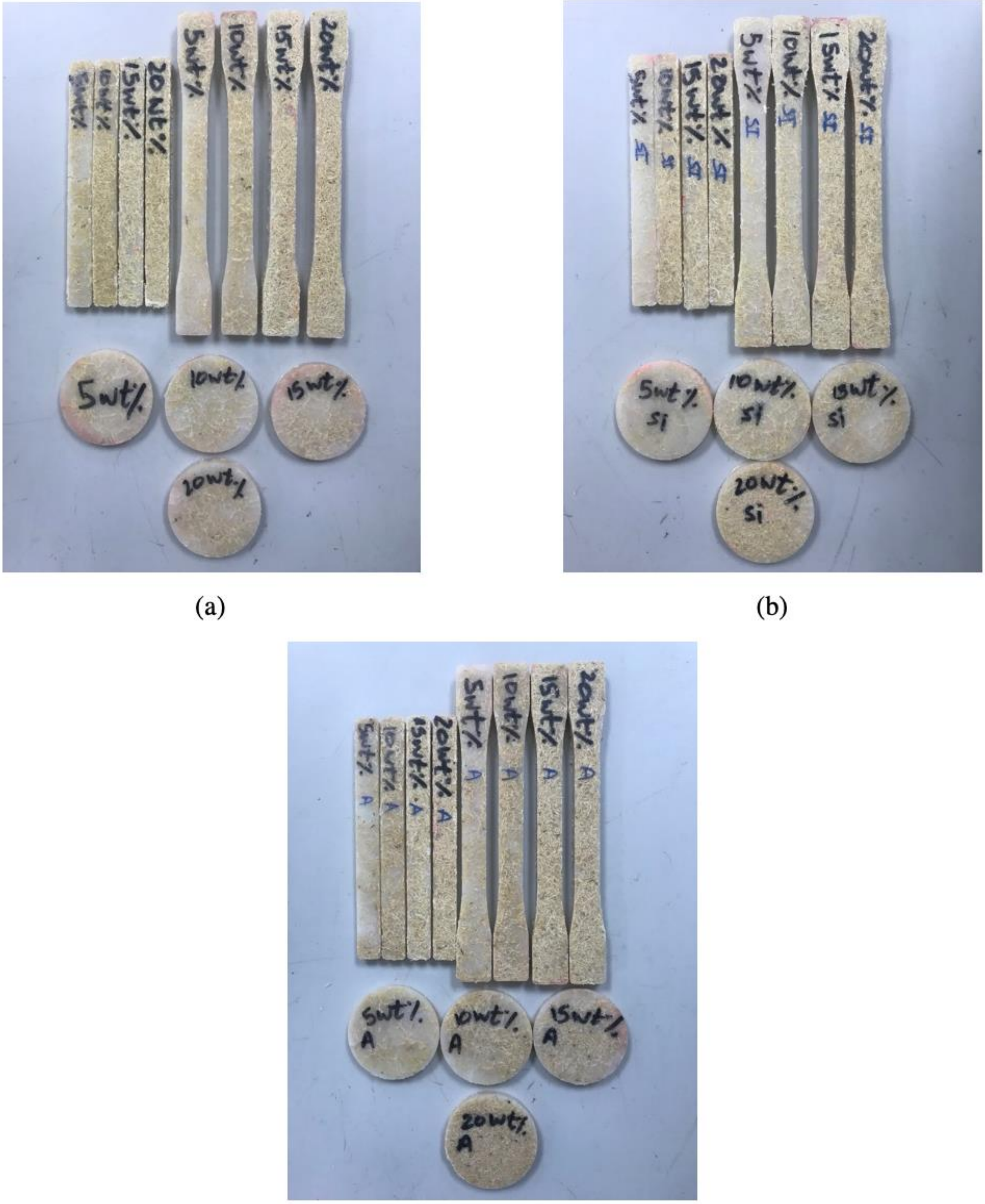

(a) (b)

(c)

Figure 30: Shows (a) Sodium hydroxide treated, (b) Silane Treated and (c) Acetylated LC-PLA composites with varying fiber volumes (5-20 %wt).

3.1.7 Testing and Characterization of LC-PLA Bio-Composites

3.1.7.1 Tensile Testing

The GOTECH Universal Testing Machine (UTM) was utilized to test the tensile strength samples, as shown in Figure 31. The testing was conducted in accordance with the ASTM D638-14 standard (ASTM 2014a). Five samples were tested for each type of fiber percentage configuration for testing purposes, as mentioned previously. Gauge length for the samples was 50mm and testing speed was 3mm/min. The average result for tensile strength was recorded

Figure 31: Tensile testing of LC-PLA composite using GOTECH UTM machine.

3.1.7.2 Flexural Testing

GOTECH Universal Testing Machine was utilized to test the flexural strength of the samples, as shown in Figure 32. The testing was conducted in accordance with ASTM D790-17 standard (ASTM 2017). Support length was 100mm and testing speed was set to 0.1mm/min. For testing, five samples were tested for each type of fiber percentage configuration, as mentioned previously. The average result for flexural strength was recorded.

Figure 32: Flexural testing of LC-PLA composite using GOTECH UTM machine.

3.1.7.3 Hardness Testing

Using the SHORE hardness meter, the hardness test was carried out, as shown in Figure 33. In addition, the SHORE hardness value was converted to the Rockwell hardness C scale in compliance with the ASTM D2240-15e1 standard, as mentioned earlier (ASTM 2015). The average value of nine readings was recorded using the SHORE hardness meter. As stated earlier, the test was conducted for each fiber percentage configuration.

Figure 33: SHORE hardness meter that was used to measure the hardness value of LC-PLA composites.

3.1.8 Characteristics of Luffa Fiber/PLA composites

3.1.8.1 Scanning Electron Microscopy (SEM)

The Scanning Electron Microscopy (SEM) study is one of the most commonly used electron microscopies to conduct a morphological analysis on the bio-composites. Hitachi Analytical table (Tabletop Microscope-3030) equipment was utilized to perform SEM analysis. Moreover, ASTM E2015-04 was utilized (ASTM 2014b). Initially, the specimens were cut and placed on metal plugs. In addition, the samples were partially coated with gold film for 60 seconds. Thickness was found out to be at 10 nm with 0.1 Torr and 18 mA. The accelerating voltage was set to 20KV with a working distance of 20 mm. The magnifications of 100x and 200x were utilized for a detailed study on the surface of the bio-composite. Different researchers in the past with different parameters had employed a similar standard approach to perform SEM analysis (A. Oushabi 2017; Saw 2017).

3.1.8.2 Thermal Analysis

3.1.8.2.1 Thermogravimetry (TGA), Derivative Thermogravimetry (DTG) and Differential Scanning Calorimetry (DSC)

The thermal analysis was performed using Pekin Elmer, simultaneous thermal analyzer, model: STA8000. ASTM E1641-18 standard was utilized (ASTM 2018). The study was performed using samples weighing 14mg. In addition to that, purified nitrogen gas with a gas flow rate of 20mg/ml was used in this study. This was to ensure that the sample only reacts with temperature (Kaewta Kaewtatip 2012; Sudhir Kumar Saw 2013). Temperature increment was set at 20 C/min, and the initial temperature value was set at 50 °C whereas, the final temperature value was set at 700 °C. The results were used to generate thermogravimetry analysis (TGA), derivative thermogravimetry (DTG), and differential scanning calorimetry (DSC) plots. Different researchers in the past had institutionalized this way to perform thermal analysis. Besides that, crystallinity (%) was calculated using the following equation (Takemura 2009).

$$\%\mathrm{X_c}\ (\text{Crystallinity }\%) = \frac{\Delta \mathrm{H_m}}{(\Delta \mathrm{H_m^0})(\mathrm{w})} \times 100 \tag{11}$$

Where; ΔH_m is the enthalpy of melting for the sample, ΔH_m^0 is the enthalpy of melting for 100% pure crystalline PLA (93J/g), in addition, “w" is the mass fraction of PLA in the bio-composite (Saurabh Chaitanya 2019).

3.1.9 Water Absorption Analysis for Luffa Fiber/PLA Composites

The water absorption tests were performed using the above stated ASTM D570-98(2018) standard (ASTM 2010). Samples were dried in the oven at 80 °C for 12 hours to make sure the moisture was removed entirely from the samples. Dry sample weight was recorded, and the samples were submerged in distilled water. Samples were removed after 24 hours of submergence and were instantly weighted to an accuracy of 0.001g. The procedure seen in Figure 34. The samples were submerged in distilled water again, and the second reading was taken after a week using a similar approach, and the third reading was recorded two weeks after the second reading. Similarly, the fourth reading was recorded two weeks after the second reading. However, the difference between the third and fourth reading was less than 5mg; therefore, it was not recorded because the samples were substantially saturated. This type of approach is known in theory as long-term immersion. The uptake percentage (%) for the moisture was analysed using the following equation (H. Demir 2006). For testing, four samples were tested for each type of fiber percentage configuration, as mentioned previously. The average result for water uptake (%) was calculated and recorded.

$$Uptake\ (\%) = \frac{M_t - M_0}{M_0} \times 100 \tag{12}$$

Where; $M_t$is the mass of the sample at a certain time whereas, M_0 is at t = 0

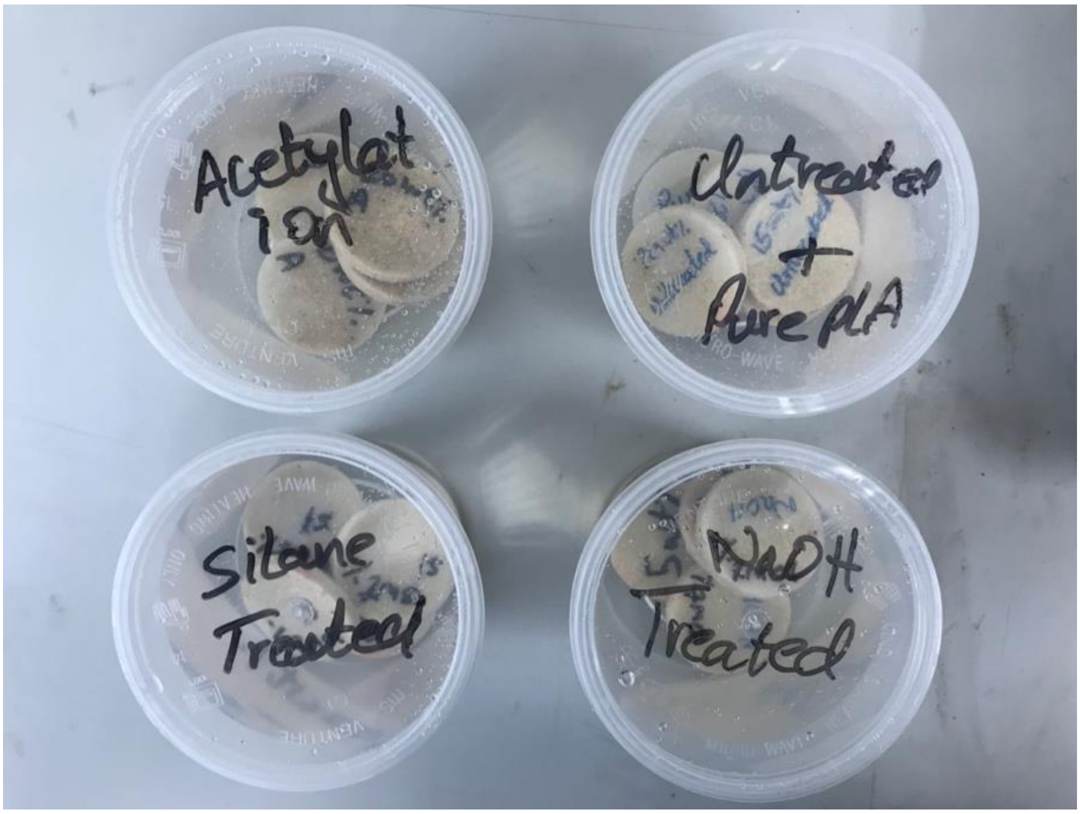

Figure 34: Submergence procedure that was utilized to test water uptake (%).

3.1.10 Methodology Flowchart

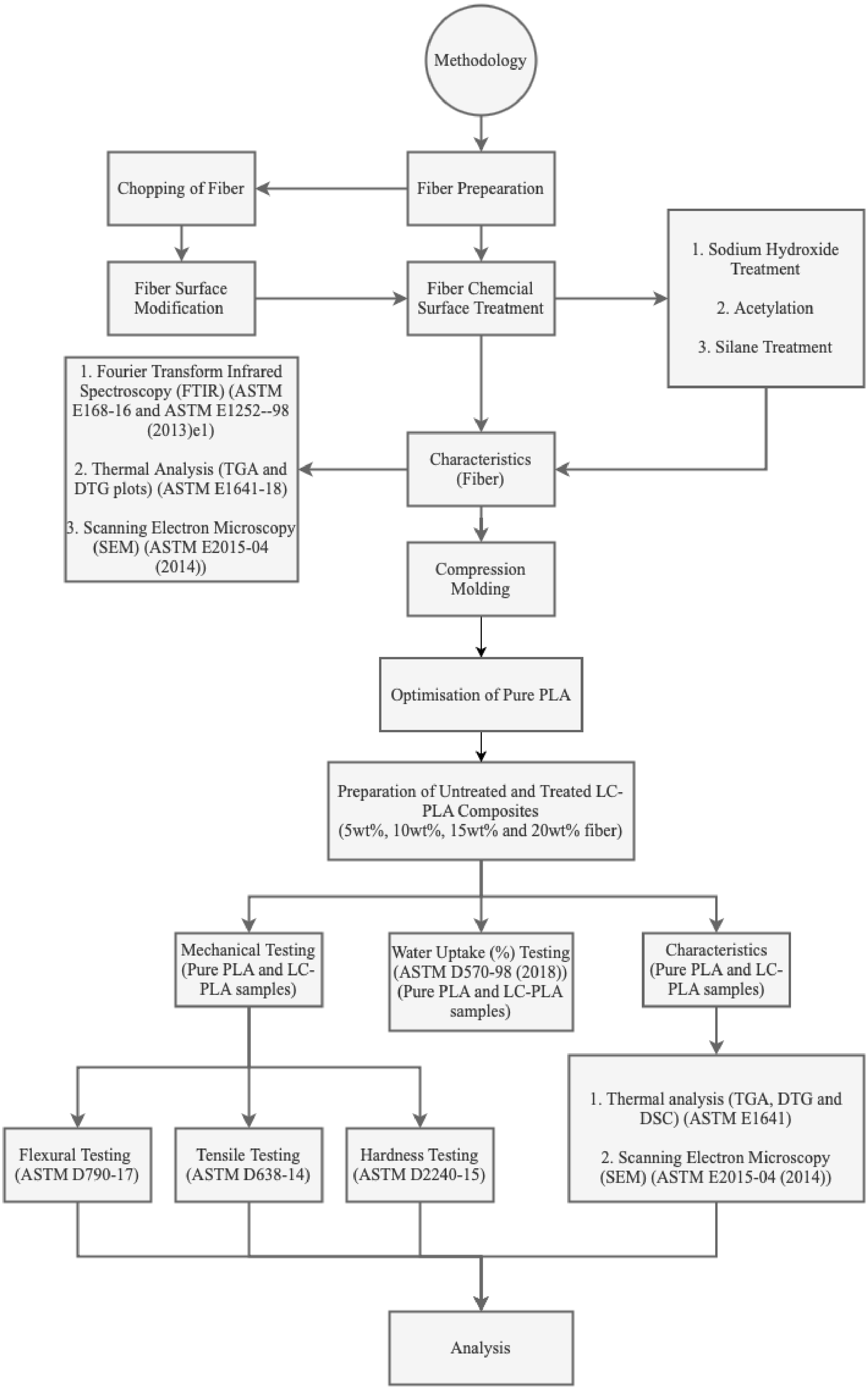

3.2 SUMMARY

This chapter was intended to clarify the methodologies that were adapted. The chapter continues with an explanation of how pure PLA samples were optimized. Utilizing baking paper, optimization of the samples was accomplished. The optimized processing temperature was 160-165 °C, processing pressure was 6 MPa, processing time was 30 minutes, and cooling time was 3 hours. These processing parameters were utilized for the preparation of pure PLA, untreated LC-PLA bio-composites, and chemically surface-treated LC-PLA bio-composites with a fiber volume of 5, 10, 15, and 20 %wt. In addition, the chapter also includes the adapted techniques to modify the surface of LC chemically. The adapted methodologies were explained in accordance with ASTM guidelines for methods related to mechanical characteristics (i.e., tensile, flexural, and hardness testing), morphological analysis (i.e., scanning electron microscopy), infrared spectroscopy (i.e., Fourier transform infrared spectroscopy), water absorption (water uptake %), and thermal analysis (i.e., thermogravimetry analysis, differential scanning calorimetry, and derivative thermogravimetry).

The results obtained are discussed and shown in the upcoming chapter (Chapter 4).

4 CHAPTER 4

4.1 RESULTS AND DISCUSSION

4.1.1 Characteristics of Chemically Surface Treated Luffa Fiber

4.1.1.1 Scanning Electron Microscopy (SEM)

Process of scanning electron microscopy (SEM), as mentioned above, provided images at a magnification of 100x, 500x, and 800x for untreated and chemically surface treated LC samples. Untreated samples of LC shown in Figure 35. A smooth fiber surface was seen due to the waxy impurities present on the surface shown in Figure 35-(a). Furthermore, Figure 35-(b) confirms the presence of voids on the surface, which were shown as black dots. Furthermore, impurities can be seen in white dots. Similar results were also shown in the research by various researchers regarding fiber surface treatments (L. Boopathi 2012; Yuxia Chen 2020). Due to the presence of waxy impurities, impurities, and voids, the adhesion between polymer and the LC was poor, which would lead to poor mechanical properties.

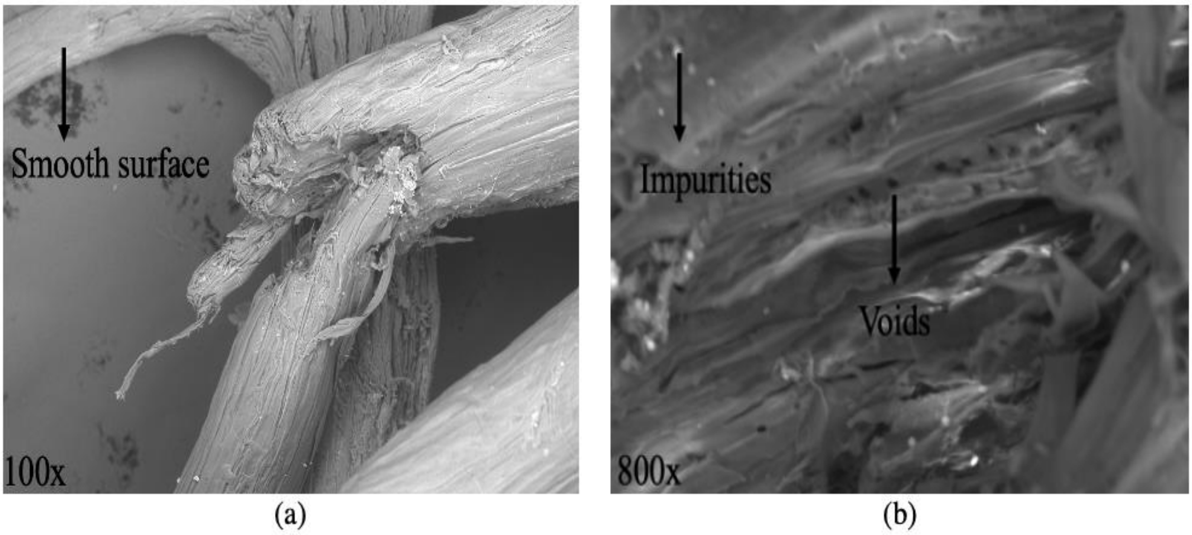

(a) (b)

Figure 35: Untreated luffa fiber samples, (a) 100x magnification and (b) 800x magnification.

Sodium hydroxide surface treated samples shown in Figure 36. Using the methodology explained earlier, 1 N of sodium hydroxide solution was used to surface treat LC chemically. Rougher fiber surface was visible, which was due to the removal of waxy impurities from the surface of LC. Removal of waxy impurities was achieved due to the impurities being soluble in sodium hydroxide solution (A. Oushabi 2017). However, some of the impurities can still be seen on the surface of LC, as shown in Figure 36-(a) and (b)’. This was due to the immersion time being only one hour. Furthermore, there was no sign of voids present on the surface of LC. Removal of waxy impurities and voids from the surface of LC was shown in other research papers as well shown by other various researchers (Lassaad Ghali & Sakli 2011; V. Fiore 2015). Better adhesion between LC and polymers was expected due to the surface being rough and without voids. Due to better adhesion, better mechanical properties were expected from LC and polymer bio-composites.

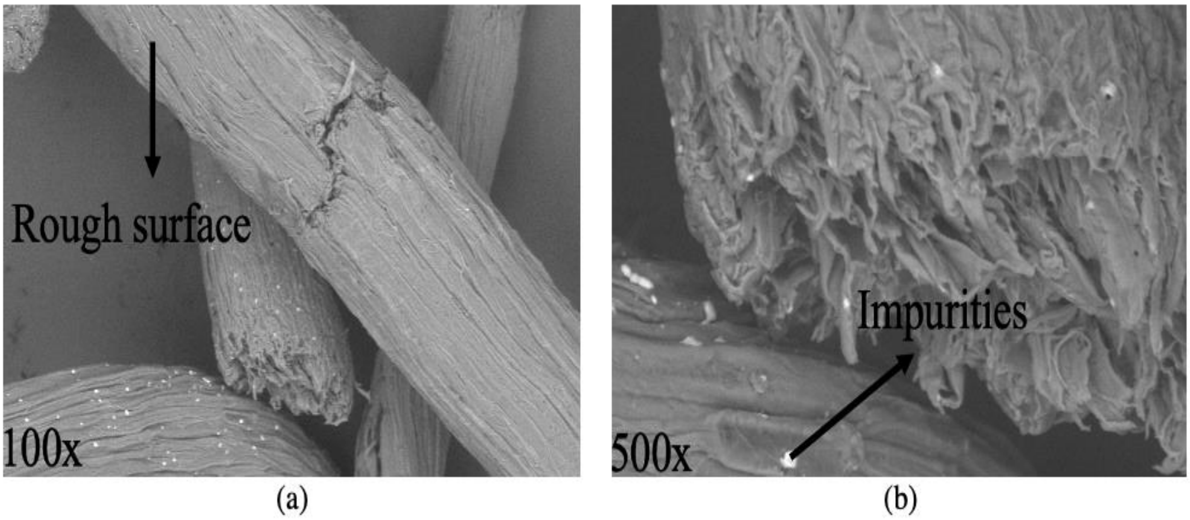

Figure 36: Sodium hydroxide surface-treated luffa fiber samples, (a) 100x magnification and (b) 500x magnification.

Silane surface treated samples shown in Figure 37. Using the methodology explained earlier, 5%wt silane solution with ethanol was used. Bis-(3-triethoxysilylpropyl) and 3-amino propyltriethoxysilane (APS) coupling agents were utilized. Shown in Figure 37-(a) and (b) that there was not much difference on the fiber surface. The surface of LC was still smooth due to silane particles sticking on the fibber's surface (Hamideh Hajiha 2014). However, Figure 37-(b) shows the removal of surface impurities, but some voids on the surface were still present (Feng Zhou 2014). This result was due to immersion time being only one hour. Furthermore, better adhesion was expected between the fiber and polymer due to the removal of waxy impurities and impurities from the LC surface. However, due to the voids present on the surface of the fiber, this may affect the overall adhesion between LC and polymer.

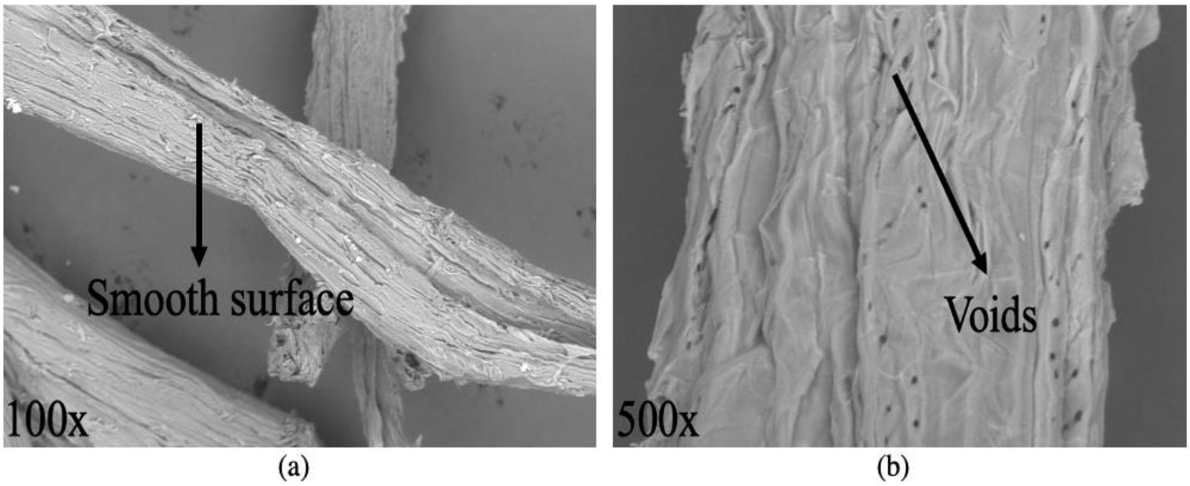

Figure 37: Silane surface-treated luffa fiber samples, (a) 100x magnification and (b) 500x magnification.

Acetylated surface treated samples shown in Figure 38. Using the methodology explained earlier, 1:1 mixing was used between acetic acid and acetic anhydride to surface treat LC samples chemically. As shown in Figure 38-(a) and (b) that the fiber surface was still smooth after the surface treatment. This was due to the acetyl functional groups replacing hydroxyl functional groups from the surface of LC (Hamideh Hajiha 2014). Furthermore, impurities from the surface were removed to some extent. However, Figure 38-(b) shows voids present on luffa fiber samples' surface. This result was expected due to immersion time being only one hour. Better adhesion was expected between the fiber surface and polymer due to the removal of waxy impurities and impurities to some extent. However, the presence of voids may not give the best mechanical properties.

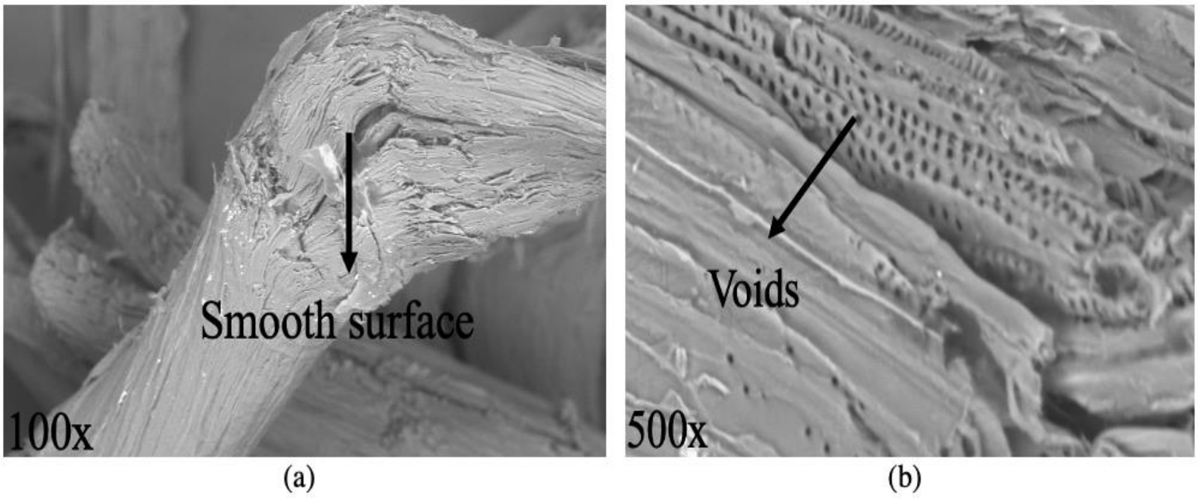

Figure 38: Acetylated surface-treated luffa fiber samples, (a) 100x magnification and (b) 500x magnification.

4.1.1.2 Thermal Analysis

4.1.1.2.1 Thermogravimetry (TGA) and Derivative Thermogravimetry (DTG)

Figure 39 shows the chart that was plotted using the data received from TGA. The decomposition process for tested specimens were seen following a similar trend shown by other researchers in their studies on thermal analysis (Sudhir Kumar Saw 2013). Chemical bonds consisting of cellulose, hemicellulose, and lignin were thermally degraded at different temperature values. This degradation resulted in mass loss percentage.

For untreated LC samples, a significant mass loss of 7% was seen in the 50-100 °C temperature range due to the removal of moisture. However, surface treated samples did not show any mass loss in this temperature range; therefore, moisture was removed with the help of chemical surface treatments. Temperature range between 200-260 °C is the decomposition temperature range for hemicellulose. Change in mass was visible for untreated samples, whereas no change was seen for chemically surface treated samples. This analysis predicts the removal of hemicellulose using all three chemical surface treatments. The temperature range of 300-400 °C is the decomposition temperature range for cellulose. All the samples during this temperature range showed single-stage decomposition. Weight loss of almost 70-75% was seen for untreated, silane treated, and acetylated samples, whereas sodium hydroxide surface treated samples showed mass loss of 60%. Cellulose is alkaline soluble; therefore, some percentage of cellulose could had been removed due to sodium hydroxide surface treatment, eventually leading to lesser mass loss. The temperature range of 250-550 °C is the decomposition range for lignin. With the TGA plot's help, lignin was removed due to fiber surface treatments because no significant mass loss was seen before 300 °C. In another research, a similar trend was evident (Kaewta Kaewtatip 2012; S. N. Pandey 1993; Valcineide O.A. Tanobe 2005). The temperature range at 500 °C and above was where carbonization occurs, thereby causing loss of material.

With the help of surface treatments, better thermal resistance was seen in the range of 50-300 °C. However, between the range of 300-400 °C, similar thermal resistance was seen for untreated, and sodium hydroxide treated samples. In this present research, silane surface treated samples predicted the highest amount of thermal resistance, and acetylated samples predicted the least amount of thermal resistance.

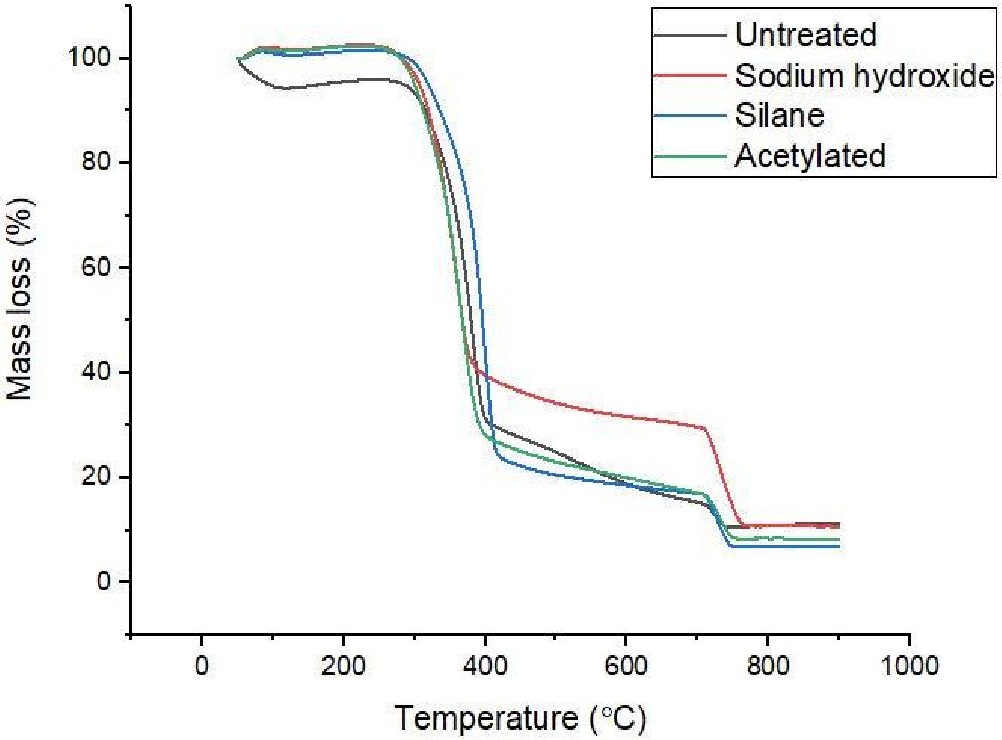

Figure 39: TGA plot for treated and untreated LC.

DTG plot shown in Figure 40. This particular method of plotting the results helps in better understanding regarding thermal degradation. Untreated samples similar to TGA showed an initial endothermic peak due to moisture removal in the range of 50-100 °C. A smaller peak followed by a dominant peak in the range of 270-400 °C showed an endothermic process. A smaller peak between 270-300 °C showed lesser mass loss compared to a dominant peak at 300-400 °C. Explanation regarding this extreme mass loss was due to active devolatilization of cellulose which is predominantly present in luffa fiber. Sodium hydroxide showed the highest amount of minimum value at 400 °C, silane treated samples showed a minimum at 350 °C, acetylated samples showed a minimum at 370 °C, and untreated samples showed a minimum at 390 °C. Endothermic peaks seen in the range of 700-800 °C were due to the carbonization of the samples. Similar research on different natural fibers and chemical surface treatments showed a similar trend (Kaewta Kaewtatip 2012; S. N. Pandey 1993; Sudhir Kumar Saw 2013).

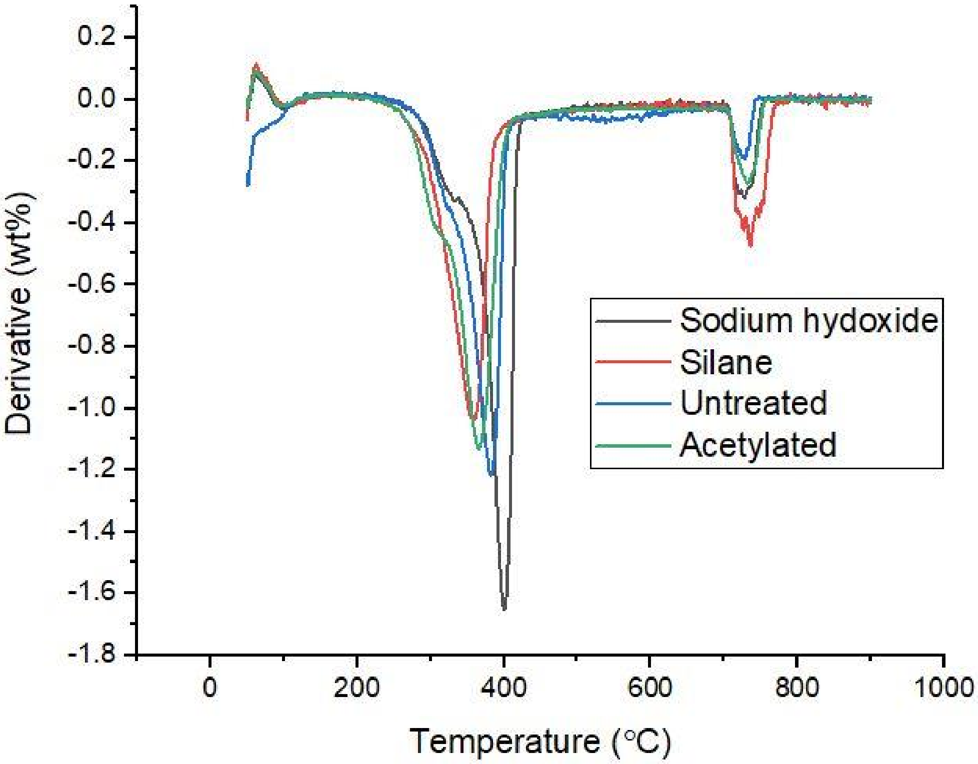

Figure 40: DTG plot for treated and untreated LC.

4.1.1.3 Fourier Transform Infrared Spectroscopy (FTIR)

Fiber surface modification was a significant step so as to get the best properties out of the bio-composite. As it has been explained, sodium hydroxide, silane, and acetylation chemical surface treatments were used in this research. Each one of these chemical surface treatments affects the fiber in a different way. As shown in Figure 41-(a), sodium hydroxide surface treatment is a procedure depicted as ionization of alcoholic bodies with hydroxyl groups. Furthermore, it removes waxy and oily impurities and lignin, prompting better mechanical properties (Mukesh 2019; Parsania 2018).

Silane surface treatment, as shown in Figure 41- (b and c), is a procedure where silanol is produced in the initial step, and then the fibers were treated. Silane, which also functions as a coupling agent, reacts with hydroxyl groups that were present in the fiber and generates covalent bonds (Mukesh 2019; Parsania 2018). Silane surface treatment then again reduces fiber cramping as the fiber is attached utilizing covalent bonds. As shown in Figure 41-(d), acetylation surface treatment is a reaction of organic compounds with acetyl ions. Fiber samples were plasticized utilizing a technique known as esterification (Mukesh 2019; Parsania

2018). Acetic acid reacts with the hydroxyl groups present inside cellulose, leading to better adhesion and mechanical properties.

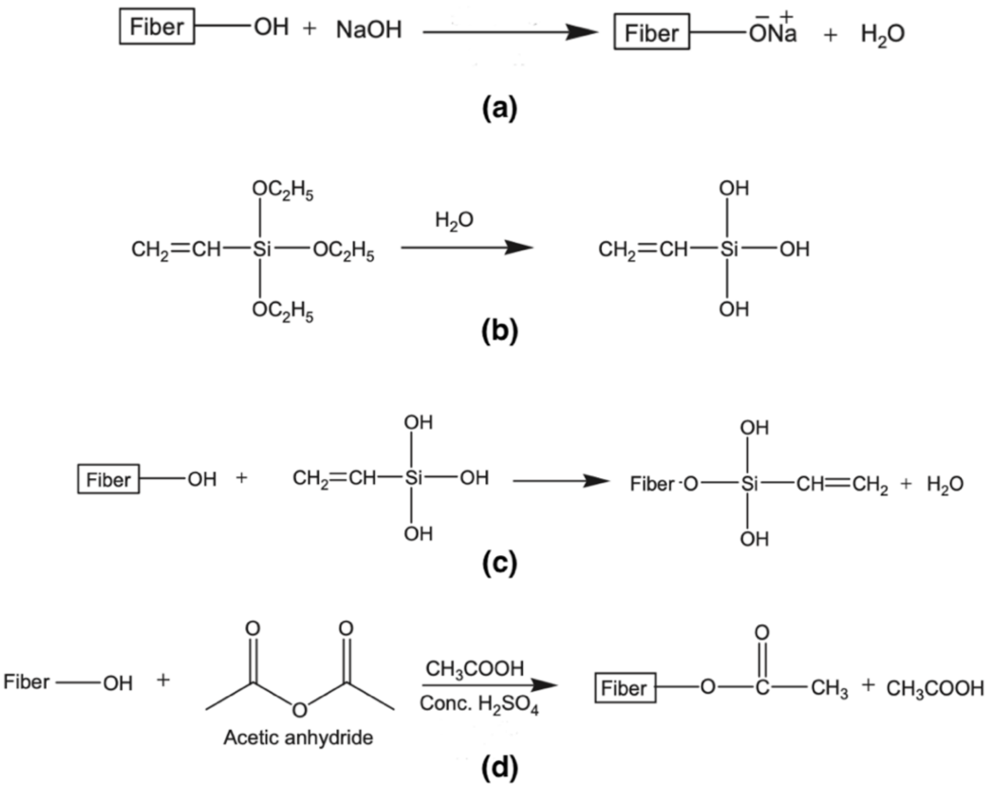

Figure 41: Chemical reactions, (a) sodium hydroxide surface treatment, (b and c) silane surface treatment, and (d) acetylation surface treatment (L. Boopathi 2012).

The plot shown in Figure 42 represents the FTIR plot for untreated LC samples. The FTIR plot presence of the – OH group was confirmed by peaks shown in the range of 3200 – 3800 cm^{-1}. The presence of peaks for – OH groups was also a characteristic of natural fibers, which is hydrophilic in nature. Moreover, a sharp peak in the range of 2300 – 2400 cm^{-1} represents the presence of lignin, cellulose, and hemicellulose. The peak shown at 2870 cm^{-1} represents the stretching of C – H bonds. The peak at 1730 cm^{-1} represents carbonyl (C = O) stretching, which was an expected peak for natural fibers due to hemicellulose and cellulose presence. Furthermore, peaks present in the range of 1600 – 1850 cm^{-1} represent the presence of waxy impurities (D. Mohana Krishnudu 2020; Mizi Fan 2012).

The FTIR plot shown in Figure 43 denotes the plot for sodium hydroxide surface-treated LC samples. It was evident that bending of CH_2 and O – H bonds were present in the 1000 – 1500 cm^{-1} range. C = O bonds' vibration was present inside cellulose was seen in the 1500 – 1700 cm^{-1} range. Peaks present in the range of 1700 – 2000 cm^{-1} were insignificant, which proves the fact that impurities such as waxy impurities were removed from the surface of LC utilizing sodium hydroxide surface treatment. In addition to that, little peaks were present in the range of 2300 – 2400 cm^{-1} predicted that hemicellulose and lignin were removed (Arun Kumar Gupta 2012; D. Mohana Krishnudu 2020; L. Boopathi 2012).

The FTIR plot shown in Figure 44 denotes the plot for silane surface-treated LC samples. The focus was to look for peaks representing Si – O – Si linkages and Si – O – Cellulose bonds. Peaks in the range of 700 – 800 cm^{-1} confirm the presence of Si – O – Cellulose bonds as well as confirm the stretching of Si – O – Si linkages. Moreover, stretching of Si – O – Cellulose bonds should represent stretching in the range of 1200 – 1250 cm^{-1}; however, no significant peaks were present in this range. Furthermore, siloxane peaks were also spotted in the range of 2100 – 2200 cm^{-1} range (Hamideh Hajiha 2014; Kumar 2010).

Figure 45 denotes the FTIR plot for acetylated LC samples. The plot shows that peaks in the range of 1500-1700 cm^{-1} represent C – H bending, which occurred due to the esterification process. Bonding of C = O within acetyl functional groups was evident in the peaks ranging from 1700 – 1800 cm^{-1}. Peaks were evident in the range of 2300 – 2400 cm^{-1}; therefore, ester linkages predicted between hydroxyl groups and acetyl ions. Furthermore, small peaks were evident in the range of 3200 – 3800 cm^{-1}; therefore, – OH groups were removed (D. Mohana Krishnudu 2020; Hamideh Hajiha 2014).

Furthermore, it was evident from the analysis of FTIR plots that the majority of – OH groups were eliminated using acetylation chemical surface treatment, and the least amount of – OH groups were eliminated using sodium hydroxide chemical surface treatment. Therefore, for acetylation chemical surface treatment, the least amount of water uptake (%) was predicted. Looking at the results for water uptake (%) shown in Figure 56 least amount of water uptake (%) was recorded for acetylation surface-treated LC-PLA bio-composites, and the highest amount of water uptake (%) was recorded for sodium hydroxide surface-treated LC-PLA bio-composites. However, most CH_2 and C = O bending was evident for sodium hydroxide surface treated samples followed by silane and acetylation surface treated samples. Therefore, the highest mechanical properties were expected for sodium hydroxide surface-treated LC-PLA bio-composite, followed by silane and the acetylation surface-treated LC-PLA bio-composites. Referring to Figure 46 and Figure 47, the highest amount of tensile and flexural strength was recorded for sodium hydroxide surface-treated LC-PLA bio-composites followed by silane and then acetylated surface-treated LC-PLA bio-composites.

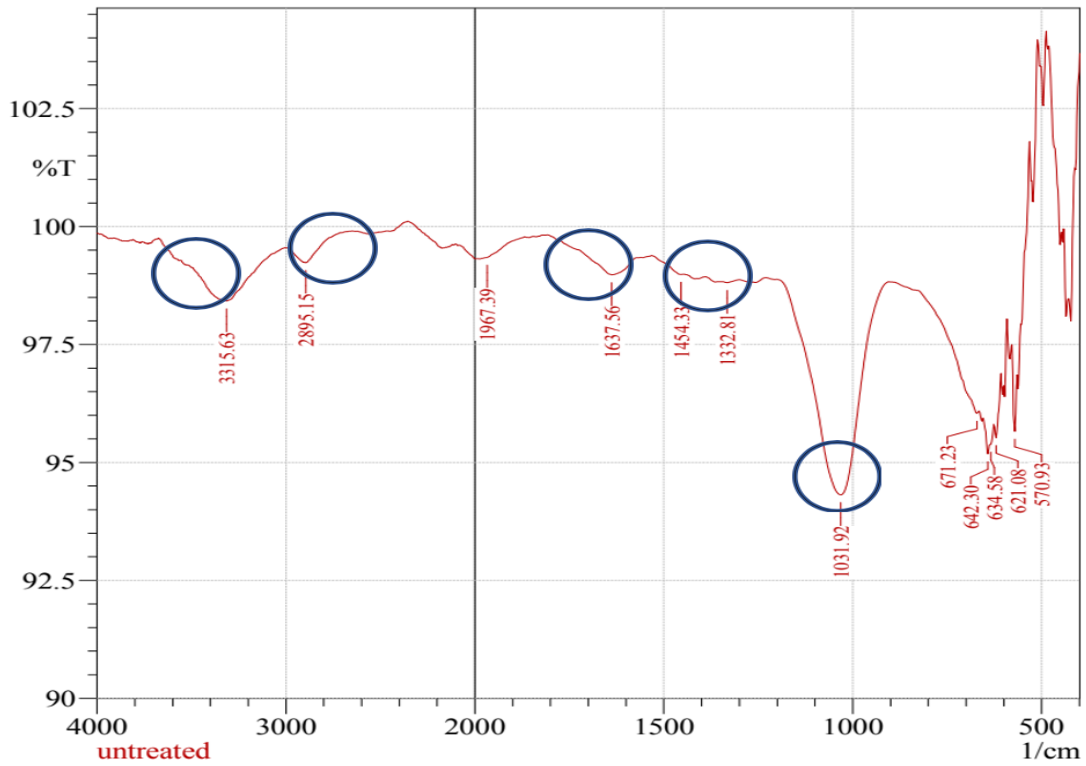

Figure 42: FTIR plot for untreated LC samples.

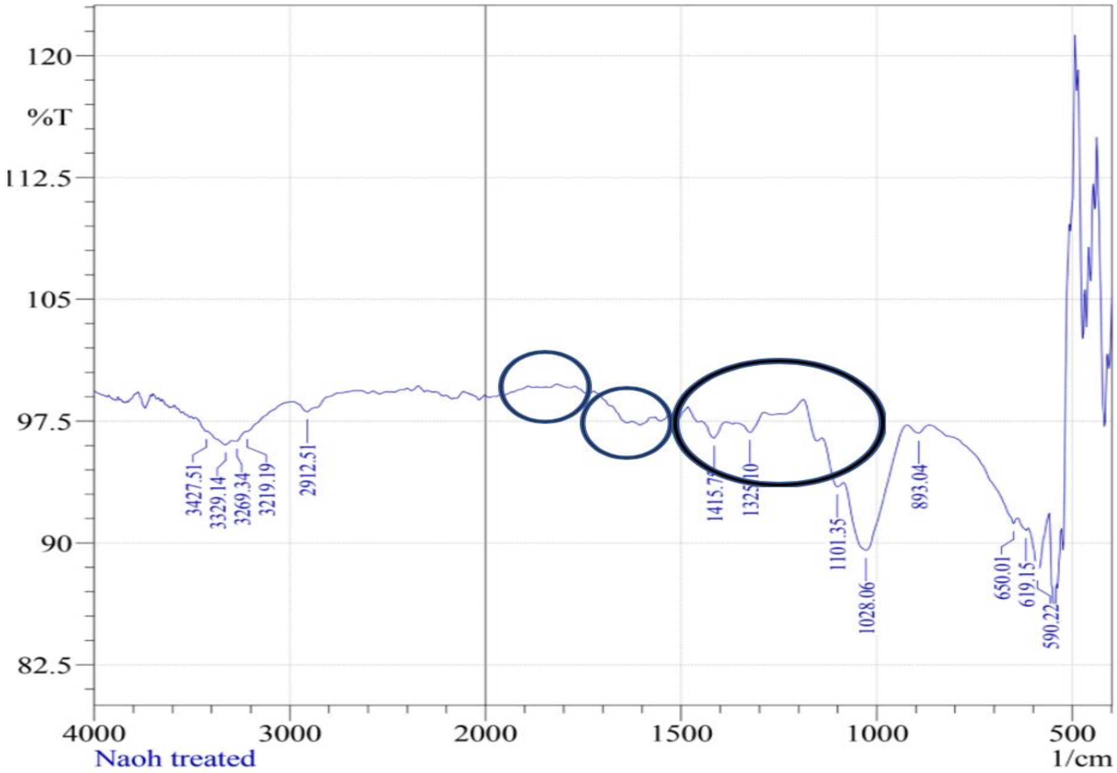

Figure 43: FTIR plot for sodium hydroxide surface-treated LC samples.

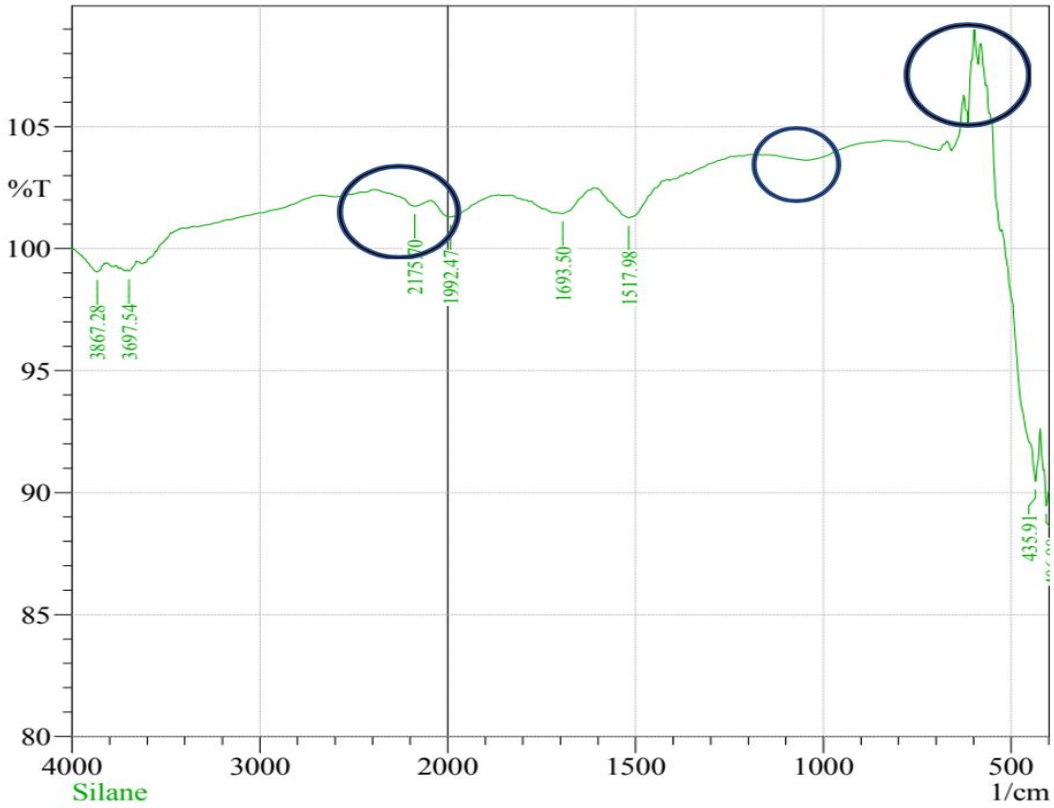

Figure 44: FTIR plot for silane surface-treated LC samples.

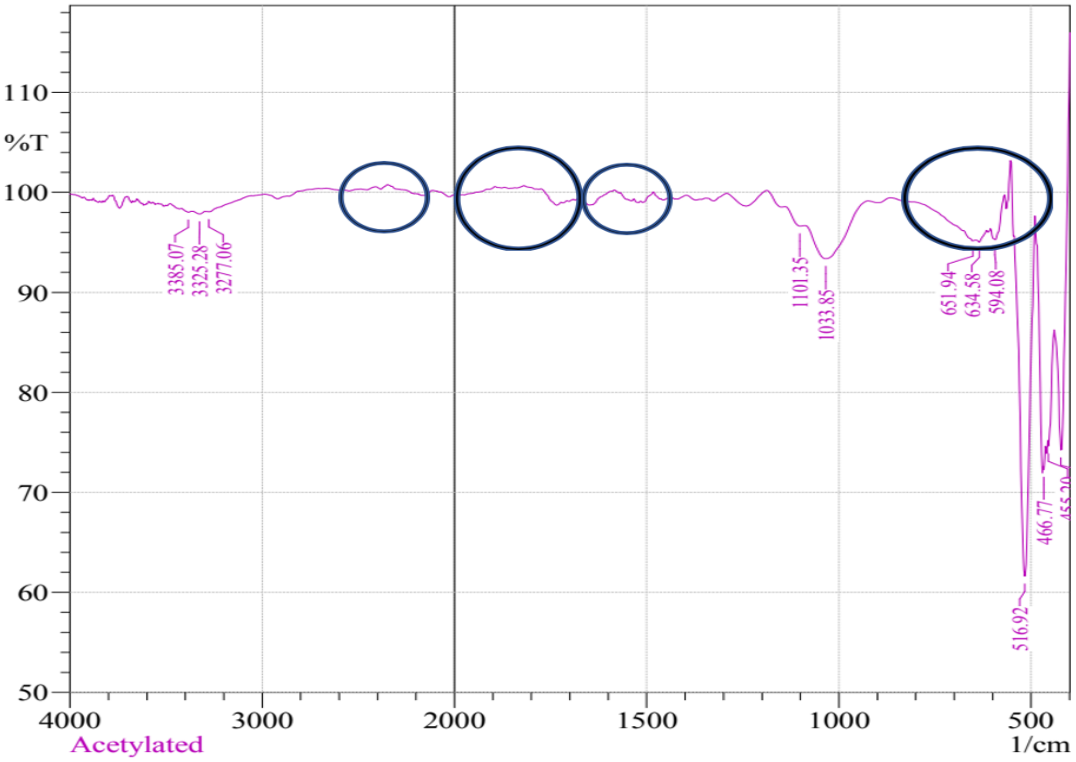

Figure 45: FTIR plot for acetylation surface-treated LC samples.

4.1.2 Optimization for tensile, flexural, hardness and water uptake (%) for bio-composite samples

As explained in previous sections, the optimization of the bio-composite was achieved for flexural, tensile, hardness, and water uptake (%) samples. ASTM (D790-17, D2240-15e1, D638-14, and D570-98(2018)) standard molds were utilized to optimize the samples (ASTM 2010, 2014a, 2015, 2017). Several magnitudes, such as the processing temperature at which the hot press compression moulding machine was set, melted the PLA, and manufactured the composites. Compression time was the time at which the PLA was heated at the processing temperature. The cooling time was the time taken for PLA to reach room temperature from processing temperature. Furthermore, compression pressure was applied to the mould to make sure it was closed and sealed properly. Optimized magnitudes shown in Table 16. Issues in samples such as uneven melting, bubbles, cracking, and voids due to overflow were faced, and each of these issues were solved, and therefore, optimized samples were achieved.

Table 16: Optimized magnitudes for flexural, tensile, and water uptake (%) samples.

Magnitudes	**Flexural**	**Tensile**	**Water Uptake (%)**
Processing temperature (°C)	160	165	165
Processing pressure (MPa)	6	6	6
Compression time (min)	30	30	25
Cooling time (h)	3	3	3
Pre heat	Yes	Yes	Yes

All of the issues, such as uneven melting and cracks in the sample, were eliminated by adjusting magnitudes like temperature and pressure. However, issues like bubbles and voids in the samples were still present. With the help of baking paper, these issues were solved. The utilization of baking paper between the plates slowed down the cooling time. Without baking paper, the top and bottom plates had to be cooled down because the PLA was sticking to the plates.

As shown, a high amount of processing temperature was not utilized in this research. The optimized temperature of 160-165 °C was 5-10 °C higher than PLA's melting temperature. A higher temperature than this range would cause the PLA to vaporize, leaving the presence of bubbles and voids. Furthermore, temperature values higher than 165 °C caused samples to crack while extracting them from the mould. Therefore, higher temperature values were not used. If 155 °C, which was the melting temperature of this specific PLA, was used, uneven melting was evident for the samples.

Hot-press compression moulding is not a commonly used technique to produce samples for PLA. More commonly utilized methods are injection moulding and extrusion. Therefore, optimization on PLA holds immense importance when using hot press compression moulding (Garkhail 1999).

4.1.3 Mechanical Properties of Pure PLA samples

Flexural and tensile samples were placed in an airtight container for two weeks before any testing. Samples were tested for tensile and flexural strength using GOTECH universal testing machine (UTM), as shown in the Figure 31 and Figure 32 earlier. The hardness was tested using the SHORE hardness meter shown in the Figure 33, and the value was converted to the Rockwell hardness C scale. The tensile strength, flexural strength, and Rockwell hardness shown in Table 17.

Table 17: Mechanical properties of pure PLA samples.

Mechanical properties	**Pure PLA**
Tensile strength	2.2 MPa
Flexural strength	7.6 MPa
Rockwell hardness C scale	59

PLA is a brittle material with low impact strength and elongation at break. However, these properties were improved with the help of synthetic fibers or natural fibers and even with fillers reinforcements, as it had been shown by several researchers (Jae-Kyoo Lim 2007; K. Oksman 2003b; Marius Murariu 2016; Tueen 2019; Yicheng Du 2014b). Furthermore, these specific properties were relevant for this specific blend of PLA prepared using above mentioned specific optimization parameters.

4.1.4 Mechanical Properties of Luffa Fiber/PLA Composites

The effect on mechanical properties due to the loading of LC in PLA is shown in Figure 46 and Figure 47. The bio-composites' mechanical properties are shown for a variable percentage of fiber loading ranging from 5-20 %wt. With the help of pure PLA mechanical testing, the sample revealed a tensile strength of 2.2 MPa, a flexural strength of 7.6 MPa, and a Rockwell hardness (C scale) of 59. The tensile strength and flexural strength almost doubled with the incorporation of 15 %wt untreated LC in the sample. At the same time, the Rockwell hardness showed an increase of 5%. The strengthening effect of LC, where the stress was transmitted from PLA to LC, suggested an increase in strength. However, the tensile strength of LC-PLA bio-composite drops drastically because of encapsulation when the fiber loading reaches 20 %wt. Encapsulation occurs when there is not enough polymer to enclose the fiber therefore, initiating the decline in the mechanical properties. The interface between the polymer and fiber was to be enhanced for better mechanical properties. Better stress transfer from polymer to fiber can, therefore, be shown (Arun Kumar Gupta 2012). One way to achieve this was through the removal of waxy impurities, voids, lignin, and hydroxyl groups from the surface of the fiber using chemical surface treatments.

In order to make sure that a natural fiber polymer composite is suitable for desired applications, it is essential to determine mechanical properties like flexural strength, tensile strength, and hardness of the composite (Jianhu Shen 2013; M.R. Sanjay 2018).

4.1.4.1 Effect of sodium hydroxide surface treatment on Tensile and Flexural Properties

The best overall mechanical properties were demonstrated for sodium hydroxide surface-treated LC-PLA samples. The tensile and flexural strength was increased by 7.1 and 6.9 %, respectively, at 15 %wt fiber volume compared to untreated LC-PLA samples shown in Figure 46 and Figure 47. This was because of LC's mercerization, which strengthens the mechanical interlocking between LC and PLA (Arun Kumar Gupta 2012; K. Anbukarasi 2015). Mercerization is a process used for decades in the textile industry. Natural fibers, such as cotton fiber, are treated using sodium hydroxide chemical surface treatment. With the help of chemical surface treatment, better strength was promoted and minimizes shrinkage. Typically, this was accomplished when cellulose molecules were rearranged in the fiber. Moreover, waxy impurities, voids, and hydroxyl groups were omitted from the surface due to sodium hydroxide surface treatment. This improves the overall surface topography of LC and thus, improves the adhesion between LC and PLA.

4.1.4.2 Effect of silane surface treatment on Tensile and Flexural Properties

The second-best overall mechanical properties were demonstrated by utilizing silane surface treatment. In comparison with untreated LC-PLA samples, an improvement of 5.7 and 1.4 % was demonstrated for tensile and flexural strength, respectively, at 15 %wt fiber volume shown in Figure 46 and Figure 47. With the increased strength, it was evident that silane interacts with carbonyl groups present in the LC, thus improving the interfacial interaction between LC and PLA (A. Orue 2016; Arun Kumar Gupta 2012). Furthermore, it is also known that silane chemical surface treatment enhances the fibber's nucleation potential, molecules in the fibers molecular structure were arranged in a pattern that improves nucleation, which leads to the better formation of crystals on the surface of the fiber, which leads to improved interfacial adhesion between the fiber and polymer (Arun Kumar Gupta 2012).

4.1.4.3 Effect of acetylation surface treatment on Tensile and Flexural Properties

The third highest mechanical properties out of the four samples were evident for acetylation surface treated samples. In comparison to untreated LC-PLA samples at fiber volume of 15 %wt, tensile and flexural strength were increased by 4.3 and 0.4 %, respectively shown in Figure 46 and Figure 47. The increase in flexural strength was negligible. However, the enhancement in tensile strength was due to the removal of hemicellulose from LC's chemical structure, which provides improved bonding between LC and PLA (Arun Kumar Gupta 2012; Hamideh Hajiha 2014). Further, by eliminating waxy impurities and voids, acetylation surface treatment enhances LC's surface topology, which improves the adhesion between LC and PLA.

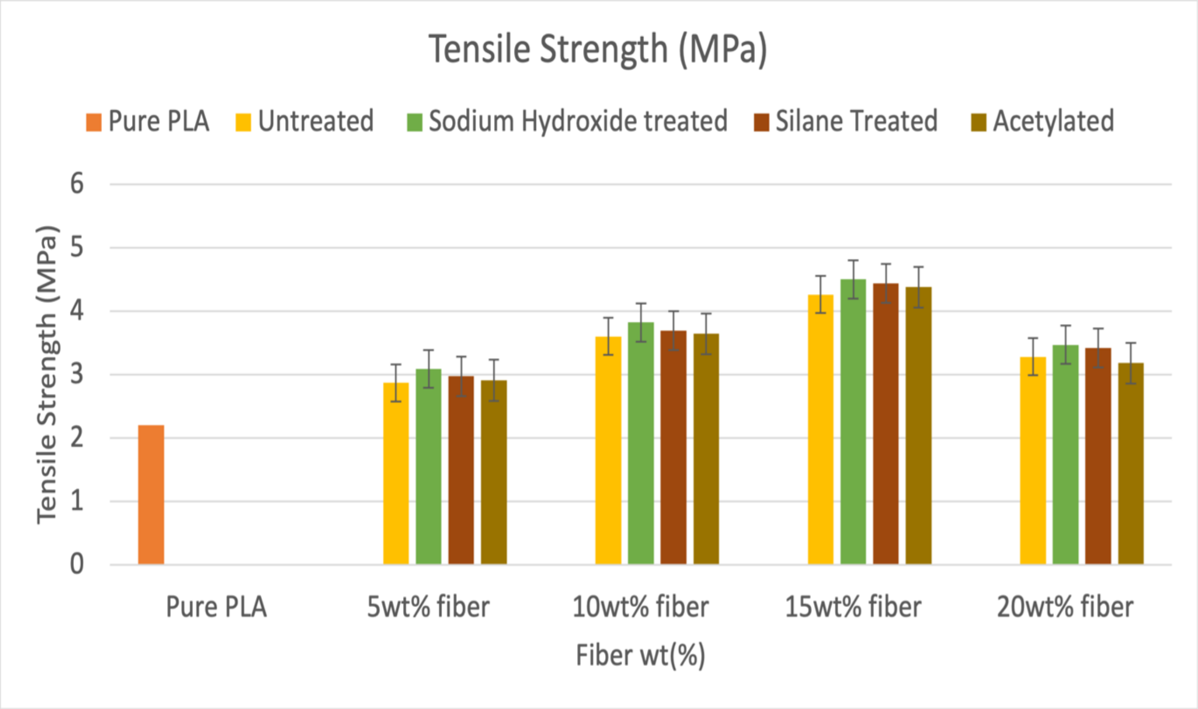

Figure 46: Plot for tensile strength for untreated and surface treated LC-PLA bio-composites.

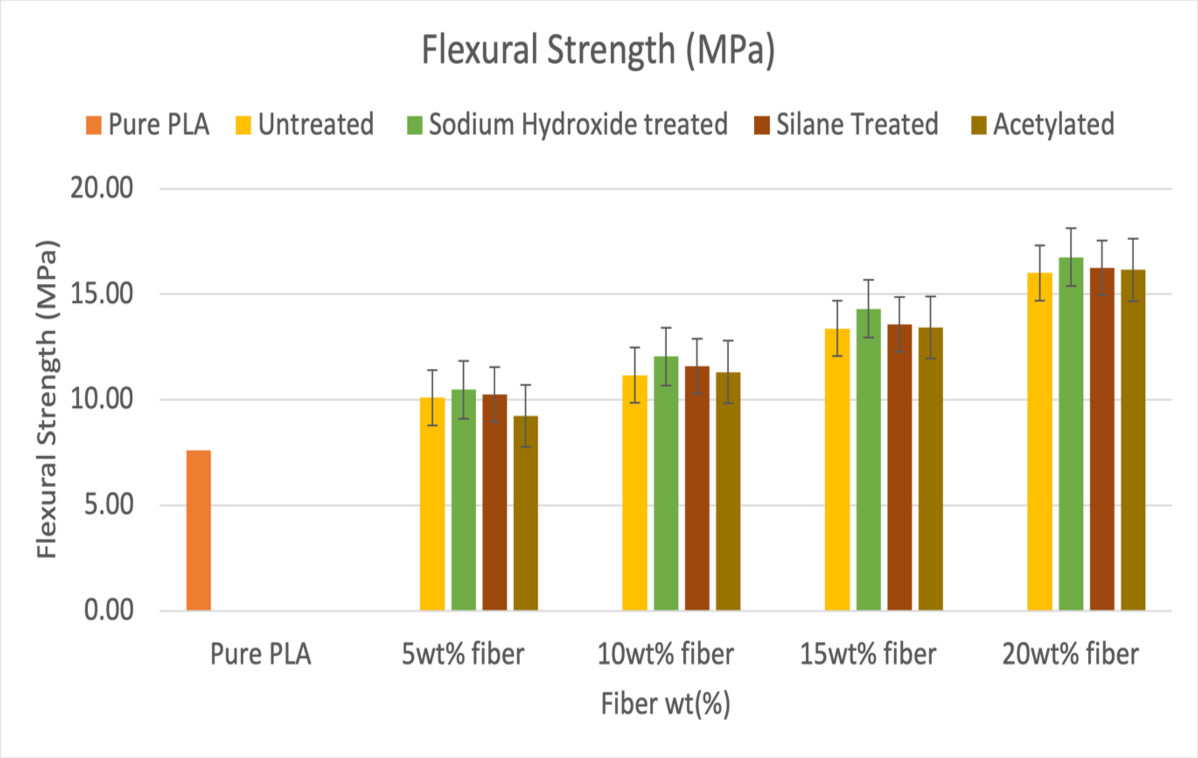

Figure 47: Plot for flexural strength for untreated and surface treated LC-PLA bio-composites.

4.1.4.4 Hardness Properties

Hardness results were for untreated and chemically surfaced treated LC-PLA bio-composite were documented and plotted as shown in Figure 48. Testing of the samples was done in accordance with ASTM D 2240-15e1 (ASTM 2015). SHORE hardness testing was meter was utilized. Unfortunately, all of the samples were tested manually, which contributed to discrepancies due to the stand's non-availability to carry the SHORE meter. In addition, nine points were checked, and the average result was recorded and plotted for each sample. The average result was converted Rockwell Hardness C scale. The hardness values for the samples were clearly not following a specific pattern like tensile and flexural plots. Moreover, as already noted, all of the samples were made using hot press compression molding, which can lead to uneven distribution of LC in the bio-composite. The potential to infiltrate only LC and PLA rather than the bio-composite as a whole thus existed. In addition, the penetration depth of the tip was recorded as 2.5mm, which may also lead to disparities. However, the plot reveals that the hardness value was between 58-63 for the LC-PLA bio-composite.

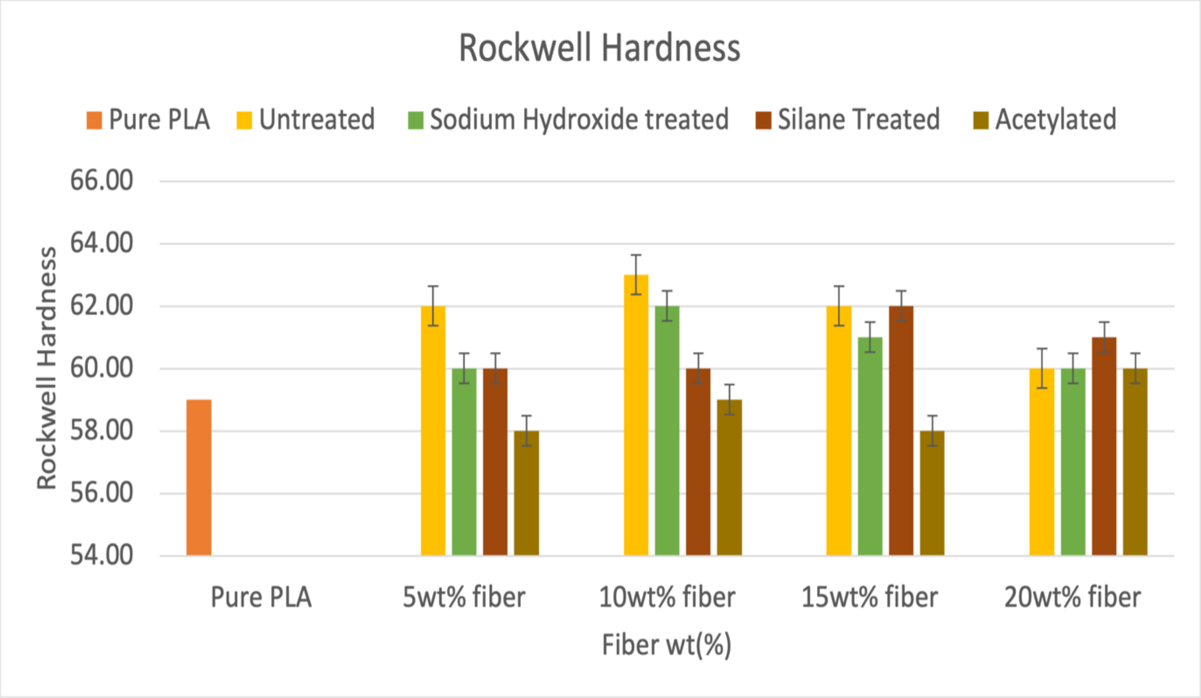

Figure 48: Plot for hardness for untreated and surface treated LC-PLA bio-composites.

4.1.4.5 Comparison between LC-PLA bio-composite (this research) with various other LC and PLA composites and bio-composites

Table 18: Comparison between mechanical characteristics of LC-PLA bio-composites evaluated in this research with various other types of LC composites.

Composite	**Tensile strength (MPa)**	**Flexural strength (MPa)**	**Reference**
	Non-biodegradable Luffa Fiber composite		
Luffa fiber reinforced epoxy composite	192.70, 17.63, 23 and 17.97	39.1, 110 and 106.67	(R.Panneerdhass 2014), (K. Anbukarasi 2015), (Saw 2017), (D.Mohana krishnudu 2018), (Sudhir Kumar Saw 2013) and (Niharika Mohanta 2015)
	Partly biodegradable Luffa Fiber composites		
Luffa Fiber/Polyester composite	16 - 19	40.25 – 52.3	(Vinay Kumar Patel 2016), (Anil Dhanola 2018), (Yuxia Chen 2020), (C. A. Boynard 2003), (Lassaad Ghali 2011), (Lassaad Ghali & Sakli 2011) (Valcineide O.A. Tanobe 2014) and (Yuxia Chen 2020)
Luffa Fiber/Polyester resin/Epoxy composite	64.15	-	(C. Sivakandhan 2018)

Luffa Fiber/Polypropylene composite	33-35	-	(H. Demir 2006), (M. Sakthivel 2014) and (A. K. Mohanty 2002)
	Fully biodegradable Luffa Fiber composites		
Poly(lactic) Acid/Luffa Fiber composite	36.45	48.64	(Chhatrapati Parida 2015a)
Thermoplastic starch/Luffa Fiber composite	1.24	-	(D. Kocak 2015) and (Kaewta Kaewtatip 2012)
Poly-hydroxybutyrate (PHBA)/Luffa Fiber composites	1.7 – 3.6	-	(Andrea Melina Avecilla-Ramirez 2020)
Poly (hydroxybutyrate-co-valerate) (PHBV)/Luffa fiber composites	-	37.31 – 90.73	(Yong Guo 2019)
Poly(lactic) Acid/Luffa Fiber composite **(THIS RESEARCH)**	2.87 – 4.50	9.23 – 16.75	-

LC and epoxy composites are widely produced as shown in the table, thanks to their high tensile and flexural strength. Epoxy, however, is not a biodegradable polymer, so the polymer pollution is enhanced once discarded. In addition, LC composites made using polyester resin and polypropylene are partially biodegradable. This means that once discarded, polymer pollution is lesser than non-biodegradable polymers but not entirely removed. Research on biodegradable polymers is therefore expected. The LC bio-composites made with PLA, PHBV, PHBA, and Thermoplastic starch are entirely biodegradable. Although the composites are entirely biodegradable, tensile strength is lesser when compared with non-biodegradable or partially biodegradable composites. One of this research's main objectives was to improve the interfacial adhesion between LC and PLA, thereby improving the bio-composites mechanical characteristics. It was evident from the methodology adopted in this research that the LC-PLA bio-composites offer better tensile strength than LC-PHBA and LC-Thermoplastic starch bio-composites.

Table 19: Comparison between mechanical characteristics of LC-PLA bio-composites evaluated in this research with various other types of PLA and natural fiber composites.

Composite	**Tensile strength (MPa)**	**Flexural strength (MPa)**	**Reference**
Poly(lactic) Acid + Jute Fiber composite	81.9, 150 - 200, 75, 40.8 and 17.8 - 22.1	175 - 225, 64.6 and 18 - 38.0	(A.K. Bledzki 2010), (Bhanu K. Goriparthi 2012), (Sean A. Hinchcliffe 2016) and (S. Ravi Theja Reddy 2020)
Poly(lactic) Acid + Abaca Fiber composite	74.0	-	(A.K. Bledzki 2010)
Poly(lactic) Acid + Hemp Fiber composite	85.7 and 87.3	87.2	(M.S. Islam 2010), (M.G. Aruan Efendy 2016), (Sean A. Hinchcliffe 2016), (V. Mazzanti 2019) and (K.L. Pickering 2016)
Poly(lactic) Acid + Kenaf Fiber composite	82.0, 58 - 62 and 46.8 - 91.5	93 - 132	(Nina Graupner 2011), (Intan S.M.A. Tawakkal 2014), (Po-Yuan Chen 2017), (Shin Serizawa 2005a) and (Panayiotis

			Georgiopoulos 2018a)
Poly(lactic) Acid + Rice Fiber composite	53.4 - 63.1		(Yang Zhao 2011) and (Longxiang Zhu 2019)
Poly(lactic) Acid + Coconut Fiber composite	72.6 and 30 - 50	-	(Jun Young Jang 2012)
Poly(lactic) Acid + Sisal Fiber composite	36.0 and 52.5 - 59.3	125.0	(Pramendra KumarBajpai 2013), (Sean A. Hinchcliffe 2016), (Parul Sahu 2018) and (M. K. Gupta 2018)
Poly(lactic) Acid + Bamboo Fiber composite	30-52	-	(Wassamon Sujaritjun & Hamada 2013)
Poly(lactic) Acid + Flax Fiber composite	49.7, 8.27 - 30.58, and 44 - 52	70.5	(Thomas Bayerl 2014), (Sean A. Hinchcliffe 2016), (Suneel Motru 2020) and (K. Oksman 2003a)
Poly(lactic) Acid + Harakeke Fiber composite	101.6		(M.G. Aruan Efendy 2016) and (K.L. Pickering 2016)

Poly(lactic) Acid + Luffa Fiber composite	36.45	48.64	(Chhatrapati Parida 2015a)
Poly(lactic) Acid + Pulp Fiber composite	88 - 122	-	(Yicheng Du 2014a)
Poly(lactic) Acid + Luffa Fiber composite **(THIS RESEARCH)**	2.87 - 4.50	9.23 - 16.75	-

PLA had been used as a polymer to produce bio-composites with diverse types of natural fibers, as shown in the table. Jute, Hemp, Kenaf, Flax, and Sisal are some of the most commonly used natural fibers. For all of the bio-composites, the tensile strength and flexural strength vary for each type. The reasons behind these variations are numerous. PLA being a brittle polymer, and its mechanical characteristics range from soft elastic material to high strength materials. As already mentioned earlier, the properties are affected differently due to parameters such as crystallinity, material formation, processing techniques, fiber volume, fiber orientation, fiber length, and fiber chemical surface treatments (Lee Tin Sin 2019). However, in this research, the processing technique was hot press compression moulding, fiber length was five mm, fiber orientation was random, fiber volume was (5, 10, 15 and 20) %wt, density of PLA was 1.24 g/cc, and grade was AI - 1001. Therefore, using these conditions, the tensile strength ranged between 2.87 - 4.50, and flexural strength ranged between 9.23 - 16.75 for chemically surface treated and untreated samples.

4.1.5 Characteristics of Luffa Fiber/PLA composites

Mechanical testing showed that the optimal amount of LC in PLA was 15%wt, and it was found that the PLA matrix was not able to encapsulate LC beyond this loading fully. In addition, with the assistance of water uptake (%), it was found that the absorption of water in the sample was significantly reduced with the help of sodium hydroxide, silane, and acetylation chemical surface treatment, regardless of the amount of LC in PLA. Thus, the following characteristics were analysed using 15%wt LC-PLA samples.

4.1.5.1 Scanning Electron Microscopy (SEM)

As noted, scanning electron microscopy (SEM) supplied images were 100x and 200x for untreated and chemically surface treated LC-PLA bio-composites. The untreated LC-PLA sample was shown in Figure 49. Due to the presence of waxy impurities on the surface of the LC, a smooth surface was seen. Hence, the interfacial adhesion between PLA and LC was weak. However, LC's rougher surface was observed when sodium hydroxide chemical surface treatment was utilized to remove waxy impurities (A. Oushabi 2017). Enhanced surface topography was seen for LC once the waxy impurities were removed. Therefore, the interfacial adhesion was improved between PLA-LC, as shown in Figure 50, whereas better mechanical characteristics were recorded. There was no substantial difference on the surface of LC using silane chemical surface treatment.

The smooth surface of LC was shown in Figure 51 because of the silane particles deposited on LC (Hamideh Hajiha 2014). As previously stated, silane surface treatment increases fibber's nucleation potential, thus improving the interfacial adhesion between PLA and LC (Arun Kumar Gupta 2012). Moreover, improved mechanical characteristics were recorded due to improved interfacial adhesion between PLA and LC. The LC's surface was smooth, similar to silane chemical surface treatment, utilizing acetylation chemical surface treatment. The smooth surface of LC is shown in Figure 52 was due to hydroxyl groups getting replaced with acetyl functional groups (A. Oushabi 2017). In addition to that, surface impurities were removed as well. The elimination of surface impurities improved the surface topography of LC and thus improved the mechanical characteristics by improving the interfacial adhesion between LC and PLA.

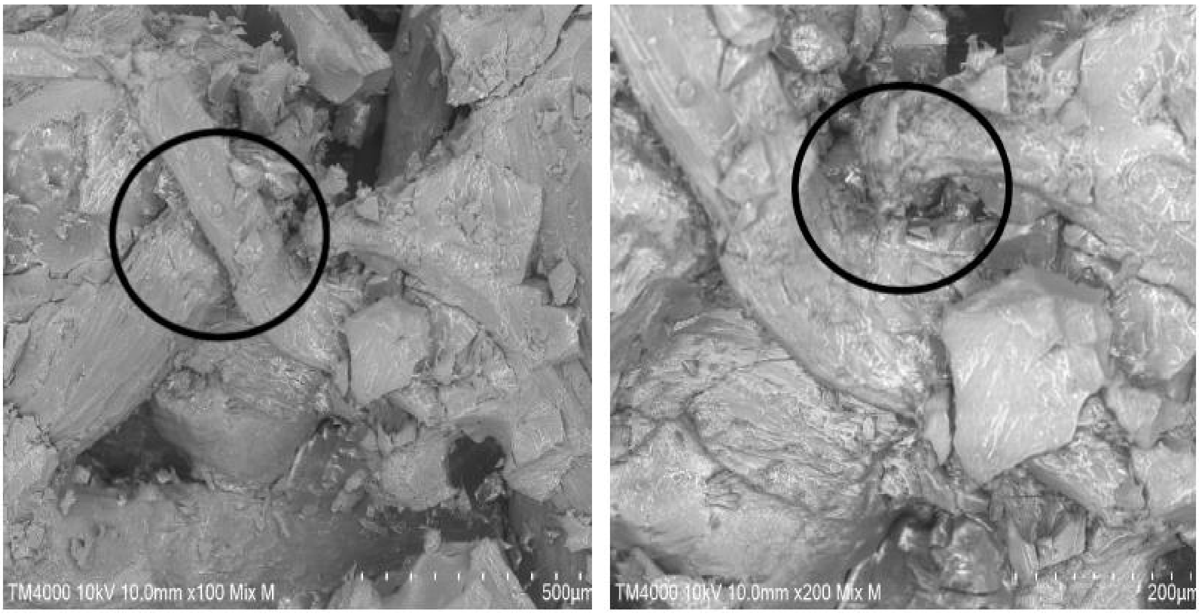

(a) (b)

Figure 49: SEM analysis for untreated LC-PLA bio-composite.

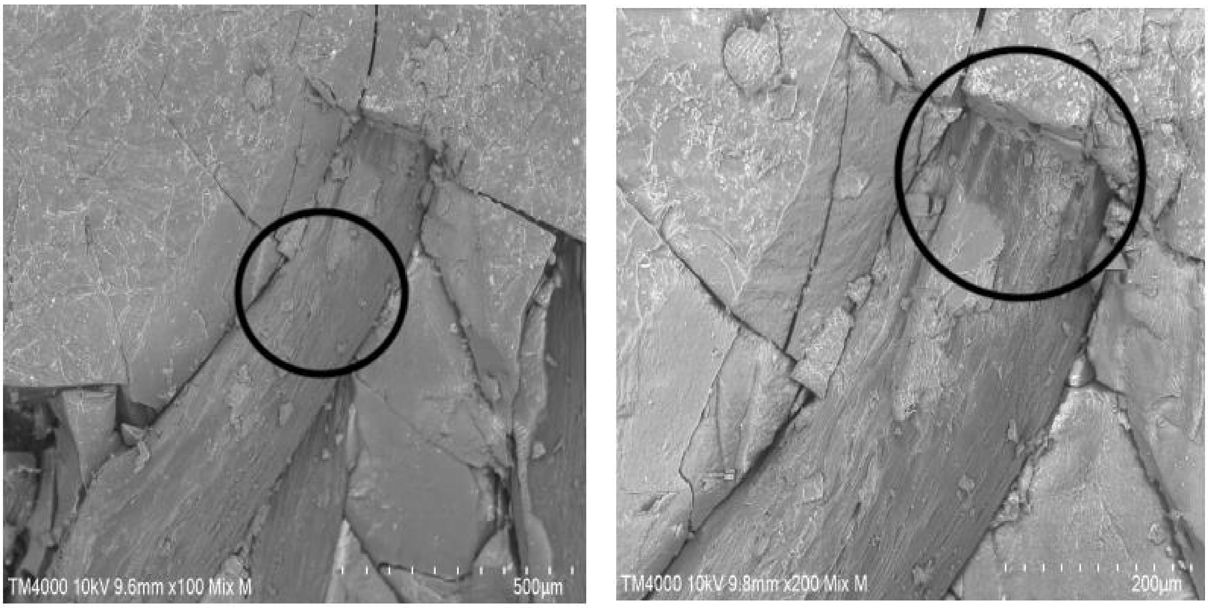

(a) (b)

Figure 50: SEM analysis for sodium hydroxide surface treated LC-PLA bio-composite.

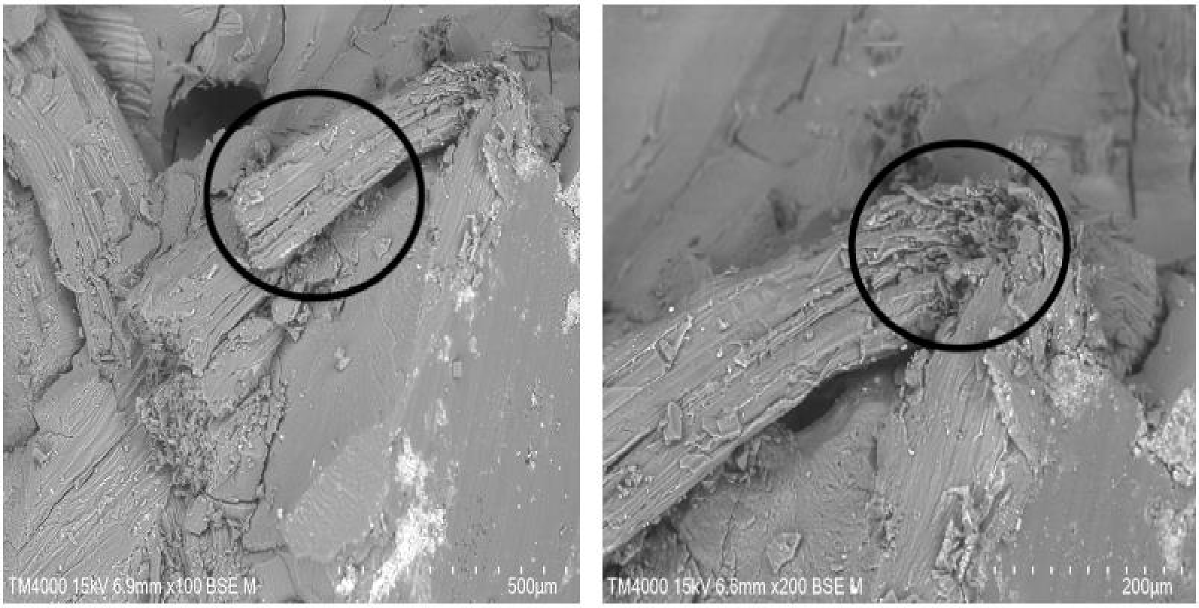

(a) (b)

Figure 51: SEM analysis for silane surface treated LC-PLA bio-composite.

(a) (b)

Figure 52: Shows the SEM analysis for acetylation surface treated LC-PLA bio-composite.

4.1.5.2 Thermal Analysis

4.1.5.2.1 Thermogravimetry (TGA) and Derivative Thermogravimetry (DTG)

Thermal analysis with the help of thermogravimetric analysis (TGA) was performed on PLA bio-composites that were enforced with untreated and chemically surface treated LC. These samples were also compared with a pure PLA matrix. Figure 53, shows the TGA plot that was achieved using the methods mentioned earlier. The plot indicated a mass loss for the untreated LC-PLA bio-composite starting from 50 °C due to the volatilization of moisture and other impurities (Arun Kumar Gupta 2012; Chhatrapati Parida 2015c). However, there is no substantial mass loss in this temperature range for treated LC-PLA bio-composite and pure PLA matrix. From the plot, it was visible that pure PLA matrix starts degrading at a higher temperature than chemically surface treated LC-PLA bio-composites. This explains that the addition of LC in the PLA matrix decreases the PLA matrix's thermal stability. However, in between the temperature range of 300-400 °C, all of the samples degrade approximately 85-90 %. It was evident that thermal stability for chemically surface treated LC-PLA was better than untreated LC-PLA bio-composites. The interfacial bonding between LC-PLA may explain this phenomenon. With the aid of chemical surface treatments, the interfacial bonding improves between LC-PLA thus, improving the thermal stability just like mechanical properties (Kaewta Kaewtatip 2012; Sudhir Kumar Saw 2013).

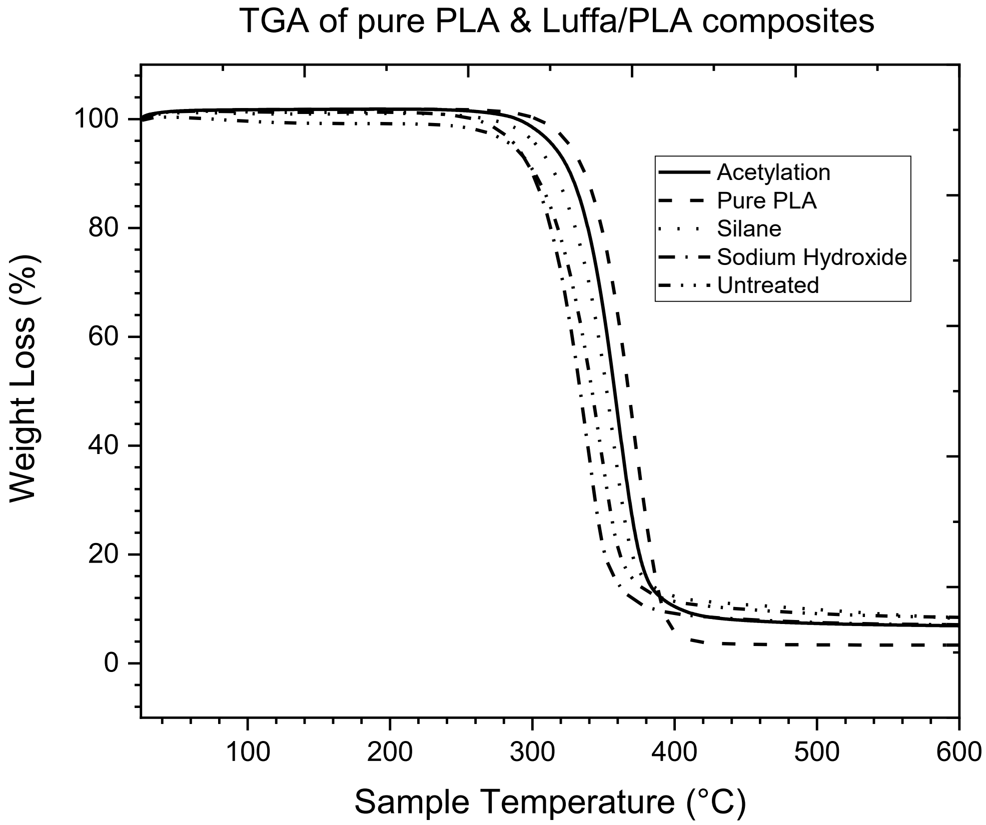

Figure 53: TGA plot for untreated and chemically surface treated LC-PLA bio-composite.

Changes are anticipated in thermal analysis with the inclusion of LCs in the PLA matrix. In Figure 54, the derivative thermogravimetry (DTG) plot was shown contrasting pure PLA, sodium hydroxide, silane, acetylated treated, and untreated bio-composites of LC-PLA. When observing the peaks in the region, it was apparent that the cellulose decomposition on LC causes these peaks. Sodium hydroxide treated LC-PLA peak was at 345 °C, silane surface-treated LC-PLA peak was at 354 °C, and acetylated surface-treated LC-PLA sample peak was at 358 °C. The peaks clearly shifted to a higher temperature range when compared to the untreated LC-PLA peak, which was at 337.6 °C. This phenomenon was due to the surface of LC had a higher level of celluloses exposed after sodium hydroxide, silane, and acetylation surface treatments (Arun Kumar Gupta 2012; Chhatrapati Parida 2015c). Therefore, the decomposition of cellulose moved to higher temperatures. Lignin, which degrades at 500 °C, showed no peaks in the plot; therefore, it was predicted that with the aid of sodium hydroxide, silane, and acetylated chemical surface treatments, lignin was eliminated from LC hence, no peaks. Moreover, the untreated LC-PLA sample's small peak was seen in the range of 50-100 °C. This peak was caused due to the elimination of moisture from LC because natural fibers are hydrophilic in nature. Whereas, for chemically surface treated samples, no peaks were seen in this temperature range. Therefore, it was safe to assume that hemicellulose was removed through the use of chemical surface treatments since hemicellulose is hydrophilic in nature (S. N. Pandey 1993).

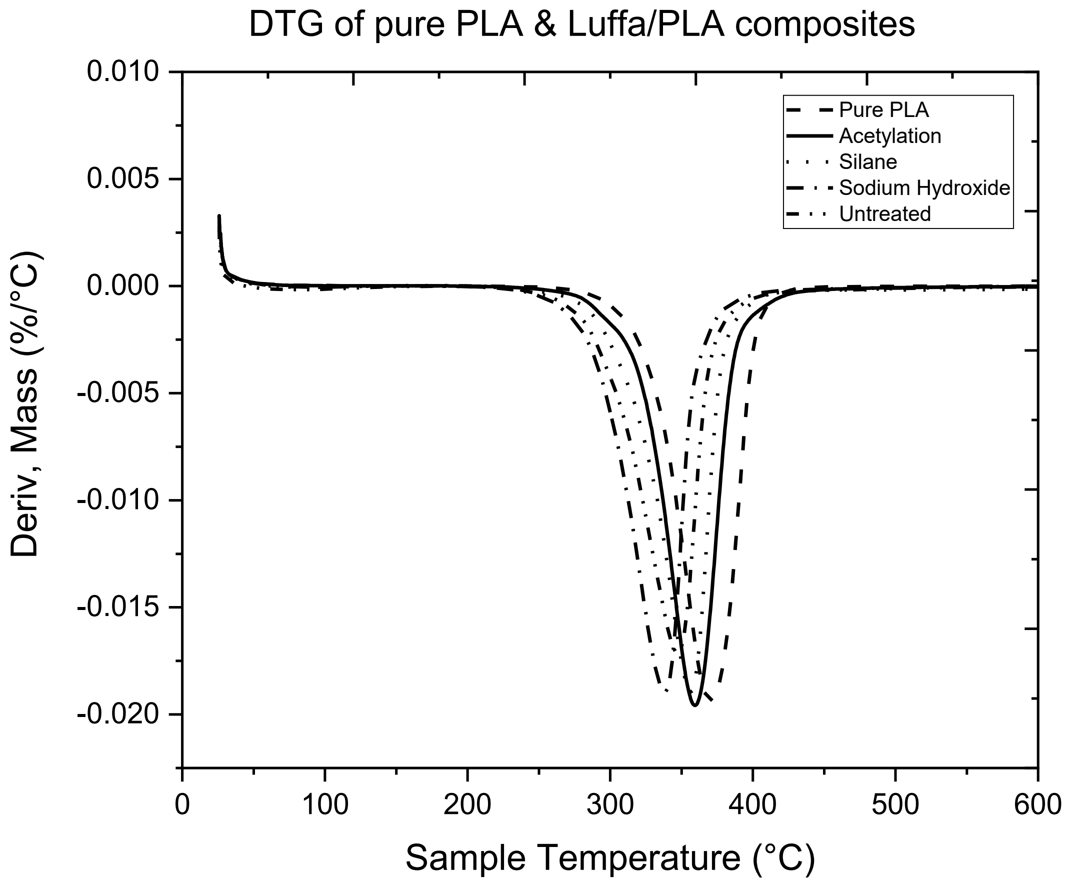

Figure 54: DTG plot for untreated and chemically surface treated LC-PLA bio-composite.

4.1.5.2.2 Differential Scanning Calorimetry (DSC)

The DSC thermogram shown in Figure 55 shows the results obtained using the previously mentioned methodology. However, as shown using the results that the enthalpy of melting was highest in pure PLA samples 25.5 J/g and that for LC-PLA bio-composites, the enthalpy of melting decreased. Untreated LC-PLA samples showed the lowest enthalpy of melting 12.7 J/g due to the presence of impurities, but with the aid of sodium hydroxide, silane, and acetylation, surface treatment enthalpy of melting was improved. In addition to that, the crystallinity percentage showed a similar trend. The above-noted crystallinity equation was used to calculate the results, and the findings are shown in Table 20. This phenomenon demonstrated that untreated fiber specimens failed to induce crystallinity due to impurities. Untreated fiber, therefore, prevented nucleation or crystalline formation (Chhatrapati Parida 2015c). However, after LC's chemical surface treatments, these impurities were eliminated, and thus better crystallization was encouraged, but not better than pure PLA. Moreover, the introduction of LC into the bio-composite helps the bio-composite to produce lumps of LC that may entangle the PLA matrix, thus, restricting the crystallization of PLA. In addition to that, the melting temperature for PLA did not get affected too much with the addition of untreated or chemically surface treated LC. Furthermore, no significant changes were visible in terms of melting temperature for pure PLA, untreated LC-PLA, silane surface-treated LC-PLA, sodium hydroxide surface-treated LC-PLA, and acetylation surface-treated LC-PLA sample, respectively.

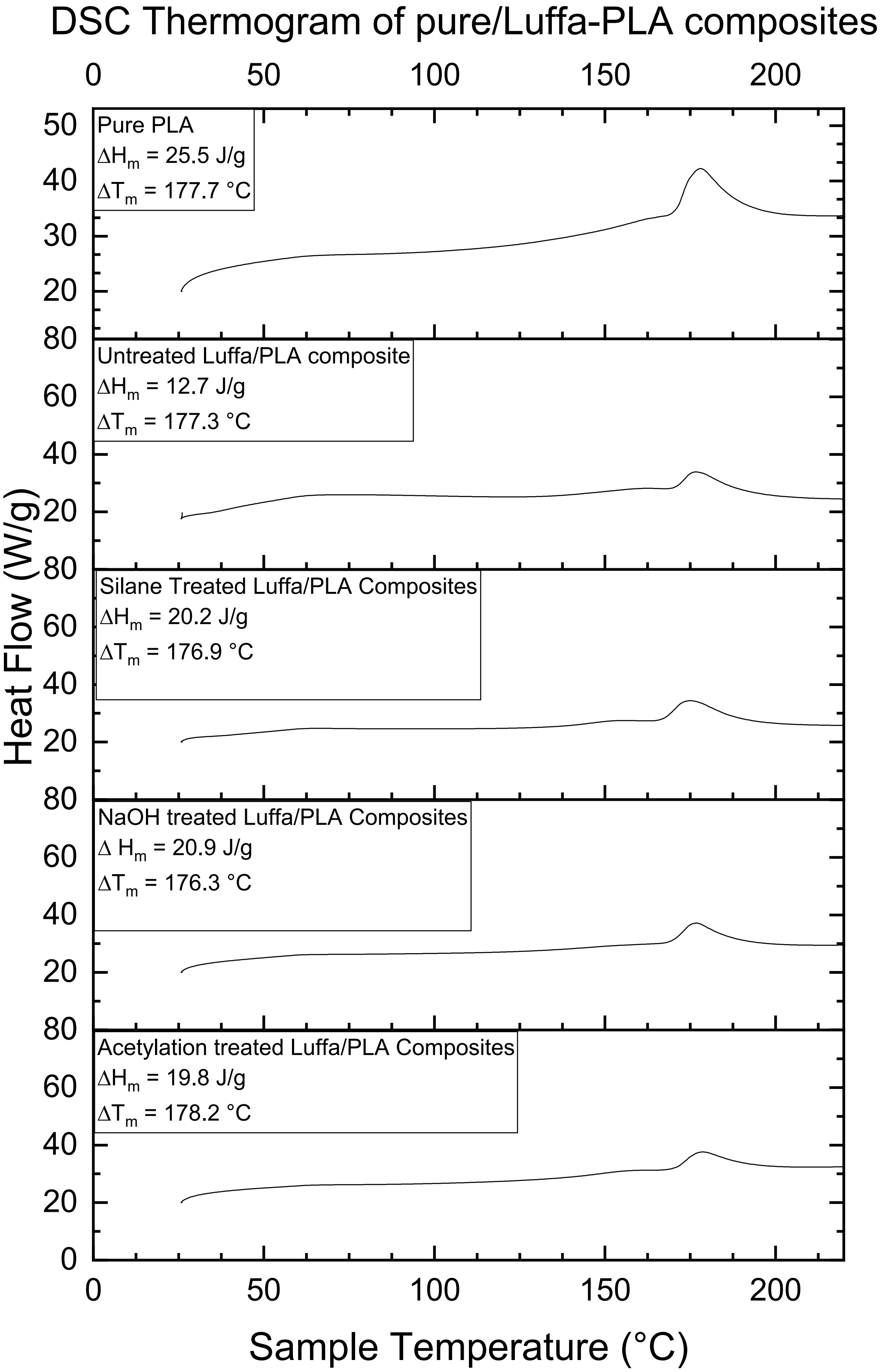

Figure 55: DSC plot for untreated and chemically surface treated LC-PLA bio-composite.

Table 20: The melting temperature (ΔTm), enthalpy of melting (ΔHm), and crystallinity % (%X) for pure PLA and LC-PLA bio-composites.

	Pure PLA	**Untreated**	**Silane**	**Sodium Hydroxide**	**Acetylation**
ΔT_m(°C)	177.7	177.3	176.9	176.3	178.2
ΔH_m(J/g)	25.5	12.7	20.2	20.9	19.8
$\%X_c$	27.4	16.1	25.6	26.4	25.1

4.1.6 Water Absorption Analysis of Pure PLA and Luffa Fiber/PLA composites

As natural fibers are hydrophilic in nature, physical property like water absorption should be measured. The methodology listed in the above section was used to analyse the water absorption of the samples. Furthermore, water uptake (%) was determined using the equation shown earlier. The result from the analysis is shown in Figure 56. It was evident that as the volume of LC increased, the uptake (%) of water rose, irrespective of the fiber chemical surface treatments. However, water uptake (%) was reduced by using chemical surface treatments. Water uptake (%) was lower due to the eradication of the alkaline soluble hydroxyl groups, silanol providing molecular continuity across the interface of the sample with the reaction between silanol and hydroxyl groups, and the reaction between hydroxyl groups and acetic groups using sodium hydroxide, silane, and acetylation chemical surface treatments respectively (Juliana Abd Halip 2019; K. Anbukarasi 2015; Yuxia Chen 2018).

The analysis of chemical surface treatments showed that the highest amount of water uptake (%) was evident for sodium hydroxide treated LC-PLA bio-composite; however, silane surface-treated LC-PLA bio-composite recorded the least amount of water uptake (%) at 5 and 10 %wt fiber volume, while the acetylated LC-PLA bio-composite recorded minimum water uptake (%) at 15 and 20 %wt fiber volume.

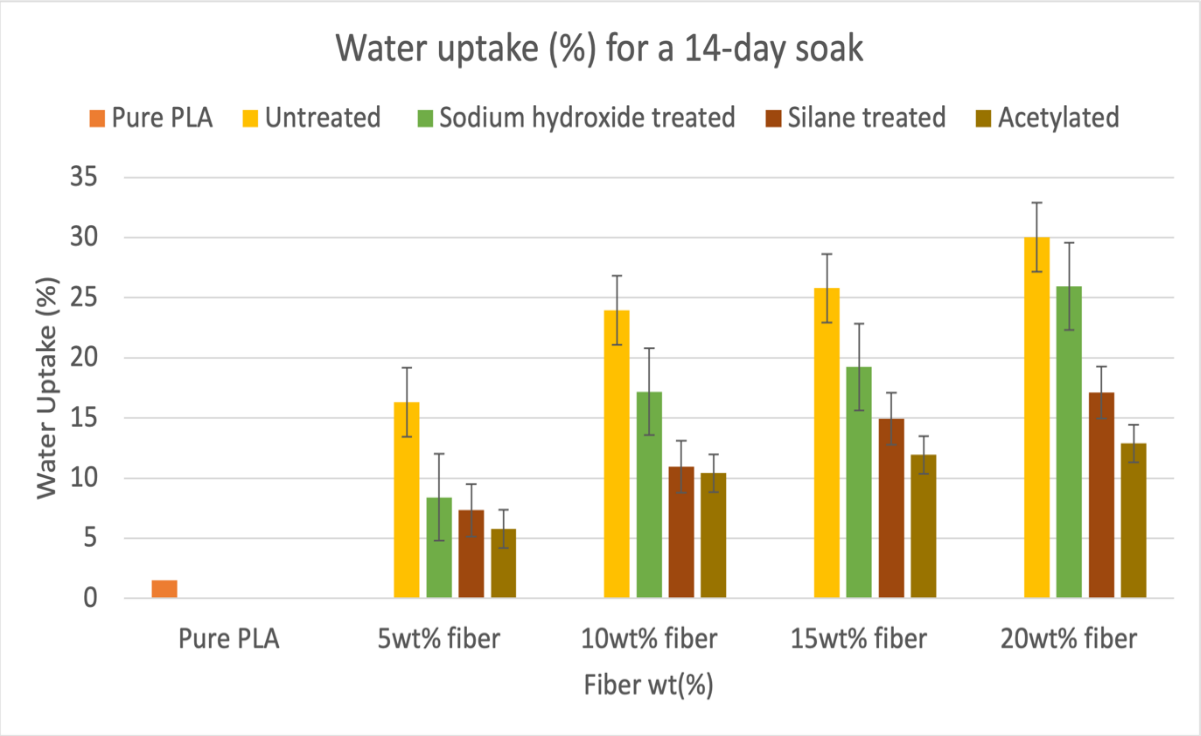

Figure 56: Water uptake (%) for chemically surface treated and untreated LC-PLA bio-composites for various fiber volumes (0-20 %wt).

4.2 SUMMARY

This chapter discussed using and comparing sodium hydroxide, silane, and acetylation chemical surface treatments and the techniques to modify LC's characteristics. The surface of LC was observed to be flaky and waxy using SEM. The surface topography of LC was improved, waxy impurities were removed, and interfacial adhesion between PLA and LC was enhanced utilizing chemical surface treatments. In addition, overall mechanical properties were improved with the addition of untreated LC in PLA. However, with the help of chemical surface treatments, the mechanical properties were improved even further. Sodium hydroxide surface-treated LC-PLA bio-composites showed the highest tensile and flexural strength, followed by silane and then acetylation surface-treated LC-PLA samples. Furthermore, LC-PLA bio-composites were also analysed for water absorption. The addition of LC in PLA significantly increased the water uptake (%) due to natural fibers being hydrophilic in nature. However, with the help of chemical surface treatments, the water uptake (%) was decreased considerably due to the removal of hemicellulose and –OH groups. Acetylation surface-treated LC-PLA bio-composites showed minimum water uptake (%), and sodium hydroxide surface-treated LC-PLA bio-composite showed the highest. Furthermore, with the help of chemical surface treatments, LC-PLA bio-composites thermal stability was improved due to improved interfacial bonding between LC and PLA. With the addition of untreated LC in PLA, enthalpy of melting (ΔH_m) was significantly reduced due to impurities; however, utilizing chemical surface treatments, the enthalpy of melting was improved. A similar trend was seen for the percentage of crystallinity ($\%X_c$) as well. Untreated LC fiber specimens failed to induce crystallinity due to impurities. Untreated fiber, therefore, prevented nucleation or crystalline formation. However, after LC's chemical surface treatments, these impurities were eliminated, and thus better crystallization was encouraged, but not better than pure PLA.

Conclusion, applications, and future work is explained in the upcoming chapter (Chapter 5)

5 CHAPTER 5

5.1 CONCLUSIONS AND FUTURE WORK

5.1.1 Conclusions

Different kinds of materials are available for the production of bio-composites, including natural fibers and biodegradable polymers. Besides being biodegradable and eco-friendly, natural fibers hold advantages like low cost and good mechanical properties. At the same time, biodegradable polymers have advantages such as low-cost, decent mechanical properties as well as biodegradability. As addressed in this thesis, the main focus of this research was on *Luffa Cylindrica* (LC) reinforced Polylactic Acid (PLA) bio-composites, which were prepared using a hot press compression moulding process.

This research illustrated the use of sodium hydroxide, silane, and acetylation chemical surface treatments and the techniques to modify LC's characteristics. The surface of LC was observed to be flaky and waxy using scanning electron microscopy (SEM). The results shown in the previous section show that the untreated surface of LC consists of waxy impurities, which causes smooth surface, other impurities, and voids. These factors play a huge role in decreasing the interfacial adhesion between the fiber and the polymer, leading to poor mechanical properties. However, by utilizing chemical surface treatments, these factors were tackled. Sodium hydroxide chemical surface treatment was able to remove waxy impurities and voids from the surface of LC but struggled to remove other impurities altogether. On the other hand, silane chemical surface treatment showed a smoother surface due to silane particles being deposited on the surface of LC, and the impurities were removed significantly. However, voids were not removed completely. Acetylation chemical surface treatment showed a smoother surface as well because the acetyl groups replaced the hydroxyl groups in the molecular structure of LC. Furthermore, impurities were removed to some extent; yet voids were still present on the surface after the chemical surface treatment. Overall, with the help of SEM analysis, it was predicted that each of the chemical surface treatments utilized in this research according to the methodology was successful. However, each of the chemical surface treatments affected LC differently. In addition, the surface topography of LC was improved, waxy impurities were removed, and interfacial adhesion between PLA and LC was enhanced using sodium hydroxide, silane, and acetylation chemical surface treatments.

Similar to SEM analysis, once all the chemical surface treatments were completed, FTIR analysis was performed, and plots were created for untreated and treated LC samples for further analysis. A significant amount of change was seen when a plot of untreated LC sample was compared with chemically surface treated LC sample plots. Sodium hydroxide-treated LC samples demonstrated no peak at 1637.56 cm^{-1}; therefore, it was predicted that hemicellulose had been removed. With the silane FTIR plot's assistance, peaks were found in the range of 700-800 cm^{-1}. These peaks predicted the existence of Si-O-cellulose and Si-O-Si linkages. Whereas acetylation treated, LC samples indicated bending of C-H bonds because of the esterification in the range of 1500-1700 cm^{-1}. Furthermore, small peaks in the range of 2300-2400 cm^{-1} affirmed ester linkages between acetyl ions and hydroxyl groups. With FTIR analysis's assistance, it was confirmed that every one of the chemical surface treatments was successful and affected the LC samples accordingly.

With the help of thermal analysis, plots for thermogravimetry (TGA) and derivative thermogravimetry (DTG) were plotted. Based on the plots for TGA and DTG, it was concluded that with the help of sodium hydroxide, silane, and acetylation chemical surface treatments, moisture was removed entirely from the fiber. Furthermore, maximum mass loss was observed between the range of 300-400 °C due to the decomposition of cellulose. However, using the methodology in this research, sodium hydroxide treated LC samples showed the minimum mass loss in this temperature range. This could had been due to the removal of some percentage of cellulose during the sodium hydroxide chemical surface treatment process. Furthermore, using the methodology explained in this research, silane surface-treated LC samples predicted the highest amount of thermal resistance, whereas acetylated LC samples predicted the lowest. However, DTG plots showed endothermic peaks for this specific thermal analysis, where silane-treated LC samples showed a minimum peak at 350 °C followed by acetylated samples at 370 °C. However, sodium hydroxide-treated LC samples showed a minimum peak at 400 °C.

Optimization and fabrication of pure PLA was a big task. As mentioned earlier, hot press compression moulding is not a widely utilized technique to fabricate PLA samples. However, this research focused on optimizing and fabricating PLA samples using hot press compression moulding. Magnitudes such as processing temperature, processing time, processing pressure, cooling time, and molds were changed continuously depending on each batch's outcome. Optimized samples were prepared at a processing temperature of 160-165 °C, the processing time of 25-30 minutes, processing pressure of 6 MPa, the cooling time of 3 hours, and ASTM (D790-17, D2240-15e1, D638-14, and D570-98(2018)) molds were utilized. Similar processing parameters were utilized to prepare LC-enforced PLA bio-composites.

With the addition of untreated LC in PLA, overall mechanical properties were drastically improved. Moreover, with the addition of LC in PLA, the bio-composites tensile strength showed an increase of almost 50%, whereas the flexural strength showed an increase of 43.2% at 15 %wt fiber volume. However, with the help of chemical surface treatments, the mechanical properties were improved even further. Sodium hydroxide surface-treated LC-PLA bio-composites showed the uppermost improvement of 7.1 and 6.9% respectively for tensile and flexural strength, followed by silane surface-treated LC-PLA bio-composites, which showed an increase of 5.7 and 1.4% respectively for tensile and flexural strength. However, acetylated LC-PLA bio-composites showed the least amount of improvement of 4.3 and 1.4%, respectively, for tensile and flexural strength at 15%wt fiber volume.

Furthermore, LC-PLA bio-composites were also analysed for water absorption. The addition of LC in PLA significantly increased water uptake (%) due to natural fibers being hydrophilic in nature However, with the help of sodium hydroxide, silane, and acetylation chemical surface treatments, the water uptake (%) was decreased considerably due to the removal of hemicellulose and –OH groups. Acetylation surface-treated LC-PLA bio-composites showed minimum water uptake (%), and sodium hydroxide surface-treated LC-PLA bio-composite showed the highest.

With the help of chemical surface treatments, LC-PLA bio-composites thermal stability was improved due to improved interfacial bonding between LC and PLA. With the addition of untreated LC in PLA, enthalpy of melting (ΔH_m) was significantly reduced due to impurities; however, utilizing chemical surface treatments, the enthalpy of melting was improved. A similar trend was seen for the percentage of crystallinity ($\%X_c$) as well. Untreated LC fiber specimens failed to induce crystallinity due to impurities. Untreated fiber, therefore, prevented nucleation or crystalline formation. However, after LC's chemical surface treatments, these impurities were eliminated, and thus better crystallization was encouraged, but not better than pure PLA. Sodium hydroxide treated LC-PLA bio-composite showed the highest amount of crystallinity (%), whereas acetylated LC-PLA bio-composite showed the least amount of crystallinity.

5.1.2 Applications

As mentioned in the previous section, there are various engineering applications for PLA. Based on the results already demonstrated, it was evident that the enforcement of untreated LC significantly improves the tensile strength and flexural strength for PLA. In addition, these properties were further improved by enforcing PLA with chemically surface treated LC.

Thus, the LC-enforced PLA bio-composite may be used as flooring in offices or houses; although the LC-enforced PLA bio-composite is durable, it is also lightweight. Furthermore, PLA is also notably used for interior panels in the automotive industry because it is biodegradable. The pure PLA panels can be substituted by LC-enforced PLA bio-composite due to improved tensile and flexural properties. Moreover, improved mechanical characteristics will improve the safety and longevity of the interior panels.

Helmets for construction workers and bike riders are two main domestic applications for PLA (Tueen 2019). Thus, the improvement in PLA's strength due to the enforcement of LC can provide construction workers and bike riders with additional safety. However, rainwater is going to be a problem. The water uptake (%) results demonstrated in the previous section showed that the water uptake (%) were significantly lowered but not completely removed with the help of acetylation chemical surface treatment. Solutions such as waterproof coatings or paint can therefore be utilized.

5.1.3 Future work

Future research or work on LC and LC bio-composites should focus more on thermal stability as not enough research has been conducted in this area. Furthermore, more research is required if LC bio-composites are to be used in automotive, aerospace, sports, and other industries. Thus, it is demonstrated in this research that further research should be undertaken in terms of analytical analysis using Hirsch's, Halpin-Tsai models, and Fourier's heat conduction equation to predict tensile strength, Young's modulus, and thermal characteristics, respectively. Using analytical analysis, one can save both time and resources. Finally, more research needs to be done when considering recycled polymer matrices to make bio-composites with LC. Thus, environmental pollution can be mitigated with the utilization of natural fibers like LC, where research provides a solution through the sustainable use of green bio-composites and the incorporation of natural fibers in them.

Moreover, due to the lack of time, many modifications, tests, and studies are there to be performed in the future (i.e., the modifications, tests, and studies that were left out due to being time-consuming or unavailability of testing equipment). The studies that will be performed in the future will require further study of the existing processes, novel ideas, and application of various manufacturing or testing approaches.

There are some experiments and processing techniques for prospective researchers that can be recommended. All that depends, though, on resource availability.

5.1.3.1 Chemical Surface Treatments

The processing parameters, including chemical concentration, immersion time, and immersion temperature for chemical surface treatment, were maintained continuously, as described earlier in the methodology section. Therefore, one can analyse the effect of varying processing parameters. As previous researchers have shown, different concentrations, immersion times, and immersion temperature can cause changes to the bio-composites overall physical properties. However, where the concentration and immersion time differ, one has to be very attentive since the surface of the fiber can be destroyed at too high of a concentration and at too long of an immersion time, resulting in poor physical properties. However, different combinations can be applied. Furthermore, in this research, sodium hydroxide, silane, and acetylation chemical surface treatments were utilized. However, there are other chemical treatments that can be used, such as strontium titanate, permanganate, benzoylation, and acrylation.

5.1.3.2 Processing Techniques

The processing technique used in this research was hot press compression moulding. The processing techniques such as extrusion, injection moulding, additive manufacturing, 3D printing, and filament winding are still available to be explored. Thus, in the future various processing techniques can be adapted by an individual where the processing parameters as mentioned in this thesis can be used as a reference.

5.2 References

A. Arbelaiz, BFn, G. Cantero, R. Llano-Ponte, A. Valea, I. Mondragon 2005, 'Mechanical properties of flax fibre/polypropylene composites. Influence of fibre/matrix modification and glass fibre hybridization', *Composite Part A: Applied Science and Manufacturing*, vol. 36, pp. 1637-1644.

A. K. Mohanty , LTDMM 2002, 'Engineered natural fiber reinforced polypropylene composites: influence of surface modifications and novel powder impregnation processing', *Journal of Adhesion Science and Technology*, vol. 16, no. 8, pp. 999-1015.

A. Orue, AJ, U. Unsuain, J. Labidi, A. Eceiza, A. Arbelaiz 2016, 'The effect of alkaline and silane treatments on mechanical properties and breakage of sisal fibers and poly(lactic acid)/sisal fiber composites', *Composite Part A: Applied Science and Manufacturing*, vol. 84, pp. 186-195.

A. Oushabi, SS, F. Oudrhiri Hassani, Y. Abboud, O. Tanane, A. El Bouari 2017, 'The effect of alkali treatment on mechanical, morphological and thermal properties of date palm fibers (DPFs): Study of the interface of DPFePolyurethane composite', *South African Journal of Chemical Engineering*, vol. 23, pp. 116-123.

A. Rubio-López, AO, A. Díaz-Álvarez, C. Santiuste 2015, 'Manufacture of compression moulded PLA based biocomposites: A parametric study', *Composite Structures* vol. 131, pp. 995-1000.

A.K. Bledzki, AJ 2010, 'Mechanical performance of biocomposites based on PLA and PHBV reinforced with natural fibres – A comparative study to PP', *Composites Science and Technology*, vol. 70, pp. 1687-1696.

A.M. Mohd Edeerozey, HMA, A.B. Azhar, M.I. Zainal Ariffin 2007, 'Chemical modification of kenaf fibers', *Materials Letters*, vol. 61, pp. 2023-2025.

Adewale Adewuyi, FVP 2017, 'Isolation and surface modification of cellulose from underutilized Luffa cylindrica sponge: A potential feed stock for local polymer industry in Africa', *Journal of the Association of Arab Universities for Basic and Applied Sciences*, vol. 24, pp. 39-45.

Al-Snafi, AE 2019, 'Constituents and pharmacology of Luffa cylindrica- A review', *IOSR Journal Of Pharmacy*, vol. 9, no. 9, pp. 68-79.

Amar K. Mohanty, MM, Lawrence T. Drzal 2005, *Natural Fuber, Biopolymers, and Biocomposites,* 1st Edition edn., CRC press, Boca Raton.

Anand R. Sanadi, DFC, Rodney E. Jacobson and Roger M. Rowelltg 1995, 'Renewable Agricultural Fibers as Reinforcing Fillers in Plastics: Mechanical Properties of Kenaf Fiber-Polypropylene Composites', *Industrial & Engineering Chemistry Research*, vol. 34, pp. 1889-1896.

Andrea Melina Avecilla-Ramirez, MdRL-C, Berenice Vegara-Porras, Asriana I. Rodriguez and Edgar Vazquez-Nunez 2020, 'Characterization of Poly-hydroxybutyrate/Luffa Fiber Composite Material ', *BioResources* vol. 15, pp. 7159-7177.

Anike David Chukwudi, OTU, Ugochukwu-Aniefuna Anthonia Azuka, Ezuh Cyprian Sunday 2015, 'Comparison of Acetylation and Alkali Treatments on the Physical and Morphological Properties of Raffia Palm Fibre Reinforced Composite', *Science Journal of Chemistry* vol. 3, pp. 72-77.

Anil Dhanola, AsB, Anil Kumar and Aman Kumar 2018, 'Influence of natural fillers on physico-mechanical properties of luffa cylindrica/ polyester composites', *Materials Today: Proceedings*, vol. 5, pp. 17021-17029.

Arun Kumar Gupta, MB, S. Mohanty, and S. K. Nayak 2012, 'Mechanical, Thermal Degradation, and Flammability Studies on Surface Modified Sisal Fiber Reinforced Recycled Polypropylene Composites', *Advances in Mechanical Engineering*, vol. 2012, 12 November 2012, pp. 1-13.

ASTM 2010, *ASTM D570-98(2018), Standard Test Method of Water Absoption of Plastics*, USA.

ASTM 2013, *ASTM E1252-98(2013)e1, Standard Practice for General Techniques for Obtaining Infrared Spectra for Qualitative Analysis*, USA.

ASTM 2014a, *ASTM D638-14, Standard Test Method for Tensile Properties of Plastics*, USA.

ASTM 2014b, *ASTM E2015-04(2014), Standard Guide for Preparation of Plastics and Polymeric Specimens for Microstructural Examination*, USA.

ASTM 2015, *ASTM D2240-15e1, Standard Test Method for Rubber Property—Durometer Hardness, ASTM International, West Conshohocken*, USA.

ASTM 2016, *ASTM E168-16, Standard Practices for General Techniques of Infrared Quantitative Analysis*, USA.

ASTM 2017, *ASTM D790-17, Standard Test Methods for Flexural Properties of Unreinfroced and Reinforced Plastics and Electrical Insulating Materials*, USA.

ASTM 2018, *ASTM E1641-18, Standard Test Method for Decomposition Kinetics by Thermogravimetry Using the Ozawa/Flynn/Wall Method*, USA.

B V Lingesh, RMRaBNR 2014, 'Effect of short glass fibers on mechanical properties of polyamide66 and polypropylene (PA66/PP) thermoplastoc blend composite ', *Procedia Materials Science*, vol. 5, pp. 1232-1240

Bhanu K. Goriparthi, KNSS, Nalluri Mohan Rao 2012, 'Effect of fiber surface treatments on mechanical and abrasive wear performance of polylactide/jute composites', *Composites: Part A*, vol. 43, pp. 1800-1808.

Breuer, KFaU 2015, *Multifunctionality of Polymer Composites*.

C. A. Boynard, SNM, J. R. M. d'Almeida 2003, 'Aspects of Alkali Treatment of Sponge Gourd (Luffa cylindrica) Fibers on the Flexural Properties of Polyester Matrix Composites', *Journal of applied polymer science*, vol. 87, pp. 1927-1932.

C. Parida, SCD, S.K. Dash 2012, 'Mechanical Analysis of Bio Nanocomposite Prepared from Luffa cylindrica', *Procedia Chemistry*, vol. 4, pp. 53-59.

C. Sivakandhan, RB, Ganesh Babu Loganathan, D. Madan, G. Murali 2018, 'Investigation of mechanical behaviour on sponge/ridge gourd (Luffa aegyptiaca) natural fiber using epoxy and polyester resin', *Materials Today: Proceedings*,

Campilho, RDSG 2015, *Natural Fiber Composites,* 1st Edition edn., CRC Press, Boca Raton.

Chaohong Dong, LS, Xingbo Ma, Zhou Lu, Pengshuang He, and Ping Zhu 2019, 'Synthesis of a Novel Linear α, ω-Di (Chloro Phosphoramide) Polydimethylsiloxane and Its Applications in Improving Flame-Retardant and Water-Repellent Properties of Cotton Fabrics', *Polymers*, vol. 11,

Chhatrapati Parida, SKD, and Sarat Chandra Das 2015a, 'Effect of Fiber Treatment and Fiber Loading on Mechanical Properties of Luffa-Resorcinol Composites', *Indian Journal of Materials Science* pp. 1-6.

Chhatrapati Parida, SKD, Pinaki Chaterjee 2015b, 'Mechanical Properties of Injection Molded Poly(lactic) Acid—Luffa Fiber Composites', *Soft Nanoscience Letters* vol. 5, pp. 65-72.

Chhatrapati Parida, SKDaPC 2015c, 'The Thermal and Crystallization Studies of Luffa Fiber Reinforced Poly Lactic Acid Composites', *Open Journal of Composite Materials*, vol. 6, pp. 1-7.

D. Kocak, SIMaMA 2015, 'The use of Luffa cylindrica fibres as reinforcements in composites', in OFaM Sain (ed.) *Biofiber Reinforcements in Composite Materials*, Elsevier, pp. 689-699.

D. Mohana Krishnudu, DS, P. Venkateshwar Reddy 2020, 'Synthesis and Characterization of PLA/Luffa Cylindrica Composite Films', *International Journal of Integrated Engineering*, vol. 12, pp. 1-7.

D.Mohana krishnudu , DS, N.Ramesh 2018, 'Synthesis, Characterization, and Properties of Epoxy Filled Luffa cylindrica reinforced composites', *Materials Today: Proceedings*, vol. 5, pp. 3835-3841.

Debanth, S 2017, 'Sustainable production of bast fibres', in SS Muthu (ed.) *Sustainable Fibres and Textiles*, pp. 60-85.

Debes Bhattacharyya, ASaNKK 2015, 'Natural fibers: Their composites and flammability characterizations', in *Multifunctionality of Polymer Composites*, Elsevier, pp. 102-143.

Deepak Pathania, AS, Vandana sethi 2017, 'Microwave induced graft copolymerization of binary monomers onto luffa cylindrica fiber: removal of congo red', *Procedia Engineering*, vol. 200, pp. 408-415.

Dutta, A 2017, 'Fourier Transform Infrared Spectroscopy', in, Elsevier, pp. 73-93.

Éder J. Siqueira, VRB 2013, 'Luffa cylindrica fibres/vinylester matrix composites: Effects of 1,2,4,5- benzenetetracarboxylic dianhydride surface modification of the fibres and aluminum hydroxide addition on the properties of the composites', *Composites Science and Technology*, vol. 82, pp. 76-83.

Faris M. AL-Oqla, OYA, M. Jawaid, S.M. Sapuan, and M.H. Es-Saheb 2014, 'Processing and Properties of Date Palm Fibers and Its Composites', in, pp. 1-25.

Faris M. AL-Oqla, SMS 2013, 'Natural fiber reinforced polymer composites in industrial applications: feasibility of date palm fibers for sustainable automotive industry', *Journal of Cleaner Production*, 7 November 2013, pp. 347-354.

Feng Zhou, GC, Bo Jiang 2014, 'Effect of silane treatment on microstructure of sisal fibers', *Applied Surface Science*, vol. 292, pp. 806-812.

Garkhail, SK, Meurs, E., Van de Beld, T.and Peijs T. 1999, 'Thermoplastic composites based on biopolymers and natural fibres', in, pp. 1-10.

Gilberto Siqueira, JB, Nadège Follain, Sabrina Belbekhouche, Stéphane Marais, Alain Dufresne 2013, 'Thermal and mechanical properties of bio-nanocomposites reinforced by Luffa cylindrica cellulose nanocrystals', *Carbohydrate Polymers*, vol. 91, pp. 711-717.

Giovanna Frisoni, MB, and Mariastella Scandola 2001, 'Natural Cellulose Fibers: Heterogeneous Acetylation Kinetics and Biodegradation Behavior', *Biomacromolecules*, vol. 2, pp. 476-482.

Gonzalo Martínez-Barrera, EV-S, Miguel Martínez-López, Maria C.S. Ribeiro, Antonio J.M. Ferreira, Witold Brostow 2013, 'Luffa fibers and gamma radiation as improvement tools of polymer concrete', *Construction and Building Materials* vol. 47, pp. 86-91.

H. Demir, UA, D. Balko ̈se, F. Tıhmınlıog ̆lu 2006, 'The effect of fiber surface treatments on the tensile and water sorption properties of polypropylene–luffa fiber composites', *Composite Part A: Applied Science and Manufacturing*, vol. 37, pp. 447-456.

Hamid Abdelhafid Ghouti, AZ, Mehdi Derradji, Li-wu Zu, Wan-an Cai, Jun Wang, Abdul Qadeer Dayo , Wen-bin Liu 2019, 'Structural and mechanical characteristics of silane-modified PIPD/basalt hybrid fiber-reinforced polybenzoxazine composites', *Materials Chemistry and Physics*, vol. 237,

Hamideh Hajiha, MSLHM 2014, 'Modification and Characterization of Hemp and Sisal Fibers', *Journal of Natural Fibers*, vol. 11, pp. 144-168.

Hasan Koruk , GG 2019, 'Acoustic and mechanical properties of luffa fiber-reinforced biocomposites', in MTaNS Mohammad Jawaid (ed.) *Mechanical and Physical Testing of Biocomposites, Fibre-Reinforced Composites and Hybrid Composites*, Woodhead, pp. 478.

Heather Simmons, PT, James E. Colwell, Marianna Kontopoulou 2019, 'Improvements in the crystallinity and mechanical properties of PLA by nucleation and annealing', *Polymer Degradation and Stability*, vol. 166, pp. 248-257.

Hossein Ebrahimnezhad-Khaljiri, RE-F, and Saeid Taleb 2020, 'Investigating the High Velocity Impact Behavior of the Laminated Composites of Aluminum/Jute Fibers- Epoxy Containing Nanoclay Particles', *Fibers and Polymers*, vol. 21, pp. 2607-2613.

Intan S.M.A. Tawakkal, MJC, Stephen W. Bigger 2014, 'Effect of kenaf fibre loading and thymol concentration on themechanical and thermal properties of PLA/kenaf/thymol composites', *Industrial Crops and Products*, vol. 61, pp. 74-83.

Jae-Kyoo Lim, RH 2007, 'Fabrication and Mechanical Properties of Completely Biodegradable Hemp Fiber Reinforced Polylactic Acid Composites', *Journal of Composite Materials*, vol. 41, pp. 1655-1669.

Jerico Biagiotti, DP, Luigi Torre and Jose M. Kenny 2004, 'A Systematic Investigation on the Influence of the Chemical Treatment of Natural Fibers on the Properties of Their Polymer Matrix Composites', *Polymer Composites*, vol. 25, pp. 470-479.

Jianhu Shen, YMX, Xiaodong Huang, Shiwei Zhou, Dong Ruan 2013, 'Behaviour of luffa sponge material under dynamic loading', *International Journal of Impact Engineering*, pp. 17-26.

Jintao Wang, YZ, Aiqin Wang 2013, 'Investigation of acetylated kapok fibers on the sorption of oil in water', *Journal of Environmental Sciences*, vol. 25, pp. 246-253.

Juliana Abd Halip, LSH, Zaidon Ashaari, Paridah Md Tahir, Lum Wei Chen and Mohd Khairun Anwar Uyup 2019, 'Effect of treatment on water absorption behavior of natural fiberereinforced polymer

composites', in MTaNS Mohammad Jawaid (ed.) *Mechanical and Physical Testing of Biocomposites, Fuber-Reinforced Composites and Hybrid Composites*, Woodhead, pp. 478.

Jun Young Jang, TKJ, Hwa Jin Oh, Jae Ryoun Youn, Young Seok Song 2012, 'Thermal stability and flammability of coconut fiber reinforced poly(lactic acid) composites', *Composites: Part B*, vol. 43, pp. 2434-2438.

Justine Muller, CG-M, Amparo Chiralt 2017, 'Poly(lactic) acid (PLA) and starch bilayer films, containing cinnamaldehyde, obtained by compression moulding', *European Polymer Journal*, vol. 95, pp. 56-70.

K. Anbukarasi, SK 2015, 'Study of effect of fibre volume and dimension on mechanical, thermal, and water absorption behaviour of luffa reinforced epoxy composites', *Materials & Design (1980-2015)*, vol. 66, pp. 321-330.

K. Majeed, MJ, A. Hassan, A. Abu Bakar, H.P.S. Abdul Khalil, A.A. Salema, I. Inuwa 2013, 'Potential materials for food packaging from nanoclay/natural fibres filled hybrid composites', *Materials & Design*, pp. 391-410.

K. Oksman, MS, J.-F. Selin 2003a, 'Natural fibres as reinforcement in polylactic acid (PLA) composites', *Composites Science and Technology*, vol. 63, pp. 1317-1324.

K. Oksman, MSaJ-FS 2003b, 'Natural fibres as reinforcement in polylactic acid (PLA) composites', *Composotes sceince and technology* vol. 63, pp. 1317-1324.

K.L. Pickering, MGAE 2016, 'Preparation and mechanical properties of novel bio-composite madeof dynamically sheet formed discontinuous harakeke and hemp fibremat reinforced PLA composites for structural applications', *Industrial Crops and Products*, vol. 84, pp. 139-150.

Kaewta Kaewtatip, JT 2012, 'Studies on the structure and properties of thermoplastic starch/luffa fiber composites', *Materials & Design* vol. 40, pp. 314-318.

Kevin J. Edgar, CMB, John S. Debenham, Paul A. Rundquist, Brian D. Seiler, Michael C. Shelton, Debra Tindall 2001, 'Advances in cellulose ester performance and application', *Progress in Polymer Science*, vol. 26, pp. 1605-1688.

Kumar, 2010, 'Effect of Silanes on Mechanical Properties of Bamboo Fiber-epoxy Composites', *Journal of Reinforced Plastics and Composites*, vol. 29, pp. 1-10.

Kuruvilla Joseph, RDTdF, Beena James, Sabu Thomas & Laura Hecker de Carvalho 1999, 'A review on sisal fiber reinforced polymer composites', *Brazilian Journal of Agricultural and Environmental Engineering*, vol. 3, pp. 367-379.

L. Boopathi, PSS, K. Mylsamy 2012, 'Investigation of physical, chemical and mechanical properties of raw and alkali treated Borassus fruit fiber', *Composite Part B: Engineering*, vol. 43, pp. 3044-3052.

L. Ghali, SM, M. Zidi, F. Sakli 2009, 'Effect of pre-treatment of Luffa fibres on the structural properties', *Materials Letters*, vol. 63, pp. 61-63.

Lassaad Ghali, MA, Mondher Zidi, Hachmi Bendaly, Slah M'sahli, and & Sakli, F 2011, 'Effect of chemical modification of luffa cylindrica fibers on the mechanical and hygrothermal behaviours of polyester/luffa composites', *Bioresources*, vol. 4, pp. 3836-3849.

Lassaad Ghali, SM, Mondher Zidi, Faouzi Sakli 2011, 'Effects of Fiber Weight Ratio, Structure and Fiber Modification onto Flexural Properties of Luffa-Polyester Composites', *Advances in Materials Physics and Chemistry*, vol. 1, pp. 78-85.

Lee Tin Sin, BST 2019, *Polylactic Acid,* Second edn.

Lokensgard, E 2016, *Industrial Plastics: Theory and Applications,* 6th Edition edn., Cengage learning.

Longxiang Zhu, JQ, Wendi Liu, Eiichi Sakai 2019, 'Mechanical and thermal properties of rice Straw/PLA modified by nano Attapulgite/PLA interfacial layer', *Composites Communications*, vol. 13, pp. 18-21.

Lu, JLCDZZDKHSZ 2020, 'Multifunctional flame-retarded and hydrophobic cotton fabrics modified with a cyclic phosphorus/polysiloxanecopolymer', *Cellulose*, vol. 27, pp. 3531–3549.

M. A. Martins, LHCM 2003, 'Short Sisal Fiber-Reinforced Tire Rubber Composites: Dynamic and Mechanical Properties', *Journal of applied polymer science*, vol. 91, pp. 670-677.

M. K. Gupta, RS 2018, 'Flexural and Dynamic Mechanical Analysis (DMA) of Polylactic Acid (PLA) Coated Sisal Fibre Reinforced Polyester Composite', *Materials Today: Proceedings*, vol. 5, pp. 6109-6114.

M. Sakthivel, SV, S. Ramesh 2014, 'Production and Characterization of Luffa/Coir Reinforced Polypropylene Composite', *Procedia Materials Science*, vol. 5, pp. 739-745.

M.A. Norul Izani, MTP, U.M.K. Anwar, M.Y. Mohd Nor, P.S. H'ng 2013, 'Effects of fiber treatment on morphology, tensile and thermogravimetric analysis of oil palm empty fruit bunches fibers', *Composite Part B: Engineering*, vol. 45, pp. 1251-1257.

M.G. Aruan Efendy, KLP 2016, 'Fibre orientation of novel dynamically sheet formed discontinuous natural fibre PLA composites', *Composites: Part A*, vol. 90, pp. 82-89.

M.R. Sanjay, PM, Mohammad Jawaid, P. Senthamaraikannan, S. Senthil, S. Pradeep 2018, 'Characterization and properties of natural fiber polymer composites: A comprehensive review', *Journal of Cleaner Production*, vol. 172, pp. 566-581.

M.S. Huda, LTD, A.K. Mohanty, M. Misra 2007, 'The effect of silane treated- and untreated-talc on the mechanical and physico-mechanical properties of poly(lactic acid)/newspaper fibers/talc hybrid composites', *Composite Part B: Engineering*, vol. 38, pp. 367-379.

M.S. Islam, KLP, N.J. Foreman 2010, 'Influence of accelerated ageing on the physico-mechanical properties of alkali-treated industrial hemp fibre reinforced poly(lactic acid) (PLA) composites', *Polymer Degradation and Stability*, vol. 95, pp. 59-65.

Marius Murariu, PD 2016, 'PLA composites: From production to properties', *Advanced Drug Delivery Reviews*, vol. 107, pp. 17-46.

Mizi Fan, DDaBH 2012, 'Fourier Transform Infrared Spectroscopy for Natural Fibres', in *Fourier Transform - Material Analysis*, InTech, pp. 45-68.

MM Alam, MMaMM 2014, 'Application and Advances in Microprocessing of Natural Fiber (Jute)–Based Composites', in GFB Saleem Hashmi, Chester J. Van Tyne and Bekir Yilbas (ed.) *Comprehensive Materials Processing*, vol. 7, Elsevier, pp. 243-260.

Mohamad Alhijazi, BS, Qasim Zeeshan, Mohammed Asmael, Arameh Eyvazian and Zhaoye Qi 2020, 'Recent Developments in Luffa Natural Fiber Composites: Review', *Sustainability*, vol. 12, pp. 1-25.

Mudhoo, SKSaA 2011, *A Handbook of Applied Biopolymer Technology: Synthesis, Degradation and Applications,* Royal Society of Chemistry, London.

Mukesh , SSG 2019, 'Effect of chemical modification of fiber surface on natural fiber composites: A review', *Materials Today: Proceedings*, vol. 18, pp. 3428-3434.

Musibau Adewuyi Azeez, OSB, Adewumi Omobola Adedeji 2013, 'Traditional and medicinal uses of Luffa cylindrica : a Review', *Journal of Medicinal Plants Studies*, vol. 1, no. 5, pp. 102-111.

N. Karthi, KK, S. Sathish, S. Gokulkumar, L. Prabhu, N. Vigneshkumar 2020, 'An overview: Natural fiber reinforced hybrid composites, chemical treatments and application areas', *Materials Today: Proceedings*, vol. 27, pp. 2828-2834.

N. Venkateshwaran, AEP, D. Arunsundaranayagam 2013, 'Fiber surface treatment and its effect on mechanical and visco-elastic behaviour of banana/epoxy composite', *Materials & Design*, vol. 47, pp. 151-159.

NAB, M 2007, *Synthesis, characterization, and propertoes of the new unsaturated polyester resins for composite application*, thesis, MARA University of Technology, pp. 45-56.

Nadège Follaina, SB, Julien Bras, Gilberto Siqueira, Stéphane Marais, Alain Dufresne 2013, 'Water transport properties of bio-nanocomposites reinforced by Luffa cylindrica cellulose nanocrystals', *Journal of Membrane Science*, pp. 218-229.

Nhlapo, LP 2010, 'Thermal and mechanical properties of ldpe/sisal fibre composites compatibilized with paraffin waxes', March 2010, pp. 1-74.

Nicole M. Stark, LMM 2004, 'Surface chemistry changes of weathered HDPE/wood-flour composites studied by XPS and FTIR spectroscopy', vol. 86, pp. 1-9.

Niharika Mohanta, SKA 2015, 'Investigation of mechanical properties of luffa cylindrica fibre reinforced epoxy hybrid composite', *International Journal of Engineering Science and Technology*, vol. 7, pp. 1-10.

Nina Graupner, JMs 2011, 'A comparison of the mechanical characteristics of kenaf and lyocell fibre reinforced poly(lactic acid) (PLA) and poly(3-hydroxybutyrate) (PHB) composites', *Composites: Part A*, vol. 42, pp. 2010-2019.

Omar Faruk, AKB, Hans-Peter Fink and Mohini Sain 2012, 'Biocomposites reinforced with natural fibers: 2000–2010', *Progress in Polymer Science*, vol. 37, pp. 1552-1596.

Ozbakkaloglu, AGaT 2019, 'A review of natural fiber composites: properties, modification and processing techniques, characterization, applications', *Journal of Materials Science*, vol. 55, pp. 829-892.

P.J. Herrera-Franco, AV-Gl 2005, 'A study of the mechanical properties of short natural-fiber reinforced composites', *Composites Part B: Engineering*, vol. 36, pp. 597-608.

Panayiotis Georgiopoulos, EK, George Georgousis 2018a, 'Effect of silane treatment loading on the flexural properties of PLA/flax unidirectional composites', *Composites Communications*, vol. 10, pp. 6-10.

Panayiotis Georgiopoulos, EKaGG 2018b, 'Effect of silane treatment loading on the flexural properties of PLA/flax unidirectional composites', *Composites Communications*, vol. 10, pp. 6-10.

Parsania, JPPaPH 2018, 'Biodegradable and Biocompatible Polymer Composites', in *Characterization, testing, and reinforcing materials of biodegradable composites*, Elsevier, pp. 438.

Parul Sahu, MKG 2018, 'PLA Coated Sisal Fibre Reinforced Polyester Composite: Static and Dynamic Mechanical Properties', *Materials Today: Proceedings*, vol. 5, pp. 19799-19807.

Po-Yuan Chen, H-YL, Yeng-Fong Shih, Su-Mei Chen-Wei, Ru-Jong Jeng 2017, 'Preparation, characterization and crystallization kinetics of Kenaf fiber/multi-walled carbon nanotube/polylactic acid (PLA) green composites', *Materials Chemistry and Physics*, vol. 196, pp. 249-255.

Polymer Blends Handbook, 2014, Second edn., Springer Science+Business Media Dordrecht.

Pramendra KumarBajpai, I, JitendraMadaan 2013, 'Tribological behavior of natural fiber reinforced PLA composites', *Wear*, vol. 297, pp. 829-840.

Pritchard, G 2012, *Developments in reinforced plastics—4,* Elsevier, New York.

Pumchusak, 2014, 'Improvement of mechanical properties of poly(lactiic acid) by elastomer', *The Malaysian Journal of Analytical Sciences*, vol. 18, pp. 669-675.

Qiuping Yang, YZ, Xiaofeng Li, Huizhi Li 2018, 'Synthesis of Fe3O4/Pr-BiOCl/Luffa composites with enhanced visible light T photoactivity for organic dyes degradation', *Materials Research Bulletin*, vol. 106, pp. 409-417.

R.Panneerdhass, AG, K.Rajkumar 2014, 'Mechanical Properties of Luffa Fiber and Ground nut Reinforced Epoxy Polymer Hybrid Composites', *Procedia Engineering* pp. 2042-2051.

S. N. Pandey, ADaMDM 1993, 'Thermal Analysis of Chemically Treated Jute Fibers', *Textile Research Journal*, vol. 3, pp. 143-150.

S. Ravi Theja Reddy, AVRP, K. Ramanaiah 2020, 'Tensile and flexural properties of biodegradable jute fiber reinforced poly lactic acid composites', *Materials Today: Proceedings*, vol. -, pp. -.

S.M. Luz, JDT, G.J.M. Rocha, A.R. Gonçalves, A.P. Del'Arco Jr. 2008, 'Cellulose and cellulignin from sugarcane bagasse reinforced polypropylene composites: Effect of acetylation on mechanical and thermal properties', *Composite Part A: Applied Science and Manufacturing*, vol. 39, pp. 1362-1369.

Saurabh Chaitanya, IS, Jung Il Song 2019, 'Recyclability analysis of PLA/Sisal fiber biocomposites', *Composites Part B* vol. 173,

Saw, SK 2017, 'Effect of stacking patterns on morphological and mechanical properties of luffa/coir hybrid fiber-reinforced epoxy composite laminates', in MKT Vijay Kumar Thakur, Raju Kumar Gupta (ed.) *Hybrid Polymer Composite Materials Structure and Chemistry*, vol. 1, Woodhead Publishing, pp. 313-333.

Sean A. Hinchcliffe, KMH, Wil V. Srubar III 2016, 'Experimental and theoretical investigation of prestressed natural fiber-reinforced polylactic acid (PLA) composite materials', *Composites Part B*, vol. 95, pp. 346-354.

Seung Goo Lee, S-SC, Won Ho Park, Donghwan Cho 2003, 'Characterization of Surface Modified Flax Fibers and Their Biocomposites with PHB', *Macromolecular Symposia*, vol. 197, pp. 89-99.

Sha Yin, HW, Jiani Li, Robert O. Ritchie, Jun Xu 2019, 'Light but tough bio-inherited materials: Luffa sponge based nickel-plated composites', *Journal of the Mechanical Behavior of Biomedical Materials*, vol. 94, pp. 10-18.

Sherely Annie Paul, AB, Laurent Ibos, Yves Candau, Kuruvilla Joseph, Sabu Thomas 2008, 'Effect of fiber loading and chemical treatments on thermophysical properties of banana fiber/polypropylene commingled composite materials', *Composite Part A: Applied Science and Manufacturing*, vol. 39, pp. 1582-1588.

Shin Serizawa, KI, Masatoshi Iji 2005a, 'Kenaf-Fiber-Reinforced Poly(lactic acid) Used for Electronic Products', *Journal of Applied Polymer Science*, vol. 100, pp. 618-624.

Shin Serizawa, KIaMI 2005b, 'Kenaf-Fiber-Reinforced Poly(lactic acid) Used for Electronic Products', *Journal of applied polymer science*, vol. 100, pp. 618-624.

Shouzheng Su, QL, Jingyuan Liu, Hongsen Zhang, Rumin Li, Xiaoyan Jing, Jun Wang 2018, 'Polyethyleneimine-functionalized Luffa cylindrica for efficient uranium extraction', *Journal of Colloid and Interface Science*, vol. 530, pp. 538-546.

Shu Hong, YS, Yang Yuan, Hailan Liana, Henrikki Liimatainen 2020, 'Production and characterization of lignin containing nanocellulose from luffa through an acidic deep eutectic solvent treatment and systematic fractionation', *Industrial Crops and Products*, vol. 143,

Shun Li , FL, Yiping Su , Ningning Shao , Dongfang Yu , Yong Liu , Weishu Liu, Zuotai Zhang 2019, 'Luffa sponge-derived hierarchical meso/macroporous boron nitride fibers as superior sorbents for heavy metal sequestration', *Journal of Hazardous Materials*, vol. 378,

Siddesh Naik V, PBSaRS 2017, 'Mechanical Properties of Sisal Fiber Reinforced Thermoplastic Starch Bio-Composites', *International Journal of Mechanical and Material Sciences Research*, vol. 7, pp. 1-7.

Sinha, R 2004, *Outlines of Polymer Technology,* Prentice-Hall of India Private Limited, India.

Sudhir Kumar Saw, RP, Sourabh Nandy, Joyjeet Ghose, and Gautam Sarkhel 2013, 'Fabrication, Characterization, and Evaluation of Luffa cylindrica Fiber Reinforced Epoxy Composites', *Bioresources*, vol. 8, pp. 4805-4826.

Suhara Panthapulakkal, MS 2006, 'Injection-Molded Short Hemp Fiber/Glass Fiber-Reinforced Polypropylene Hybrid Composites— Mechanical, Water Absorption and Thermal Properties', *Journal of applied polymer science*, vol. 103, 30 August 2006, pp. 2432-2441.

Sun-Mou Lai, Y-HK, Yu-Kuo Liu, Fang-Chyou Chiu 2016, 'Preparation and properties of luffa fiber- and kenaf fiber-filled poly(butylene succinate-co-lactate)/starch blend-based biocomposites', *Polymer Testing*, vol. 50, pp. 191-199.

Suneel Motru, AVH, Bharath J, Guruprasad R 2020, 'Development and Evaluation of Mechanical Properties of Biodegradable PLA/Flax Fiber Green Composite Laminates', *Materials Today: Proceedings*, vol. 24, pp. 641-649.

Takao Iijima, TTaMT 1991, 'Modification of Epoxy Resins with Poly (aryl ether ketone)s', *Journal of applied polymer science*, vol. 43, pp. 1685-1692.

Takemura, MTaA 2009, 'Thermal Degradation of Natural Fiber-reinforced Polypropylene Composites', *Journal of Thermoplastic Composite Materials*, vol. 23, pp. 281-298.

Thomas Bayerl, MG, Arcot A. Somashekar, Debes Bhattacharyya 2014, 'Influence of fibre architecture on the biodegradability of FLAX/PLA composites', *International Biodeterioration & Biodegradation*, vol. 96, pp. 18-25.

Tueen, 2019, *Polylactic Acid,* second edn.

V. Fiore, GDB, A. Valenza 2015, 'The effect of alkaline treatment on mechanical properties of kenaf fibers and their epoxy composites', *Composite Part B: Engineering*, vol. 68, pp. 14-21.

V. Mazzanti, RP, A. Bonanno, O. Ruiz de Ballesteros, F. Mollica, G. Filippone 2019, 'Reinforcing mechanisms of natural fibers in green composites: Role of fibers morphology in a PLA/hemp model system', *Composites Science and Technology*, vol. 180, pp. 51-59.

V. Vilay, MM, R. Mat Taib, Mitsugu Todo 2008, 'Effect of fiber surface treatment and fiber loading on the properties of bagasse fiber–reinforced unsaturated polyester composites', *Composites Science and Technology* vol. 68, pp. 631-638.

Valcineide O.A. Tanobe, THDS, Marilda Munaro, Sandro C. Amico 2005, 'A comprehensive characterization of chemically treated Brazilian sponge-gourds (Luffa cylindrica)', *Polymer Testing*, vol. 24, pp. 474-482.

Valcineide O.A. Tanobe, THSF-S, Sandro C. Amico, Graciela I.B. Muniz, and K.G. Satyanarayana 2014, 'Sponge Gourd (Luffa Cylindrica) Reinforced Polyester Composites: Preparation and Properties', vol. 64, pp. 273-280.

Vinay Kumar Patel, AD 2016, 'Influence of CaCO3, Al2O3, and TiO2 microfillers on physico-mechanical properties of Luffa cylindrica/polyester composites', *Engineering Science and Technology, an International Journal*, vol. 19, pp. 676-683.

Vinod Kumar Guptaa, DP, Shilpi Agarwal, Shikha Sharma 2014, 'Amputation of congo red dye from waste water using microwave induced grafted Luffa cylindrica cellulosic fiber', *Carbohydrate Polymers*, pp. 556-566.

Volova, T 2004, *Polyhydroxyalkanoates—plastic materials of the 21st century: production, properties, applications,* Niva Publishers, New Yorl.

W. Z. W. Zahari , RNRLB, H. Ardyananta , D. Kurniawan and F. M. Nor 2015, 'Mechanical Properties and Water Absorption Behavior of Polypropylene / Ijuk Fiber Composite by Using Silane Treatment', *Procedia Chemistry*, vol. 2, pp. 573-578.

Wassamon Sujaritjun, PU, Weraporn Pivsa-Art, & Hamada, H 2013, 'Mechanical property of surface modified natural fiber reinforced PLA biocomposites', *Energy Procedia*, vol. 34, pp. 664-672.

Weifeng Cao, YW, Jianquan Luo, Junxiang Yin, Jianmin Xing, Yinhua Wan 2018, 'Succinic acid biosynthesis from cane molasses under low pH by Actinobacillus succinogenes immobilized in luffa sponge matrices', *Bioresource Technology* vol. 268, pp. 45-51.

Xue Li, LGTaSP 2007, 'Chemical Treatments of Natural Fiber for Use in Natural Fiber-Reinforced Composites: A Review', *Journal of Polymers and the Environment*, vol. 15, pp. 25-33.

Yadong Wu , WH, Ruishi Xie , Xun Liu , Dingming Yang , Peng Chen , Jing Zhang, Fangshu Zhang 2018, 'Composite of nano-goethite and natural organic luffa sponge as template: Synergy of high efficiency adsorption and visible-light photocatalysis', *Inorganic Chemistry Communications*, vol. 98, pp. 115-119.

Yang Zhao, JQ, Huixia Feng, Min Zhang, Lin Lei, Xueli Wu 2011, 'Improvement of tensile and thermal properties of poly(lactic acid) composites with admicellar-treated rice straw fiber', *Chemical Engineering Journal*, vol. 173, pp. 659-666.

Yicheng Du, TW, Ning Yan, Mark T. Kortschot, Ramin Farnood 2014a, 'Fabrication and characterization of fully biodegradable natural fiber-reinforced poly(lactic acid) composites', *Composites: Part B*, vol. 56, pp. 717-723.

Yicheng Du, TW, Tongfei Wu, Mark T. Kortschot and Ramin Farnood 2014b, 'Fabrication and characterization of fully biodegradable natural fiber-reinforced poly(lactic acid) composites', *Composites Part B: Engineering*, vol. 56, pp. 717-723.

Yong Guo, LW, Yuxia Chen, Panpan Luo and Tong Chen 2019, 'Properties of Luffa Fiber Reinforced PHBV Biodegradable Composites', *Polymers*, vol. 11, pp. 1-16.

Yucheng Liu, JX, Na Wu, Lidong Wang, Yunhai Ma, Jin Tong 2019, 'Influence of silane treatment on the mechanical, tribological and morphological properties of corn stalk fiber reinforced polymer composites', *Tribology International* vol. 131, pp. 398-405.

Yuxia Chen, FY, Qin Su, Canming Yu, Kaiting Zhang, PanPan Luo, Dingfeng Hu, Yong Guo 2020, 'A novel sound absorbing material comprising discarded luffa scraps and polyester fibers', *Journal of Cleaner Production*, vol. 245, pp. 1-8.

Yuxia Chen, NS, Kaiting Zhang, Shiliu Zhu, Zhenzhen Zhu, Wenlian Qin, Yiwen Yang, Yunjiao Shi, Shanshan Fan, Zhongkai Wang, Yong Guo 2018, 'Effect of fiber surface treatment on structure, moisture absorption and mechanical properties of luffa sponge fiber bundles', *Industrial Crops and Products*, vol. 123, pp. 341-352.

Zhe Wang, HM, Benjamin Chu, Benjamin S. Hsiao 2017, 'Super-hydrophobic modification of porous natural polymer “luffa sponge” for oil absorption', *Polymer*, vol. 126, pp. 470-476.

Zhi Liu, YP, Kai Shi, Weicai Wang, Chao Peng, Wei Li, Di Sha, Zhe Wang, Xiangling Ji 2016, 'Preparation of hydrophilic luffa sponges and their water absorption performance', *Carbohydrate Polymers*, vol. 147, pp. 178-187.

Zquez, 2003, 'Thermal degradation of cellulose derivatives/starch blends and sisal fibre biocomposites', *Polymer degradation and stability*, vol. 84, pp. 13-21.

5.3 Appendices

5.3.1 Datasheets

Polylactic acid datasheet:

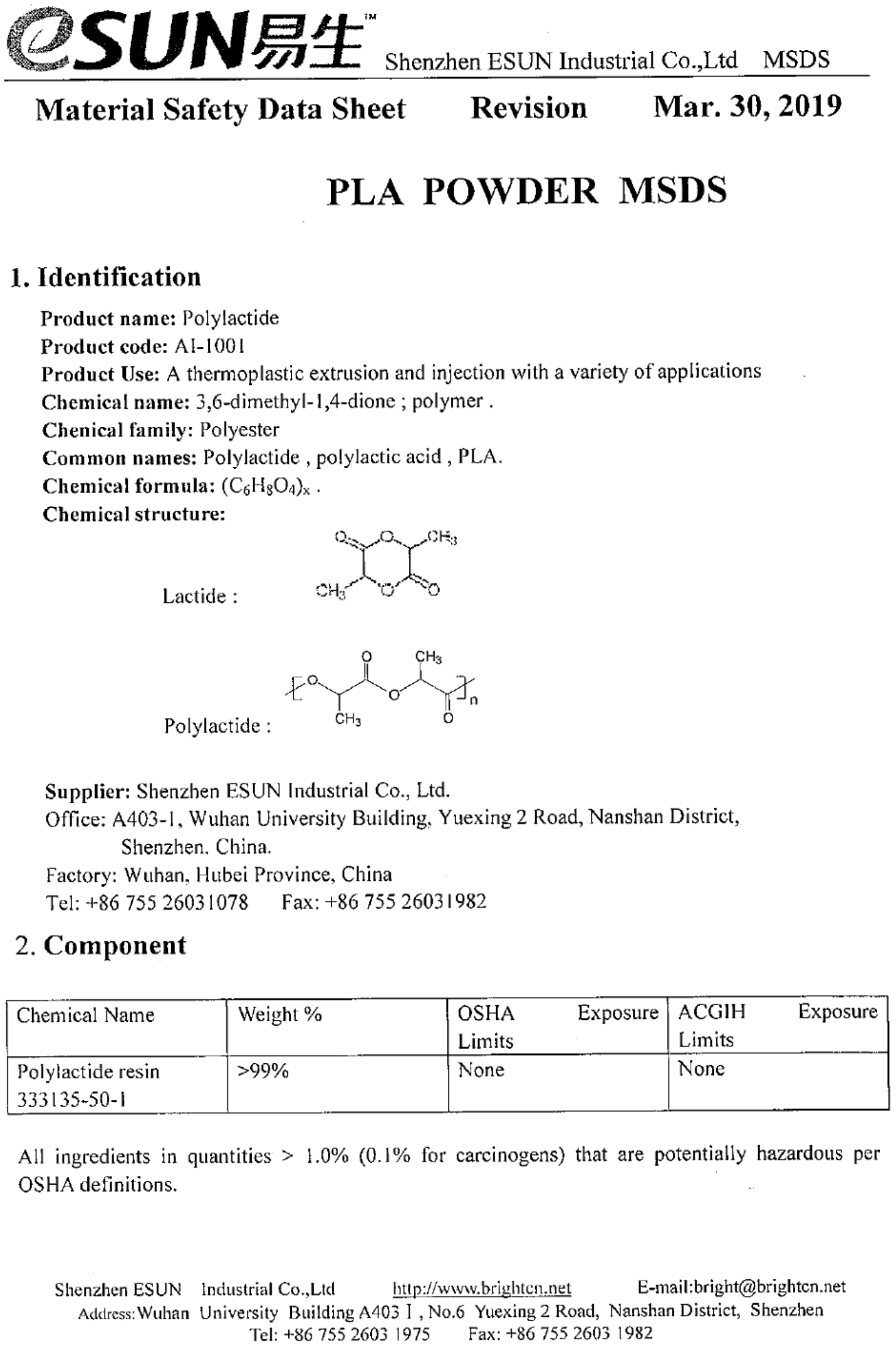

eSUN易生™ Shenzhen ESUN Industrial Co.,Ltd MSDS

Material Safety Data Sheet **Revision** **Mar. 30, 2019**

PLA POWDER MSDS

1. Identification

Product name: Polylactide
Product code: AI-1001
Product Use: A thermoplastic extrusion and injection with a variety of applications
Chemical name: 3,6-dimethyl-1,4-dione ; polymer .
Chenical family: Polyester
Common names: Polylactide , polylactic acid , PLA.
Chemical formula: $(C_6H_8O_4)_x$.
Chemical structure:

Lactide :

Polylactide :

Supplier: Shenzhen ESUN Industrial Co., Ltd.
Office: A403-1, Wuhan University Building, Yuexing 2 Road, Nanshan District,
Shenzhen. China.
Factory: Wuhan, Hubei Province, China
Tel: +86 755 26031078 Fax: +86 755 26031982

2. Component

Chemical Name	Weight %	OSHA Exposure Limits	ACGIH Exposure Limits
Polylactide resin 333135-50-1	>99%	None	None

All ingredients in quantities > 1.0% (0.1% for carcinogens) that are potentially hazardous per OSHA definitions.

Shenzhen ESUN Industrial Co.,Ltd http://www.brightcn.net E-mail:bright@brightcn.net
Address:Wuhan University Building A403 I , No.6 Yuexing 2 Road, Nanshan District, Shenzhen
Tel: +86 755 2603 1975 Fax: +86 755 2603 1982

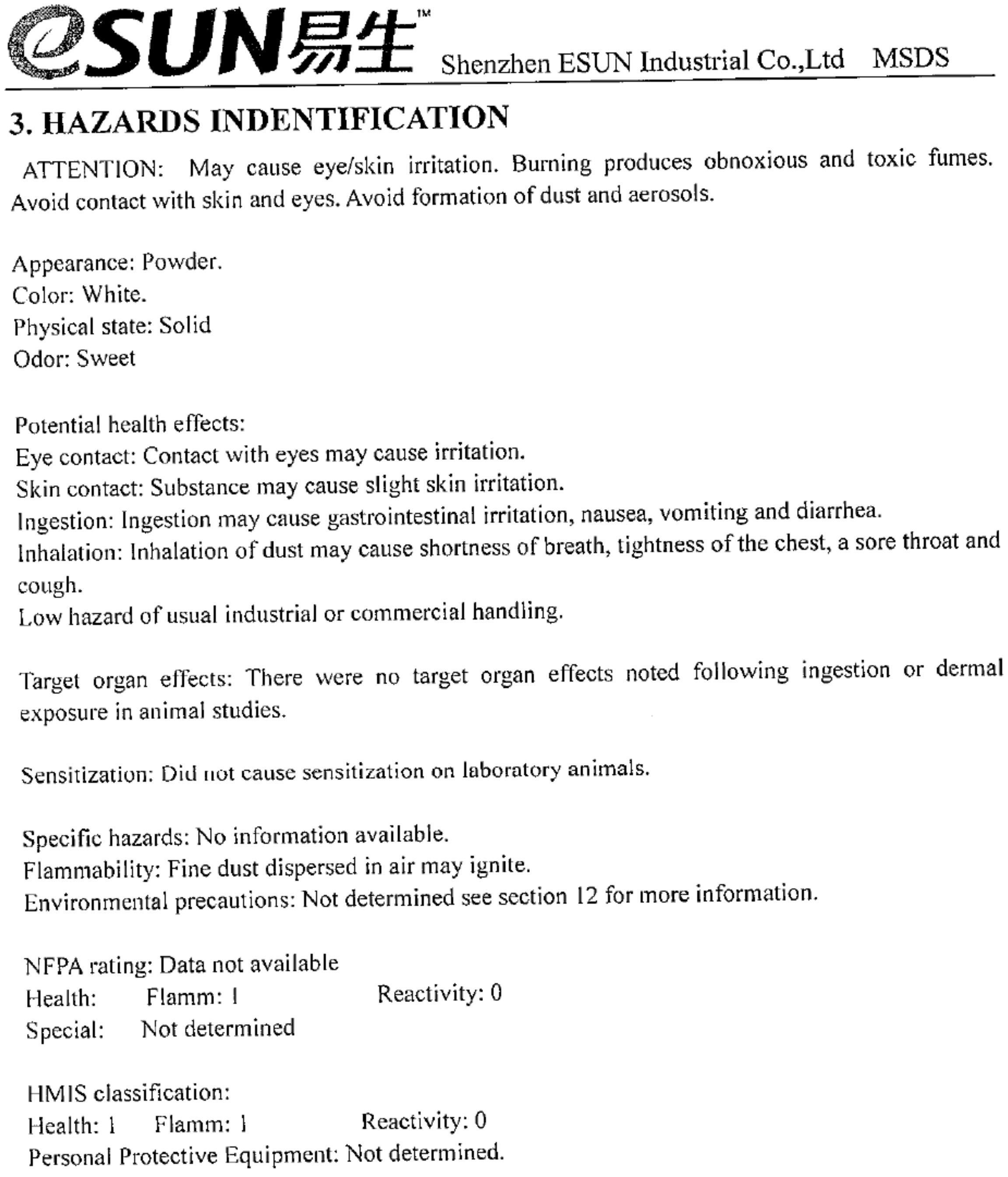

ESUN易生™ Shenzhen ESUN Industrial Co.,Ltd MSDS

3. HAZARDS INDENTIFICATION

ATTENTION: May cause eye/skin irritation. Burning produces obnoxious and toxic fumes. Avoid contact with skin and eyes. Avoid formation of dust and aerosols.

Appearance: Powder.
Color: White.
Physical state: Solid
Odor: Sweet

Potential health effects:
Eye contact: Contact with eyes may cause irritation.
Skin contact: Substance may cause slight skin irritation.
Ingestion: Ingestion may cause gastrointestinal irritation, nausea, vomiting and diarrhea.
Inhalation: Inhalation of dust may cause shortness of breath, tightness of the chest, a sore throat and cough.
Low hazard of usual industrial or commercial handling.

Target organ effects: There were no target organ effects noted following ingestion or dermal exposure in animal studies.

Sensitization: Did not cause sensitization on laboratory animals.

Specific hazards: No information available.
Flammability: Fine dust dispersed in air may ignite.
Environmental precautions: Not determined see section 12 for more information.

NFPA rating: Data not available
Health: Flamm: 1 Reactivity: 0
Special: Not determined

HMIS classification:
Health: 1 Flamm: 1 Reactivity: 0
Personal Protective Equipment: Not determined.

Sodium Hydroxide Datasheet:

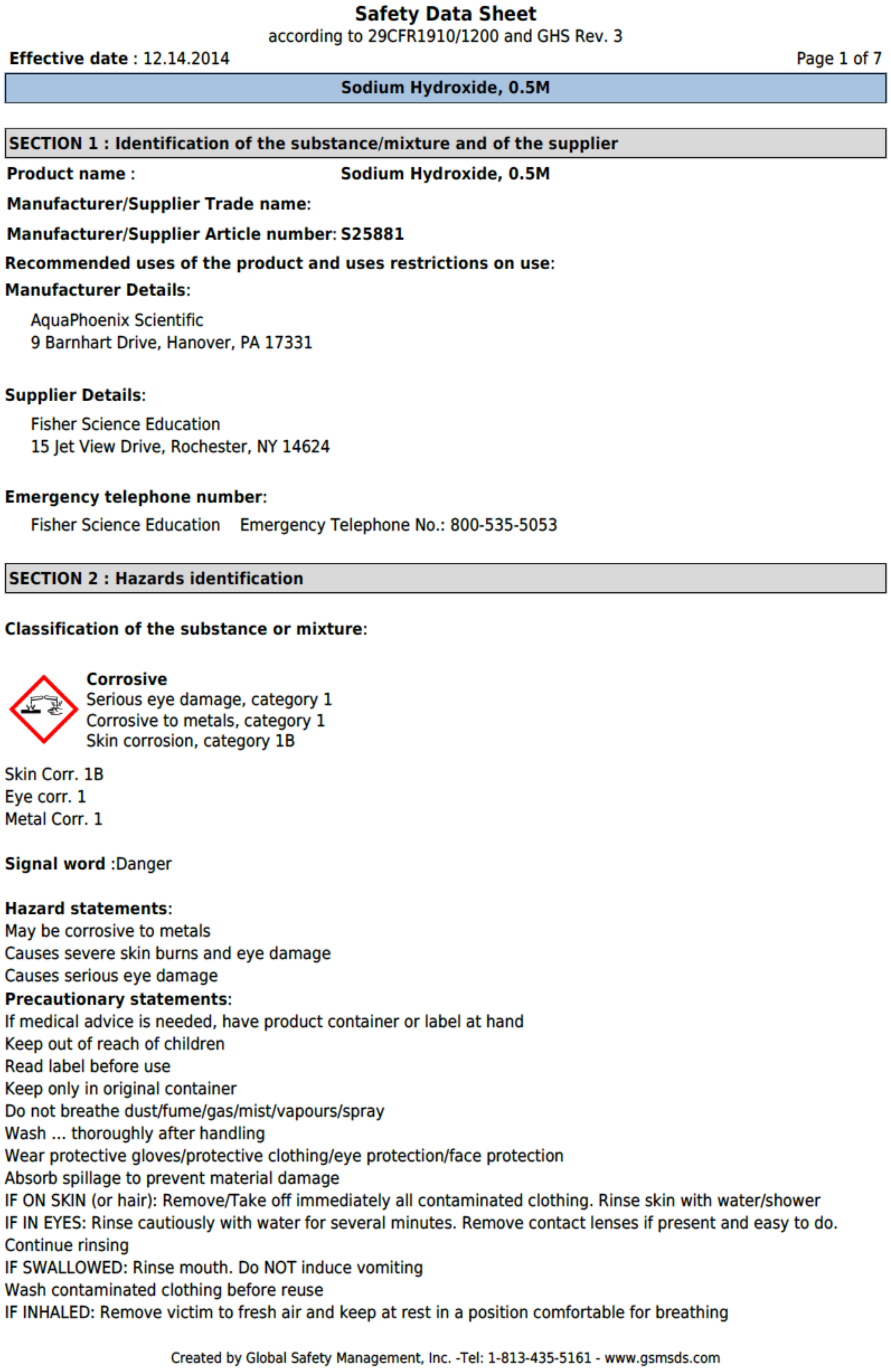

Safety Data Sheet

according to 29CFR1910/1200 and GHS Rev. 3

Effective date : 12.14.2014 Page 1 of 7

Sodium Hydroxide, 0.5M

SECTION 1 : Identification of the substance/mixture and of the supplier

Product name : **Sodium Hydroxide, 0.5M**

Manufacturer/Supplier Trade name:

Manufacturer/Supplier Article number: S25881

Recommended uses of the product and uses restrictions on use:

Manufacturer Details:

AquaPhoenix Scientific
9 Barnhart Drive, Hanover, PA 17331

Supplier Details:

Fisher Science Education
15 Jet View Drive, Rochester, NY 14624

Emergency telephone number:

Fisher Science Education Emergency Telephone No.: 800-535-5053

SECTION 2 : Hazards identification

Classification of the substance or mixture:

Corrosive
Serious eye damage, category 1
Corrosive to metals, category 1
Skin corrosion, category 1B

Skin Corr. 1B
Eye corr. 1
Metal Corr. 1

Signal word :Danger

Hazard statements:
May be corrosive to metals
Causes severe skin burns and eye damage
Causes serious eye damage
Precautionary statements:
If medical advice is needed, have product container or label at hand
Keep out of reach of children
Read label before use
Keep only in original container
Do not breathe dust/fume/gas/mist/vapours/spray
Wash … thoroughly after handling
Wear protective gloves/protective clothing/eye protection/face protection
Absorb spillage to prevent material damage
IF ON SKIN (or hair): Remove/Take off immediately all contaminated clothing. Rinse skin with water/shower
IF IN EYES: Rinse cautiously with water for several minutes. Remove contact lenses if present and easy to do. Continue rinsing
IF SWALLOWED: Rinse mouth. Do NOT induce vomiting
Wash contaminated clothing before reuse
IF INHALED: Remove victim to fresh air and keep at rest in a position comfortable for breathing

Created by Global Safety Management, Inc. -Tel: 1-813-435-5161 - www.gsmsds.com

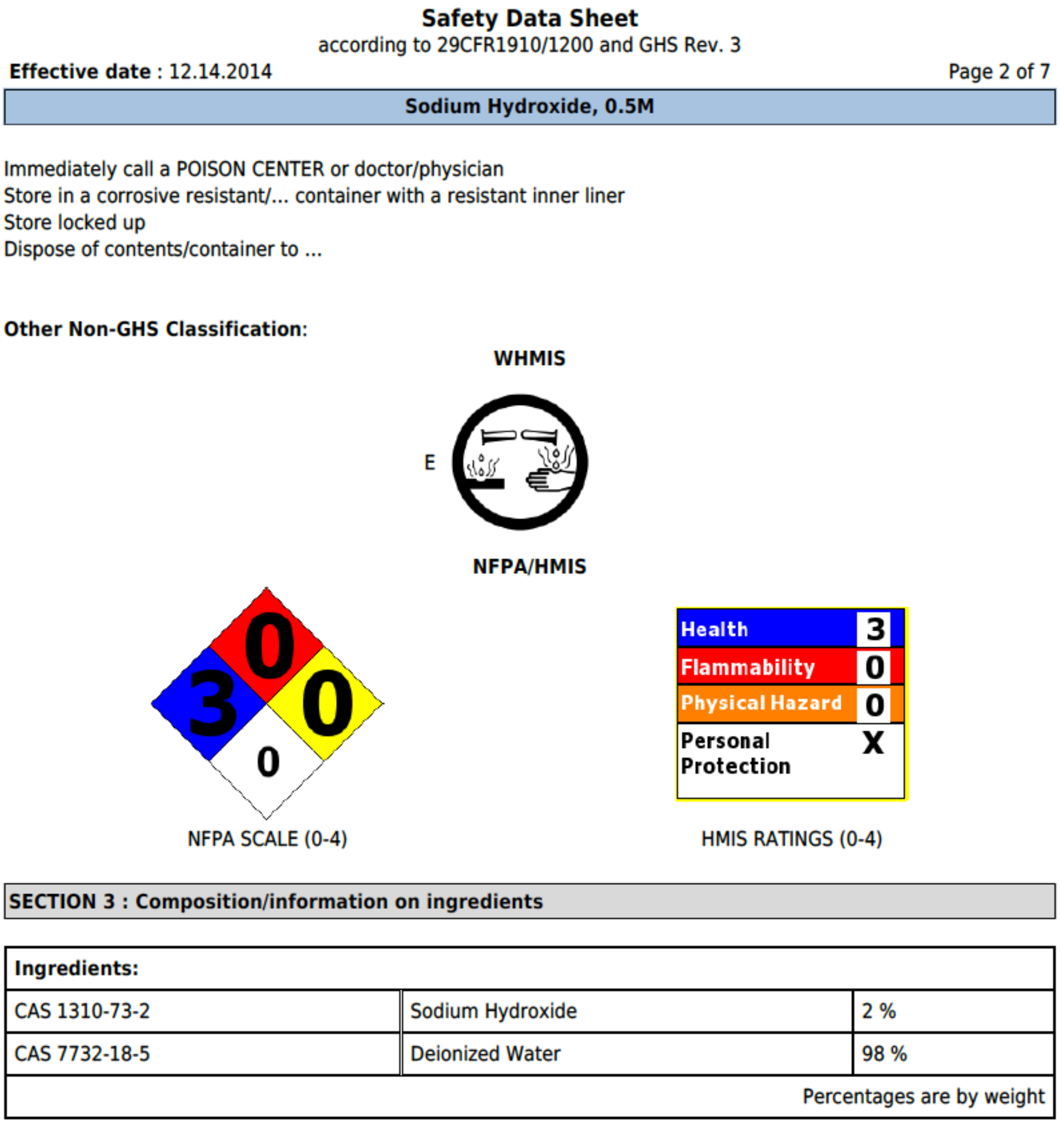

Safety Data Sheet
according to 29CFR1910/1200 and GHS Rev. 3

Effective date : 12.14.2014

Page 2 of 7

Sodium Hydroxide, 0.5M

Immediately call a POISON CENTER or doctor/physician
Store in a corrosive resistant/... container with a resistant inner liner
Store locked up
Dispose of contents/container to ...

Other Non-GHS Classification:

WHMIS

NFPA/HMIS

NFPA SCALE (0-4)

Health	**3**
Flammability	**0**
Physical Hazard	**0**
Personal Protection	**X**

HMIS RATINGS (0-4)

SECTION 3 : Composition/information on ingredients

Ingredients:		
CAS 1310-73-2	Sodium Hydroxide	2 %
CAS 7732-18-5	Deionized Water	98 %
		Percentages are by weight

Acetic Acid Datasheet:

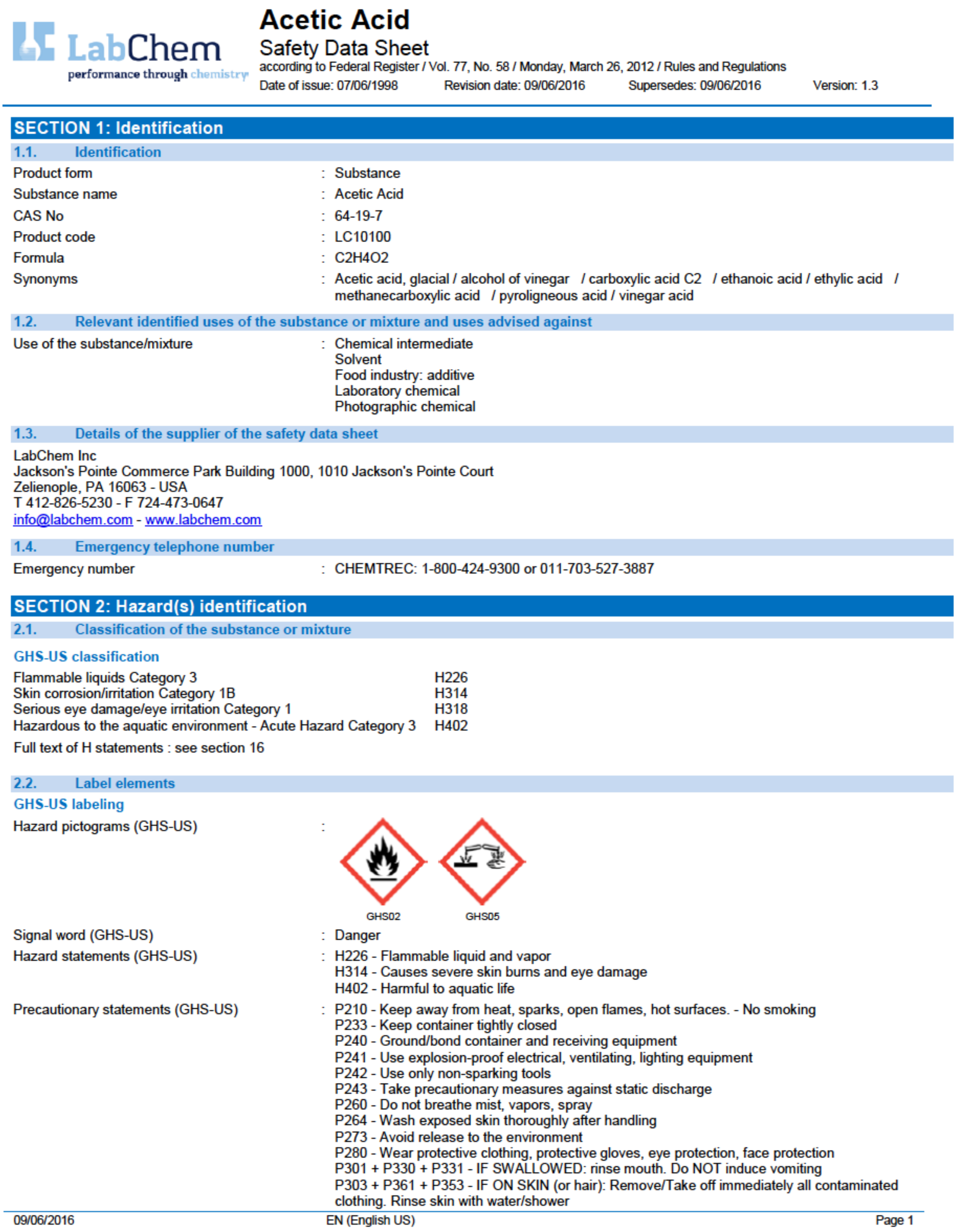

LabChem
performance through chemistry

Acetic Acid

Safety Data Sheet

according to Federal Register / Vol. 77, No. 58 / Monday, March 26, 2012 / Rules and Regulations

Date of issue: 07/06/1998 Revision date: 09/06/2016 Supersedes: 09/06/2016 Version: 1.3

SECTION 1: Identification

1.1. Identification

Product form	:	Substance
Substance name	:	Acetic Acid
CAS No	:	64-19-7
Product code	:	LC10100
Formula	:	C2H4O2
Synonyms	:	Acetic acid, glacial / alcohol of vinegar / carboxylic acid C2 / ethanoic acid / ethylic acid / methanecarboxylic acid / pyroligneous acid / vinegar acid

1.2. Relevant identified uses of the substance or mixture and uses advised against

Use of the substance/mixture	:	Chemical intermediate Solvent Food industry: additive Laboratory chemical Photographic chemical

1.3. Details of the supplier of the safety data sheet

LabChem Inc
Jackson's Pointe Commerce Park Building 1000, 1010 Jackson's Pointe Court
Zelienople, PA 16063 - USA
T 412-826-5230 - F 724-473-0647
info@labchem.com - www.labchem.com

1.4. Emergency telephone number

Emergency number	:	CHEMTREC: 1-800-424-9300 or 011-703-527-3887

SECTION 2: Hazard(s) identification

2.1. Classification of the substance or mixture

GHS-US classification

Flammable liquids Category 3	H226
Skin corrosion/irritation Category 1B	H314
Serious eye damage/eye irritation Category 1	H318
Hazardous to the aquatic environment - Acute Hazard Category 3	H402

Full text of H statements : see section 16

2.2. Label elements

GHS-US labeling

Hazard pictograms (GHS-US) :

GHS02 GHS05

Signal word (GHS-US)	:	Danger
Hazard statements (GHS-US)	:	H226 - Flammable liquid and vapor H314 - Causes severe skin burns and eye damage H402 - Harmful to aquatic life
Precautionary statements (GHS-US)	:	P210 - Keep away from heat, sparks, open flames, hot surfaces. - No smoking P233 - Keep container tightly closed P240 - Ground/bond container and receiving equipment P241 - Use explosion-proof electrical, ventilating, lighting equipment P242 - Use only non-sparking tools P243 - Take precautionary measures against static discharge P260 - Do not breathe mist, vapors, spray P264 - Wash exposed skin thoroughly after handling P273 - Avoid release to the environment P280 - Wear protective clothing, protective gloves, eye protection, face protection P301 + P330 + P331 - IF SWALLOWED: rinse mouth. Do NOT induce vomiting P303 + P361 + P353 - IF ON SKIN (or hair): Remove/Take off immediately all contaminated clothing. Rinse skin with water/shower

09/06/2016 EN (English US) Page 1

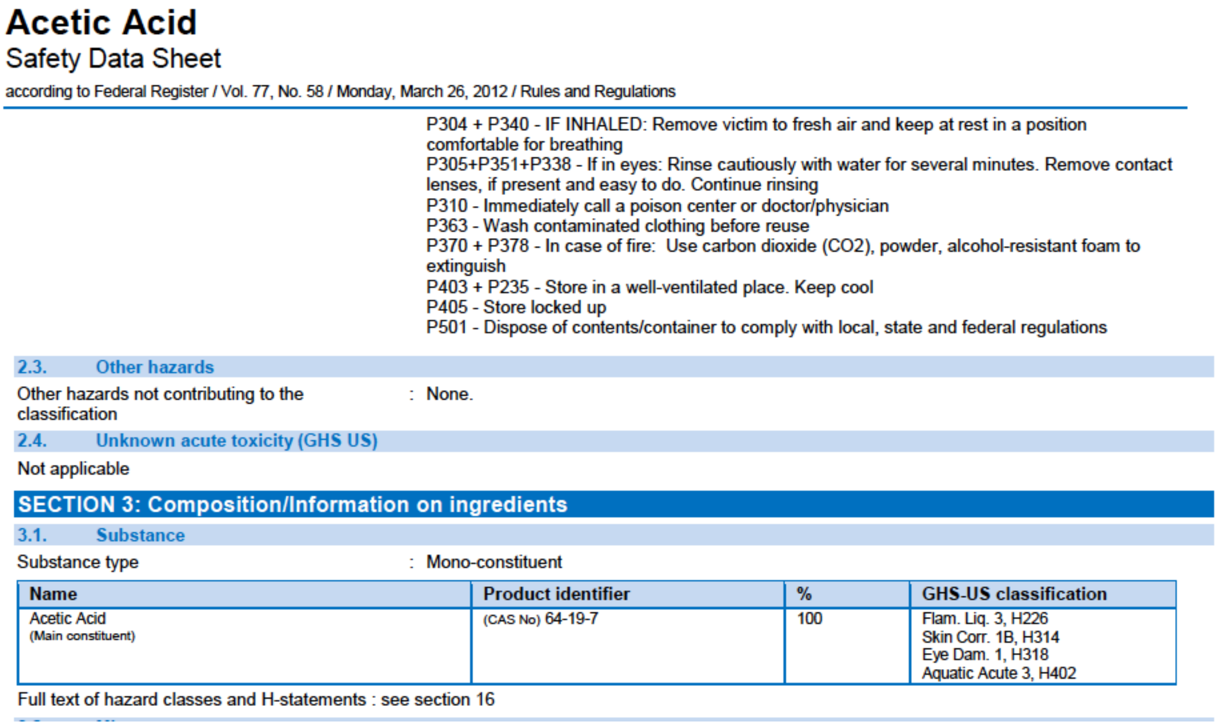

Acetic Acid

Safety Data Sheet

according to Federal Register / Vol. 77, No. 58 / Monday, March 26, 2012 / Rules and Regulations

P304 + P340 - IF INHALED: Remove victim to fresh air and keep at rest in a position comfortable for breathing
P305+P351+P338 - If in eyes: Rinse cautiously with water for several minutes. Remove contact lenses, if present and easy to do. Continue rinsing
P310 - Immediately call a poison center or doctor/physician
P363 - Wash contaminated clothing before reuse
P370 + P378 - In case of fire: Use carbon dioxide (CO2), powder, alcohol-resistant foam to extinguish
P403 + P235 - Store in a well-ventilated place. Keep cool
P405 - Store locked up
P501 - Dispose of contents/container to comply with local, state and federal regulations

2.3. Other hazards

Other hazards not contributing to the classification : None.

2.4. Unknown acute toxicity (GHS US)

Not applicable

SECTION 3: Composition/Information on ingredients

3.1. Substance

Substance type : Mono-constituent

Name	Product identifier	%	GHS-US classification
Acetic Acid (Main constituent)	(CAS No) 64-19-7	100	Flam. Liq. 3, H226 Skin Corr. 1B, H314 Eye Dam. 1, H318 Aquatic Acute 3, H402

Full text of hazard classes and H-statements : see section 16

Acetic Anhydride Datasheet:

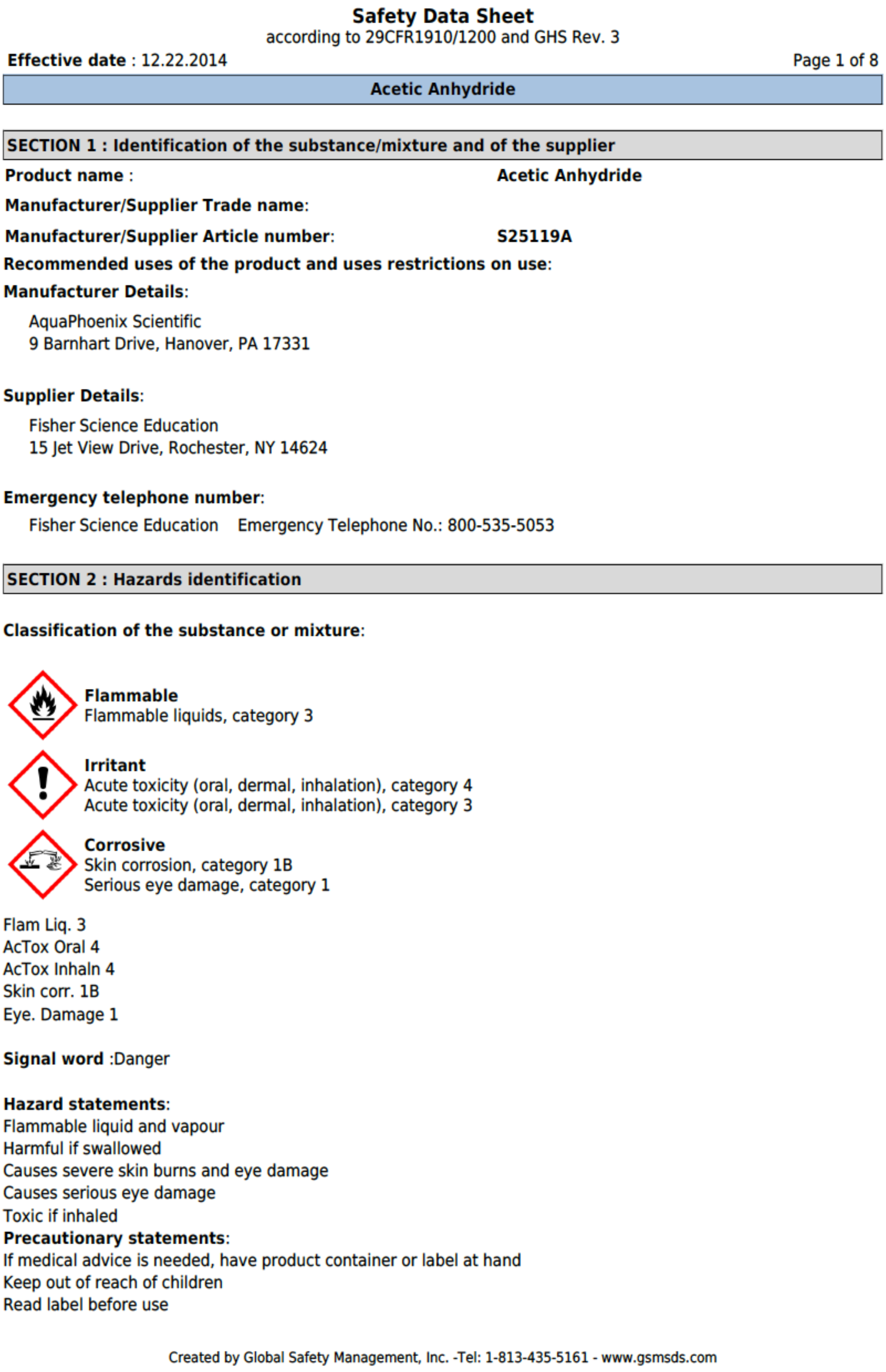

Safety Data Sheet

according to 29CFR1910/1200 and GHS Rev. 3

Effective date : 12.22.2014 Page 1 of 8

Acetic Anhydride

SECTION 1 : Identification of the substance/mixture and of the supplier

Product name :	**Acetic Anhydride**
Manufacturer/Supplier Trade name:	
Manufacturer/Supplier Article number:	**S25119A**

Recommended uses of the product and uses restrictions on use:

Manufacturer Details:

AquaPhoenix Scientific
9 Barnhart Drive, Hanover, PA 17331

Supplier Details:

Fisher Science Education
15 Jet View Drive, Rochester, NY 14624

Emergency telephone number:

Fisher Science Education Emergency Telephone No.: 800-535-5053

SECTION 2 : Hazards identification

Classification of the substance or mixture:

Flammable
Flammable liquids, category 3

Irritant
Acute toxicity (oral, dermal, inhalation), category 4
Acute toxicity (oral, dermal, inhalation), category 3

Corrosive
Skin corrosion, category 1B
Serious eye damage, category 1

Flam Liq. 3
AcTox Oral 4
AcTox Inhaln 4
Skin corr. 1B
Eye. Damage 1

Signal word :Danger

Hazard statements:
Flammable liquid and vapour
Harmful if swallowed
Causes severe skin burns and eye damage
Causes serious eye damage
Toxic if inhaled
Precautionary statements:
If medical advice is needed, have product container or label at hand
Keep out of reach of children
Read label before use

Created by Global Safety Management, Inc. -Tel: 1-813-435-5161 - www.gsmsds.com

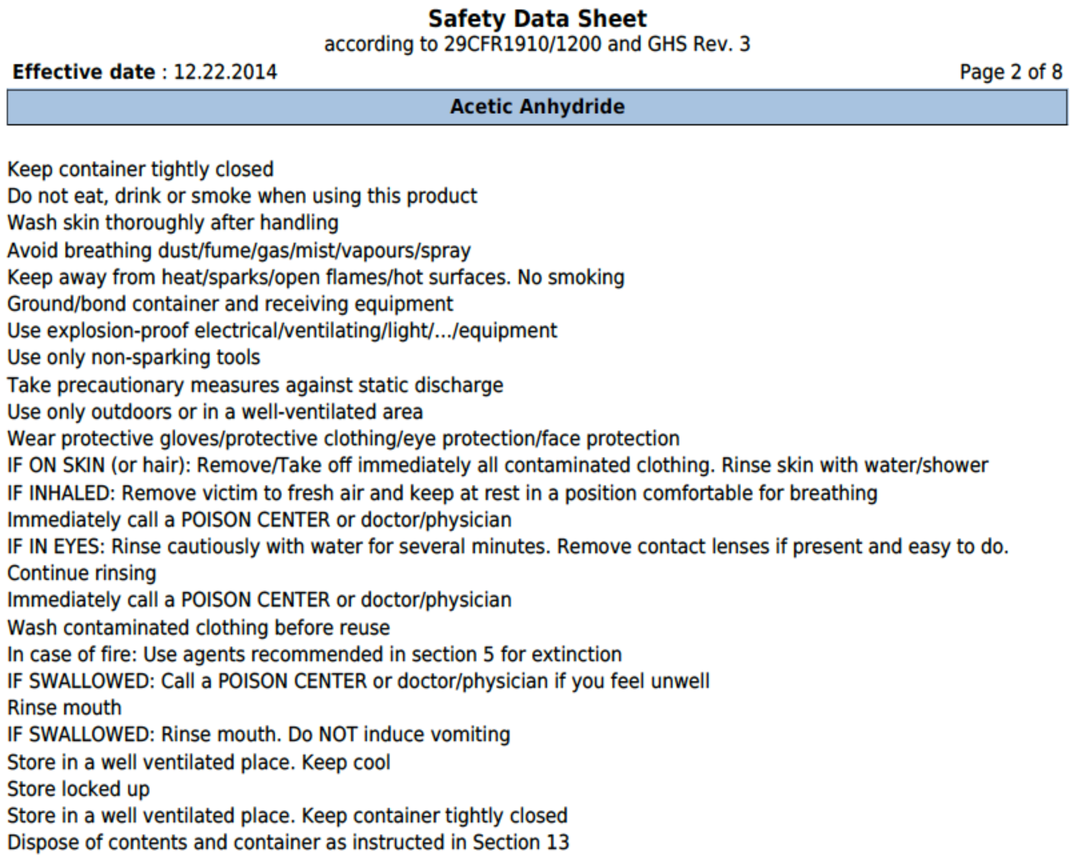

Safety Data Sheet
according to 29CFR1910/1200 and GHS Rev. 3

Effective date : 12.22.2014 Page 2 of 8

Acetic Anhydride

Keep container tightly closed
Do not eat, drink or smoke when using this product
Wash skin thoroughly after handling
Avoid breathing dust/fume/gas/mist/vapours/spray
Keep away from heat/sparks/open flames/hot surfaces. No smoking
Ground/bond container and receiving equipment
Use explosion-proof electrical/ventilating/light/.../equipment
Use only non-sparking tools
Take precautionary measures against static discharge
Use only outdoors or in a well-ventilated area
Wear protective gloves/protective clothing/eye protection/face protection
IF ON SKIN (or hair): Remove/Take off immediately all contaminated clothing. Rinse skin with water/shower
IF INHALED: Remove victim to fresh air and keep at rest in a position comfortable for breathing
Immediately call a POISON CENTER or doctor/physician
IF IN EYES: Rinse cautiously with water for several minutes. Remove contact lenses if present and easy to do.
Continue rinsing
Immediately call a POISON CENTER or doctor/physician
Wash contaminated clothing before reuse
In case of fire: Use agents recommended in section 5 for extinction
IF SWALLOWED: Call a POISON CENTER or doctor/physician if you feel unwell
Rinse mouth
IF SWALLOWED: Rinse mouth. Do NOT induce vomiting
Store in a well ventilated place. Keep cool
Store locked up
Store in a well ventilated place. Keep container tightly closed
Dispose of contents and container as instructed in Section 13

Sulphuric Acid Datasheet:

LabChem
performance through chemistry

Sulfuric Acid, ACS

Safety Data Sheet
according to Federal Register / Vol. 77, No. 58 / Monday, March 26, 2012 / Rules and Regulations
Date of issue: 10/01/1998 Revision date: 02/28/2018 Supersedes: 01/23/2018 Version: 1.3

SECTION 1: Identification

1.1. Identification

Product form : Substance
Substance name : Sulfuric Acid, ACS
CAS-No. : 7664-93-9
Product code : LC25550
Formula : H2SO4
Synonyms : battery acid / brown acid / brown oil of vitriol / dihydrogen sulfate / dipping acid / electrolyte acid / nordhausen acid / oil of vitriol / sulphuric acid

1.2. Recommended use and restrictions on use

Use of the substance/mixture : Industrial use
Laboratory chemical
Battery: component
Recommended use : Laboratory chemicals
Restrictions on use : Not for food, drug or household use

1.3. Supplier

LabChem Inc
Jackson's Pointe Commerce Park Building 1000, 1010 Jackson's Pointe Court
Zelienople, PA 16063 - USA
T 412-826-5230 - F 724-473-0647
info@labchem.com - www.labchem.com

1.4. Emergency telephone number

Emergency number : CHEMTREC: 1-800-424-9300 or 011-703-527-3887

SECTION 2: Hazard(s) identification

2.1. Classification of the substance or mixture

GHS-US classification

Skin corrosion/irritation, Category 1A	H314	Causes severe skin burns and eye damage.
Serious eye damage/eye irritation, Category 1	H318	Causes serious eye damage.

Full text of H statements : see section 16

2.2. GHS Label elements, including precautionary statements

GHS-US labelling

Hazard pictograms (GHS-US) :

GHS05

Signal word (GHS-US) : Danger
Hazard statements (GHS-US) : H314 - Causes severe skin burns and eye damage.
Precautionary statements (GHS-US) : P260 - Do not breathe mist, vapours, spray.
P264 - Wash exposed skin thoroughly after handling.
P280 - Wear protective gloves, protective clothing, eye protection, face protection.
P301+P330+P331 - IF SWALLOWED: rinse mouth. Do NOT induce vomiting.
P303+P361+P353 - IF ON SKIN (or hair): Take off immediately all contaminated clothing. Rinse skin with water/shower.
P304+P340 - IF INHALED: Remove person to fresh air and keep comfortable for breathing.
P305+P351+P338 - IF IN EYES: Rinse cautiously with water for several minutes. Remove contact lenses, if present and easy to do. Continue rinsing.
P310 - Immediately call a POISON CENTER/doctor
P363 - Wash contaminated clothing before reuse.
P405 - Store locked up.
P501 - Dispose of contents/container to comply with local, state and federal regulations

02/28/2018 EN (English) Page 1

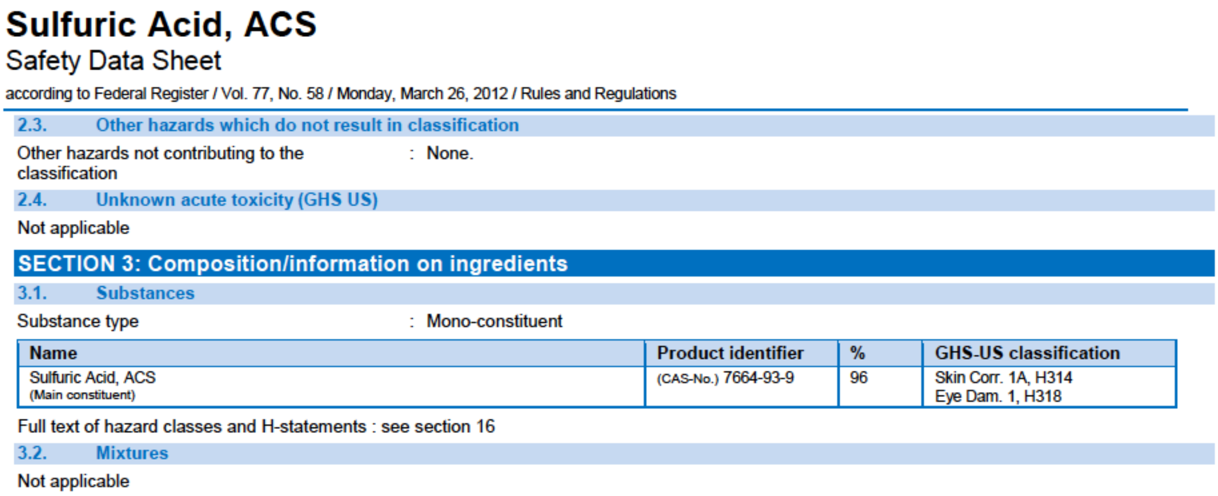

Sulfuric Acid, ACS

Safety Data Sheet

according to Federal Register / Vol. 77, No. 58 / Monday, March 26, 2012 / Rules and Regulations

2.3. Other hazards which do not result in classification

Other hazards not contributing to the classification : None.

2.4. Unknown acute toxicity (GHS US)

Not applicable

SECTION 3: Composition/information on ingredients

3.1. Substances

Substance type : Mono-constituent

Name	Product identifier	%	GHS-US classification
Sulfuric Acid, ACS (Main constituent)	(CAS-No.) 7664-93-9	96	Skin Corr. 1A, H314 Eye Dam. 1, H318

Full text of hazard classes and H-statements : see section 16

3.2. Mixtures

Not applicable

Silane Datasheet:

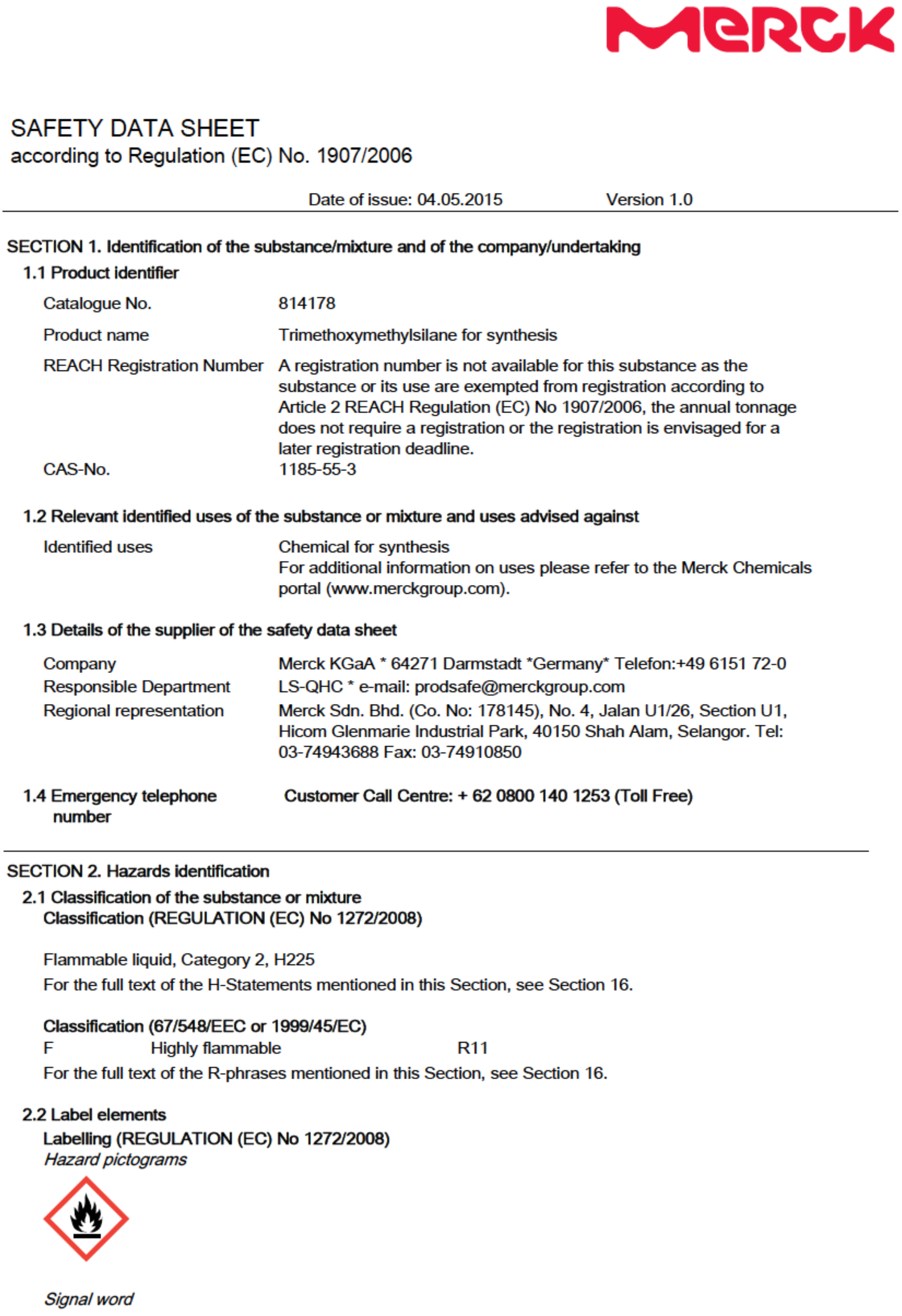

SAFETY DATA SHEET
according to Regulation (EC) No. 1907/2006

Date of issue: 04.05.2015 Version 1.0

SECTION 1. Identification of the substance/mixture and of the company/undertaking

1.1 Product identifier

Catalogue No.	814178
Product name	Trimethoxymethylsilane for synthesis
REACH Registration Number	A registration number is not available for this substance as the substance or its use are exempted from registration according to Article 2 REACH Regulation (EC) No 1907/2006, the annual tonnage does not require a registration or the registration is envisaged for a later registration deadline.
CAS-No.	1185-55-3

1.2 Relevant identified uses of the substance or mixture and uses advised against

Identified uses	Chemical for synthesis For additional information on uses please refer to the Merck Chemicals portal (www.merckgroup.com).

1.3 Details of the supplier of the safety data sheet

Company	Merck KGaA * 64271 Darmstadt *Germany* Telefon:+49 6151 72-0
Responsible Department	LS-QHC * e-mail: prodsafe@merckgroup.com
Regional representation	Merck Sdn. Bhd. (Co. No: 178145), No. 4, Jalan U1/26, Section U1, Hicom Glenmarie Industrial Park, 40150 Shah Alam, Selangor. Tel: 03-74943688 Fax: 03-74910850

1.4 Emergency telephone number	**Customer Call Centre: + 62 0800 140 1253 (Toll Free)**

SECTION 2. Hazards identification

2.1 Classification of the substance or mixture

Classification (REGULATION (EC) No 1272/2008)

Flammable liquid, Category 2, H225

For the full text of the H-Statements mentioned in this Section, see Section 16.

Classification (67/548/EEC or 1999/45/EC)

F	Highly flammable	R11

For the full text of the R-phrases mentioned in this Section, see Section 16.

2.2 Label elements

Labelling (REGULATION (EC) No 1272/2008)

Hazard pictograms

Signal word

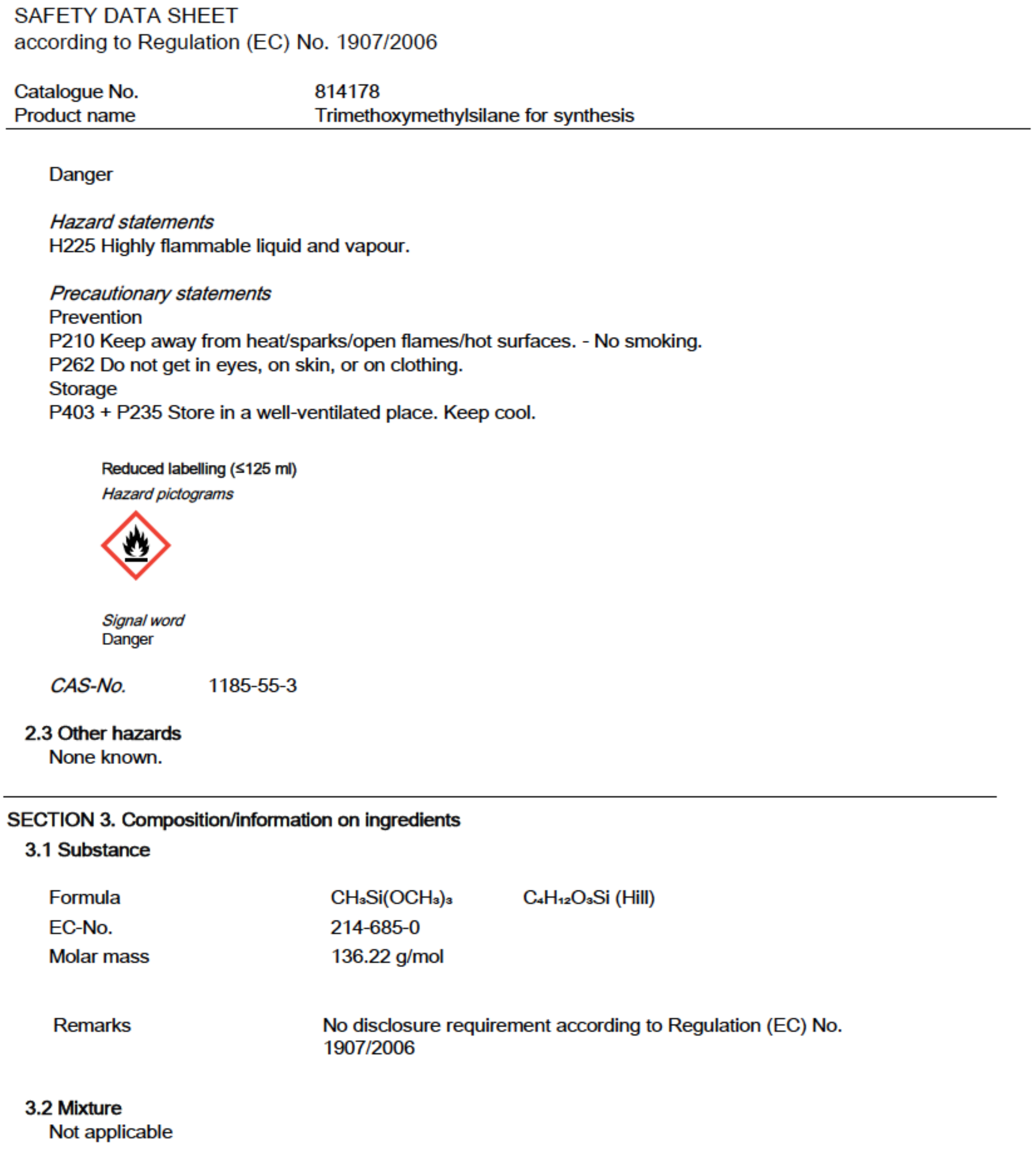

SAFETY DATA SHEET
according to Regulation (EC) No. 1907/2006

Catalogue No.	814178
Product name	Trimethoxymethylsilane for synthesis

Danger

Hazard statements
H225 Highly flammable liquid and vapour.

Precautionary statements
Prevention
P210 Keep away from heat/sparks/open flames/hot surfaces. - No smoking.
P262 Do not get in eyes, on skin, or on clothing.
Storage
P403 + P235 Store in a well-ventilated place. Keep cool.

Reduced labelling (≤125 ml)
Hazard pictograms

Signal word
Danger

CAS-No. 1185-55-3

2.3 Other hazards
None known.

SECTION 3. Composition/information on ingredients

3.1 Substance

Formula	$CH_3Si(OCH_3)_3$	$C_4H_{12}O_3Si$ (Hill)
EC-No.	214-685-0	
Molar mass	136.22 g/mol	
Remarks	No disclosure requirement according to Regulation (EC) No. 1907/2006	

3.2 Mixture
Not applicable

3-amino propyltriethoxysilane (APS) Datasheet:

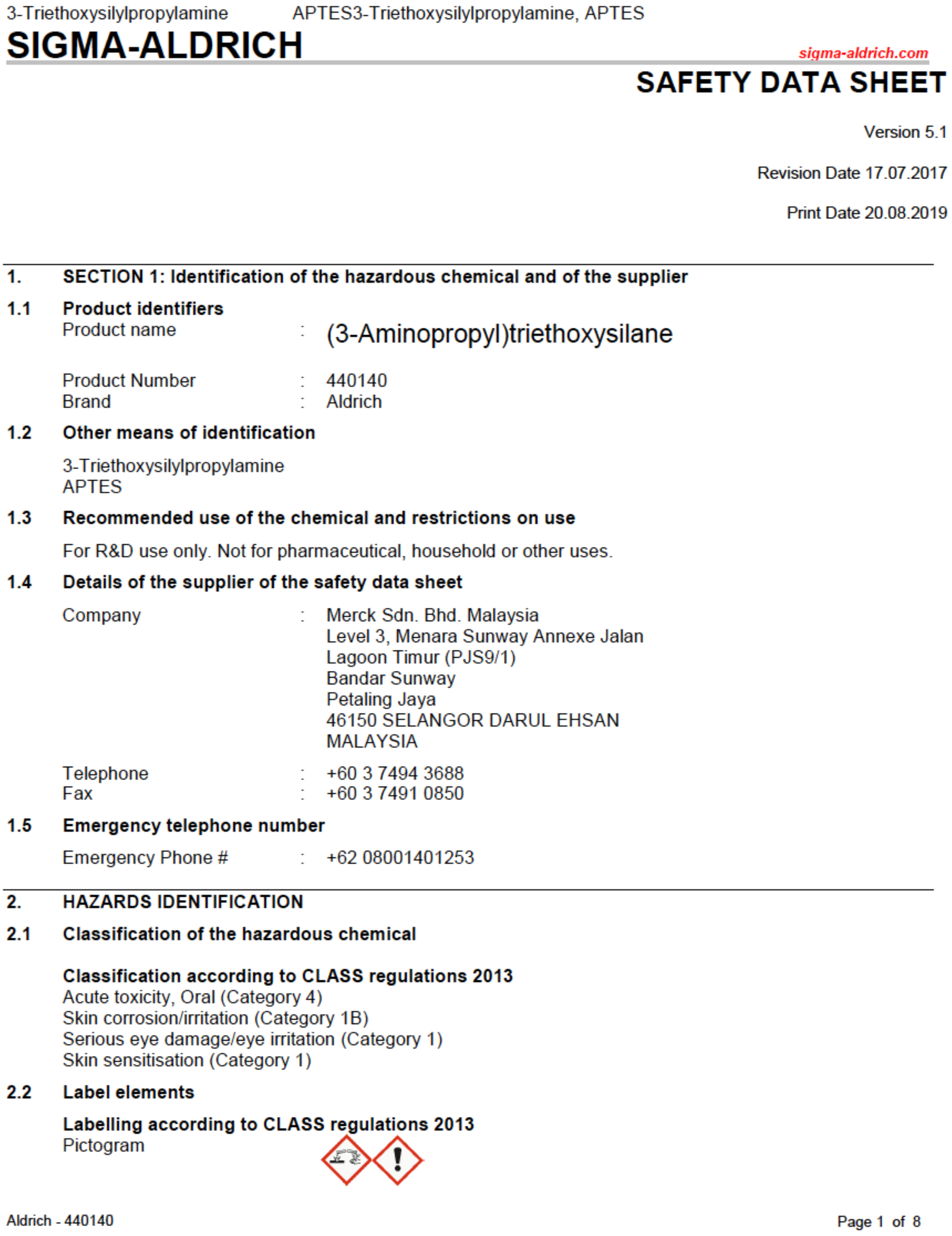

3-Triethoxysilylpropylamine APTES3-Triethoxysilylpropylamine, APTES

SIGMA-ALDRICH

sigma-aldrich.com

SAFETY DATA SHEET

Version 5.1

Revision Date 17.07.2017

Print Date 20.08.2019

1. SECTION 1: Identification of the hazardous chemical and of the supplier

1.1 Product identifiers

Product name : (3-Aminopropyl)triethoxysilane

Product Number : 440140
Brand : Aldrich

1.2 Other means of identification

3-Triethoxysilylpropylamine
APTES

1.3 Recommended use of the chemical and restrictions on use

For R&D use only. Not for pharmaceutical, household or other uses.

1.4 Details of the supplier of the safety data sheet

Company : Merck Sdn. Bhd. Malaysia
Level 3, Menara Sunway Annexe Jalan
Lagoon Timur (PJS9/1)
Bandar Sunway
Petaling Jaya
46150 SELANGOR DARUL EHSAN
MALAYSIA

Telephone : +60 3 7494 3688
Fax : +60 3 7491 0850

1.5 Emergency telephone number

Emergency Phone # : +62 08001401253

2. HAZARDS IDENTIFICATION

2.1 Classification of the hazardous chemical

Classification according to CLASS regulations 2013
Acute toxicity, Oral (Category 4)
Skin corrosion/irritation (Category 1B)
Serious eye damage/eye irritation (Category 1)
Skin sensitisation (Category 1)

2.2 Label elements

Labelling according to CLASS regulations 2013
Pictogram

Aldrich - 440140

Page 1 of 8

Signal word	Danger
Hazard statement(s)	
H302	Harmful if swallowed.
H314	Causes severe skin burns and eye damage.
H317	May cause an allergic skin reaction.
Precautionary statement(s)	
Prevention	
P261	Avoid breathing dust/ fume/ gas/ mist/ vapours/ spray.
P264	Wash skin thoroughly after handling.
P280	Wear protective gloves/ protective clothing/ eye protection/ face protection.
Response	
P303 + P361 + P353	IF ON SKIN (or hair): Remove/ Take off immediately all contaminated clothing. Rinse skin with water/ shower.
P304 + P340 + P310	IF INHALED: Remove victim to fresh air and keep at rest in a position comfortable for breathing. Immediately call a POISON CENTER or doctor/ physician.
P305 + P351 + P338 + P310	IF IN EYES: Rinse cautiously with water for several minutes. Remove contact lenses, if present and easy to do. Continue rinsing. Immediately call a POISON CENTER or doctor/ physician.

2.3 Other hazards - none

---

3. SECTION 3: Composition and information of the ingredients of the hazardous chemical

3.1 Substances
Chemical identity

Synonyms : 3-Triethoxysilylpropylamine
APTES

Formula : $C_9H_{23}NO_3Si$
Molecular weight : 221,37 g/mol
CAS-No. : 919-30-2

Component		Concentration
3-Aminopropyltriethoxysilane		
CAS-No.	919-30-2	<= 100 %
EC-No.	213-048-4	
Index-No.	612-108-00-0	

Bis-(3-triethoxysilylpropyl) Datasheet:

SIB1824.5 - BIS(3-TRIETHOXYSILYLPROPYL)AMINE, 95%

Gelest
Enabling Your Technology

BIS(3-TRIETHOXYSILYLPROPYL)AMINE, 95%
Safety Data Sheet SIB1824.5
Date of issue: 01/07/2015 Version: 1.0

SECTION 1: Identification

1.1. Identification

Product name	: BIS(3-TRIETHOXYSILYLPROPYL)AMINE, 95%
Product code	: SIB1824.5
Product form	: Substance
Physical state	: Liquid
Formula	: $C_{18}H_{43}NO_6Si_2$
Synonyms	: 3,13-DIOXA-8-AZA-4,12-DISILAPENTADECANE, 4,4,12,12-TETRAETHOXY-; 1-PROPANAMINE, 3-TRIETHOXYSILYL-N-(3-TRIETHOXYSILYL)PROPYL)
Chemical family	: ORGANOETHOXYSILANE

1.2. Recommended use and restrictions on use

Recommended use	: Chemical intermediate

1.3. Supplier

GELEST, INC.
11 East Steel Road
Morrisville, PA 19067
USA
T 215-547-1015 - F 215-547-2484 - (M-F): 8:00 AM - 5:30 PM EST
info@gelest.com - www.gelest.com

1.4. Emergency telephone number

Emergency number	: CHEMTREC: 1-800-424-9300 (USA); +1 703-527-3887 (International)

SECTION 2: Hazard(s) identification

2.1. Classification of the substance or mixture

GHS-US classification

Skin corrosion/irritation Category 1C	H314 Causes severe skin burns and eye damage
Serious eye damage/eye irritation Category 1	H318 Causes serious eye damage
Specific target organ toxicity (single exposure) Category 3	H335 May cause respiratory irritation

Full text of H statements : see section 16

2.2. GHS Label elements, including precautionary statements

GHS US labeling

Hazard pictograms (GHS US) :

Signal word (GHS US) : Danger

Hazard statements (GHS US) :
H314 - Causes severe skin burns and eye damage
H318 - Causes serious eye damage
H335 - May cause respiratory irritation

Precautionary statements (GHS US) :
P280 - Wear protective gloves/protective clothing/eye protection/face protection.
P260 - Do not breathe vapors.
P264 - Wash hands thoroughly after handling.
P271 - Use only outdoors or in a well-ventilated area.
P301+P330+P331 - If swallowed: rinse mouth. Do NOT induce vomiting
P303+P361+P353 - If on skin (or hair): take off immediately all contaminated clothing. rinse skin with water/shower
P304+P340 - If inhaled: Remove person to fresh air and keep comfortable for breathing
P305+P351+P338 - IF IN EYES: Rinse cautiously with water for several minutes. Remove contact lenses, if present and easy to do. Continue rinsing
P310 - Immediately call a doctor
P363 - Wash contaminated clothing before reuse.
P403+P233 - Store in a well-ventilated place. Keep container tightly closed.
P405 - Store locked up.
P501 - Dispose of contents/container to licensed waste disposal facility.

2.3. Hazards not otherwise classified (HNOC)

Other hazards not contributing to the classification : The hydrolysis product of this compound is ethanol. Overexposure to ethanol by skin absorption, inhalation or ingestion may have a narcotic effect (headache, nausea, drowsiness). Ethanol is metabolized to acetaldehyde and acetic acid which in large quantities result in

Print date: 04/12/2019 EN (English US) SDS ID: **SIB1824.5** Page 1

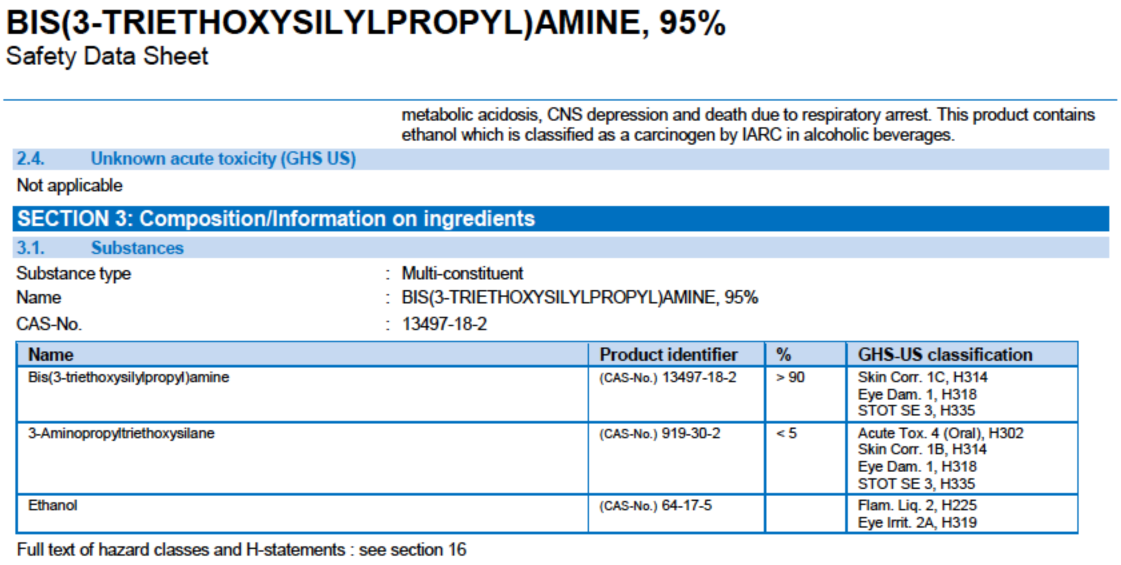

BIS(3-TRIETHOXYSILYLPROPYL)AMINE, 95%

Safety Data Sheet

metabolic acidosis, CNS depression and death due to respiratory arrest. This product contains ethanol which is classified as a carcinogen by IARC in alcoholic beverages.

2.4. Unknown acute toxicity (GHS US)

Not applicable

SECTION 3: Composition/Information on ingredients

3.1. Substances

Substance type : Multi-constituent
Name : BIS(3-TRIETHOXYSILYLPROPYL)AMINE, 95%
CAS-No. : 13497-18-2

Name	Product identifier	%	GHS-US classification
Bis(3-triethoxysilylpropyl)amine	(CAS-No.) 13497-18-2	> 90	Skin Corr. 1C, H314 Eye Dam. 1, H318 STOT SE 3, H335
3-Aminopropyltriethoxysilane	(CAS-No.) 919-30-2	< 5	Acute Tox. 4 (Oral), H302 Skin Corr. 1B, H314 Eye Dam. 1, H318 STOT SE 3, H335
Ethanol	(CAS-No.) 64-17-5		Flam. Liq. 2, H225 Eye Irrit. 2A, H319

Full text of hazard classes and H-statements : see section 16

Ethanol Datasheet:

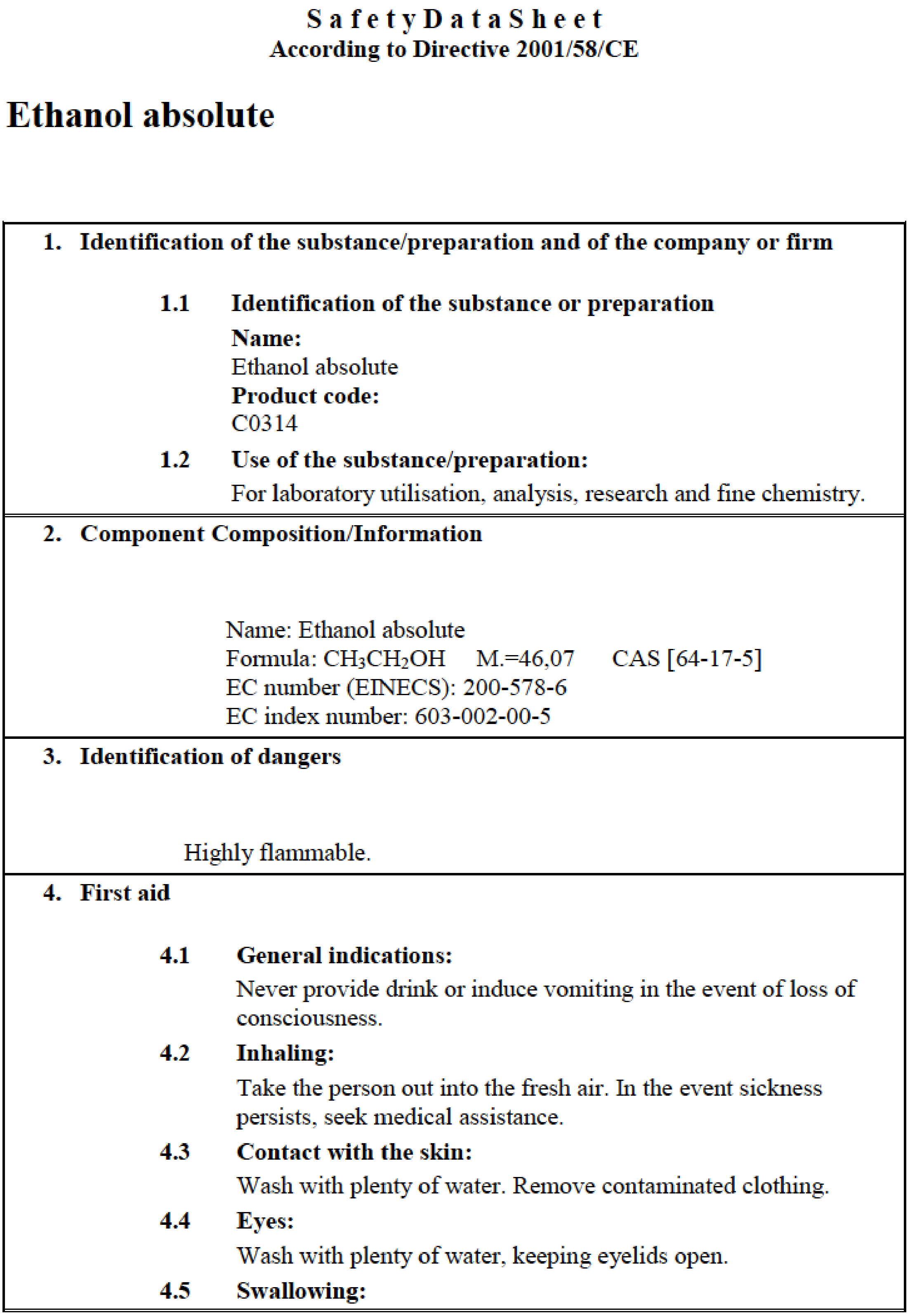

SafetyDataSheet
According to Directive 2001/58/CE

Ethanol absolute

1. Identification of the substance/preparation and of the company or firm

1.1 Identification of the substance or preparation

Name:
Ethanol absolute
Product code:
C0314

1.2 Use of the substance/preparation:
For laboratory utilisation, analysis, research and fine chemistry.

2. Component Composition/Information

Name: Ethanol absolute
Formula: CH_3CH_2OH M.=46,07 CAS [64-17-5]
EC number (EINECS): 200-578-6
EC index number: 603-002-00-5

3. Identification of dangers

Highly flammable.

4. First aid

4.1 General indications:
Never provide drink or induce vomiting in the event of loss of consciousness.

4.2 Inhaling:
Take the person out into the fresh air. In the event sickness persists, seek medical assistance.

4.3 Contact with the skin:
Wash with plenty of water. Remove contaminated clothing.

4.4 Eyes:
Wash with plenty of water, keeping eyelids open.

4.5 Swallowing:

5.3.2 Gantt Chart

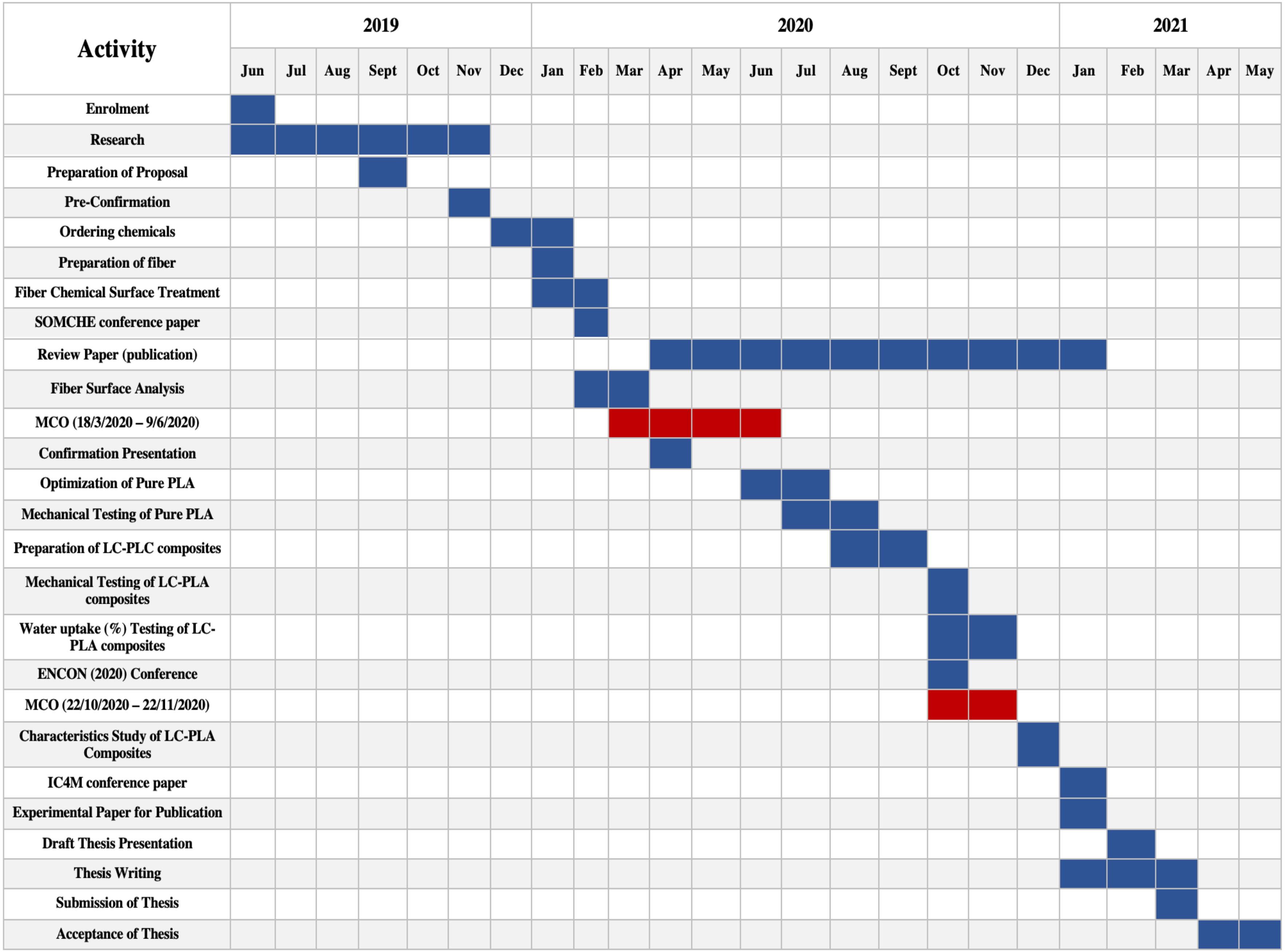

Activity	2019							2020												2021				
	Jun	Jul	Aug	Sept	Oct	Nov	Dec	Jan	Feb	Mar	Apr	May	Jun	Jul	Aug	Sept	Oct	Nov	Dec	Jan	Feb	Mar	Apr	May
Enrolment	🟦																							
Research	🟦	🟦	🟦	🟦	🟦	🟦																		
Preparation of Proposal				🟦																				
Pre-Confirmation						🟦																		
Ordering chemicals							🟦	🟦																
Preparation of fiber								🟦																
Fiber Chemical Surface Treatment								🟦	🟦															
SOMCHE conference paper									🟦															
Review Paper (publication)											🟦	🟦	🟦	🟦	🟦	🟦	🟦	🟦	🟦	🟦				
Fiber Surface Analysis									🟦	🟦														
MCO (18/3/2020 – 9/6/2020)										🟥	🟥	🟥	🟥											
Confirmation Presentation											🟦													
Optimization of Pure PLA													🟦	🟦										
Mechanical Testing of Pure PLA														🟦	🟦									
Preparation of LC-PLC composites															🟦	🟦								
Mechanical Testing of LC-PLA composites																	🟦							
Water uptake (%) Testing of LC-PLA composites																	🟦	🟦						
ENCON (2020) Conference																	🟦							
MCO (22/10/2020 – 22/11/2020)																	🟥	🟥						
Characteristics Study of LC-PLA Composites																			🟦					
IC4M conference paper																				🟦				
Experimental Paper for Publication																				🟦				
Draft Thesis Presentation																					🟦			
Thesis Writing																				🟦	🟦	🟦		
Submission of Thesis																						🟦		
Acceptance of Thesis																							🟦	🟦